



Title	Metabolic profiling of <i>Garcinia mangostana</i> : a new insight into quality after postharvest treatment
Author(s)	Parijadi, Anjaritha Aulia Rizky
Citation	大阪大学, 2019, 博士論文
Version Type	VoR
URL	https://doi.org/10.18910/73548
rights	
Note	

The University of Osaka Institutional Knowledge Archive : OUKA

<https://ir.library.osaka-u.ac.jp/>

The University of Osaka

Doctoral Dissertation

**Metabolic Profiling of *Garcinia mangostana*
(mangosteen): a new insight into quality after
postharvest treatment**

Anjaritha Aulia Rizky Parijadi

July 2019

Department of Biotechnology,
Division of Advanced Science and Biotechnology,
Graduate School of Engineering,
Osaka University

Table of Contents

Table of Contents	2
Abstract.....	7
List of Abbreviations	9
Chapter 1	11
General Introduction.....	11
1.1. Fruit ripening process	11
1.2. <i>Garcinia mangostana</i> (mangosteen)	16
1.2.1. General Information of mangosteen	16
1.3. Color measurements	22
1.4. Metabolomics	24
1.4.1. General concept.....	24
1.4.2. Metabolomics Workflow	26
1.4.3. Application to agricultural and food science	29
1.4.4. Recent research and objectives in this study	30
1.5. Research Objectives	31
1.6. Thesis outline.....	32

Chapter 2	33
Metabolomics-based approach for the study of <i>Garcinia mangostana</i> (mangosteen) ripening stages	33
2.1. Introduction	33
2.2. Experimental section	35
2.2.1. Plant materials	35
2.2.2. Color changes measurement	36
2.2.3. Samples extraction.....	36
2.2.4. Derivatization	37
2.2.5. Gas chromatography-mass spectrometry analysis.....	37
2.2.6. Data analysis.....	37
2.3. Results and discussions	38
2.3.1. Assessment of mangosteen ripening stages.....	38
2.3.2. Elucidation of metabolic changes during mangosteen ripening stages	40
2.3.3. Color changes based exploratory analysis of mangosteen ripening stages ..	43
2.3.4. Important metabolites change in mangosteen during ripening are related to color changes	45
2.3.5. Metabolites changes related to the quality of mangosteen during ripening process in flesh part	48

2.3.6. Metabolites changes related to the quality of mangosteen during ripening process in peel part	51
2.4. Conclusions	53
Chapter 3	54
Metabolomics-based approach for the evaluation of different mangosteen ripening condition	54
3.1. Introduction	54
3.2. Experimental section	55
3.2.1. Plant materials	55
3.2.2. Color changes measurement.....	56
3.2.3. Samples extraction.....	56
3.2.4. Derivatization	57
3.2.5. Gas chromatography-mass spectrometry analysis.....	57
3.2.6. Data analysis.....	57
3.3. Results and discussions	57
3.3.1. Elucidation of metabolic changes during mangosteen ripening stages in different ripening conditions	57
3.3.2. Prediction model of mangosteen ripening process in two different harvesting condition	63
3.3.3. Prediction model of different ripening condition in mangosteen	70

3.4. Conclusions	72
Chapter 4	73
Metabolomics-based approach for the evaluation of different mangosteen postharvest technologies	73
4.1. Introduction	73
4.2. Experimental section	74
4.2.1. Plant materials	74
4.2.2. Color changes measurement.....	75
4.2.3. Samples extraction.....	76
4.2.4. Derivatization	76
4.2.5. Gas chromatography-mass spectrometry analysis.....	76
4.2.6. Data analysis.....	76
4.3. Results and discussions	76
4.3.1. Physical appearance assessment of mangosteen postharvest technology	76
4.3.2. Elucidation of metabolic changes during mangosteen postharvest technology in peel part	78
2.4. Conclusions	88
Chapter 5	89
Conclusions and perspectives.....	89

References	93
Appendix	111
List of publications	139
Conferences	139
Review paper	140
Original papers	141
Acknowledgments	142

Abstract

Metabolomics, the study of total profiling of metabolites, is an important tool to support postharvest fruit development and ripening studies. Monitoring the changes in the metabolome during fruit ripening is important to obtain insight into the mechanisms involved and improve postharvest management strategies. Fruit ripening process is a complex developmental process involving coordinated regulation of numerous metabolic pathways that influence color, flavor, aroma, and texture. Based on their mode of ripening, fruits are categorized into two categories such as climacteric fruit and non-climacteric fruit. The ripening of climacteric fruit is dependent on the concomitant burst of ethylene, while non-climacteric fruit ripening is not affected by the existence of ethylene. Mangosteen, often known as the “Queen of Fruits”, is an economically important tropical fruit desired for its distinctive appearance and unique taste. Mangosteen is a climacteric fruit and the progression of ripening is indicated by changes in its peel color. Mangosteen ripening stages were categorized into seven stages based on color changes. Understanding the changes that occur during ripening is necessary in order to assess optimal harvest maturity and the quality of fruit as it is marketed to the consumer as well as to devise appropriate postharvest packaging and handling strategies. For the last decade, the study of mangosteen only focused on the elucidation of bioactive compounds such as alpha-mangosteen and gamma-mangosteen. However, there is no single study that mentions about the metabolic changes during the mangosteen ripening process.

In chapter 1 provides the general introduction concerning mangosteen as an important export commodity in Indonesia and how metabolomics can be an effective tool for mangosteen researches. In chapter 2, non-targeted GC/MS-based metabolic profiling methods were applied to obtain a general view on the metabolic changes related to the qualities during ripening process throughout mangosteen color changes. In chapter 3, in order to investigate the effects of different cultivation area, different tree, and year of harvesting were examined to confirm the metabolic changes during mangosteen ripening process. In these experiments, all samples were evaluated based on their color changes

and metabolic changes during ripening process. In chapter 4, several postharvest treatments were applied and evaluated using metabolomics approach. At last, the conclusions revealed from this study were summarized and the future perspectives were proposed.

List of Abbreviations

(in alphabetical order)

1-MCP	1-methylcyclopropane (ethylene inhibitor)
a*	Chromacity diagram red-green color in CIELAB
ACC	1-aminocyclopropane-1-carboxylic acid
ACCS	ACC synthase enzyme
ACO	ACC oxidase
ANDI	Analytical Data Interchange Protocol
b*	Chromacity diagram yellow-blue color in CIELAB
CENTROHS	Center of Tropical Horticultural Studies
CIE	Commission International d'Eclairage
CTR1	Constitutive Triple-Response1
EBF	Ethylene Insensitive3-binding F-box Proteins
EIL1	EIN3/Ethylene Insensitive3-Like1, <i>Transcription factors</i>
EIN2	Ethylene Insensitive2, <i>Transcription factors</i>
ER	Endoplasmic Reticulum
ETRs	Ethylene receptors
FID	Flame Induction Detector
GC	Gas Chromatography
HCA	Hierarchical Cluster Analysis
HS-SPME	Headspace-Solid Phase Micro Extraction
ICP	Inductively Coupled Plasma
L*	Lightness value in CIELAB
LC	Liquid Chromatography
LT	Low temperature
MeJa	Methyl Jasmonate
MS	Mass Spectrometer
MSI	Metabolites Standard Initiatives
MSTFA	<i>N</i> -methyl- <i>N</i> -trimethylsilyl-trifluoroacetamide
NIST	National Institute of Standards and Technology
OPLS-DA	Orthogonal Projections to Latent Structures-Discriminant Analysis

PC	Principal Component
PCA	Principal Component Analysis
PEREs	Primary Ethylene Response Elements
PLS	Partial Least Squares
QC	Quality Control
RI	Retention Index
RMSEE	Root Means Square Error of Estimation
RMSEP	Root Means Square Error of Prediction
ROS	Reactive Oxygen System
RSD	Relative Standard Deviation
RT	Room temperature
RT	Retention Time
SA	Salicylic Acid
SAM	S-adenosyl-L-Methionine
SI	Stress Inducer
SNI	Standard Nasional Indonesia (<i>Indonesian national standard</i>)
TA	Titrateable acid
TCA	Tricarboxylic acid
TEV	Total Explained Variance
TSS	Total Soluble Solids
UV	Unit Variance, Scaling method
VIP	Variable Importance in Projection

Chapter 1

General Introduction

In the last decade, the increasing trend of fresh products including fruits and quality of agricultural and food products have become one of the major issues in the food industry. Fruit ripening process is a process involving the coordinated regulation of numerous metabolic pathways that influence color, flavor, aroma, and texture. Additionally, countless efforts to prolong agricultural product shelf-life have deliberately accomplished by manufacturers and exporters to meet consumers' demand, is challenging. In recent years, metabolomics approach is widely used as an important tool to support postharvest fruit development and ripening studies. In this thesis, the investigation of mangosteen ripening process and its effect after postharvest treatment were presented employing metabolomics technology.

1.1. Fruit ripening process

Fruit is one of the ultimate sink organs of the plant. The growth of this sink organ directly depends on the partitioning of photosynthate from source organ to sink. The sink organ store variety of metabolites which depends on species, source strength, the composition of allocated photosynthate and plant requirement. The storage of metabolites in fruit will be depended on the requirement to be used for fruit development and fruit ripening process¹⁻³.

Fruit ripening process is significantly correlated with metabolic composition of fruit. Fruit ripening process is also well known as a complex developmental process involving the coordinated regulation of numerous metabolic pathways that influence color, flavor, aroma, and texture. Many of these attributes enhance fruit nutritional value and attractiveness, thereby promoting consumption and seed dispersal⁴⁻⁶. This process usually is induced by ethylene (C₂H₄) which acts as ripening hormones.

Ethylene (C₂H₄), as one of plant hormones, is produced to activate several processes in plant physiology such as seeds germination, embryogenesis, leaves and flower senescence, and ripening process in the fruits. Ethylene biosynthesis pathway involves the conversion of *S*-adenosyl-*L*-methionine (SAM) to 1-aminocyclopropane-1-carboxylic acid (ACC) by ACC synthase enzyme (ACS). The ethylene is produced by ACC oxidase (ACO) from ACC to ethylene (Figure 1)⁶⁻⁸.

Ethylene biosynthesis pathway as a regulator which characterized feature of ripening fruits and senescing flowers based on its exposure to exogenous ethylene or propylene due to the induction of ACS and ACO genes^{9,10}. The roles of ACS gene have been extensively studied in tomato, melon, cucumber, and citrus. Analysis of ACS genes induction in mutant fruit has been used to identify the specific ACS ethylene-regulated gene. The disrupted ACS gene in mutant fruits was reported to have an abnormal pattern of ripening such as reduced lycopene accumulation, delayed softening, and a much-reduced ethylene peak^{5,6,11-14}.

Additionally, investigation of ACO roles during ethylene biosynthesis have increased in recent years. Analysis of ACO gene expression patterns in ripening fruit shows that each gene is highly regulated with transcripts of individual members

accumulating to varying degrees at distinct developmental stages. Therefore, the previous study also reported the first step in catalytic ethylene biosynthesis by using the *de novo* synthesis of ACO enzyme, the produced-ethylene induces ACS gene expression, resulted in more ACC productions¹⁵⁻¹⁷.

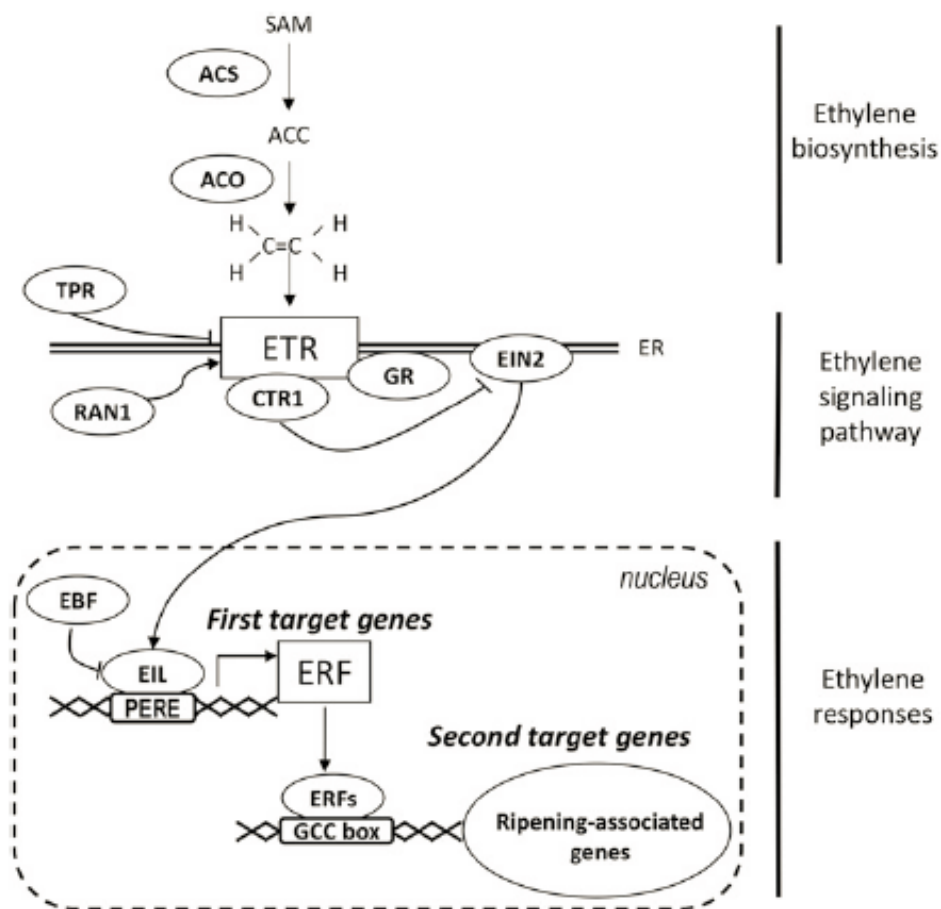


Figure 1. Simplified scheme showing ethylene synthesis and response in tomato based on Liu *et al* (2015)¹.

The function of ACS and ACO had been explained in detailed of ethylene biosynthesis process. Additionally, specific members of ACS and ACO genes were proposed to investigate its role to control two systems of ethylene production in plants,

including system-1 and system-2. System-1 is an auto-inhibitory, where the perception of ethylene by the plant inhibits further ethylene production or its biosynthesis as found in unripe fruits and vegetative tissues. In contrast, system-2 is autocatalytic, where the perception of ethylene stimulates ethylene synthesis as displayed during floral senescence and fruit ripening^{18,19}.

As mentioned earlier, ethylene plays a big role during fruit ripening process. Elucidation the mechanisms involved in ripening of fruit had been reported in several approaches for understanding the role of ethylene during the process. During ripening process, ethylene is perceived by receptors encoded by a multigene family, the ethylene receptors (ETRs) in *Arabidopsis* and tomato (Figure 1). ETRs roles have been extensively studied to understanding fruit ripening process especially in tomatoes such as its effect to fruit size, yield, or flavor-related chemical composition. ETRs are membrane proteins associated with the endoplasmic reticulum and act as negative regulators of the ethylene response pathway^{20,21}. Subsequently, ethylene will activate the transcription process of ethylene responsive genes that will induce several ripening-associated genes such as cell-wall degradation or softening process during fruit ripening process.

Polygalacturonase is one of enzymes that has the main function during softening process of peach (*Prunus persica*)^{22,23}. Polygalacturonase will degrade the fruit cell wall into simple form due to oxidation process during ripening process. Subsequently, the degradation of fruit cell wall will affect the fruit softening during ripening process. The other enzymes that are contributed to fruit cell wall degradation are cellulose, pectinesterase, pectate lyase, xylulose, polygalacturonase, and expansin. These enzymes

are actively found during banana ripening process ²¹. These textural changes during ripening is an essential attribute that makes fruit edible, more palatable, and attractive for human consumption.

Other physical changes occur during fruit ripening process is color changes. Color changes during ripening process due to the pigmentation process from chlorophyll to other pigmentation metabolites such as carotenoids and anthocyanin. The characteristic pigmentation of fruit is due to biochemical changes during ripening process. The predominant carotenoid found in tomato fruit, and beta-carotene, which are associated with the change from green to red as chloroplasts are transformed to chromoplasts. During ripening process, lycopene begins to accumulate and its concentration increases 500-fold in ripe fruit ²⁴⁻²⁶. Similar process occurs in mangosteen, which accumulates anthocyanin pigment during ripening process ²⁷. Color changes during ripening is an essential attribute that indicates fruit attractiveness for human consumption as well for vectors of fruit dispersal.

Based on their mode of ripening, fruits are categorized into two categories such as climacteric fruit and non-climacteric fruit. The ripening of climacteric fruit is dependent on the concomitant burst of ethylene, while non-climacteric fruit ripening is not affected by the existence of ethylene. The progression of ripening is indicated by changes in its peel color, texture, and taste. The example of climacteric fruits are banana, papaya, mango, and mangosteen. In contrast, strawberry, kiwi, and pepper are listed as non-climacteric fruit, which is not affected on the concomitant burst of ethylene around the fruits ^{4,5,28}.

The rapid progression of ripening process in fruit will degrade the quality of fruits. While the increasing demand for the product of fresh fruits makes countless effort to prolong fruit shelf-life. Several postharvest technologies (low temperature, edible coating) have been extensively developed to reach the most-favorable condition either for quality improvement or shelf-life improvement²⁹⁻³⁴. Understanding the changes that occur during ripening is necessary in order to assess optimal harvest maturity and the quality of fruit as it is marketed to the consumer as well as to devise appropriate postharvest packaging and handling strategies.

1.2. *Garcinia mangostana* (mangosteen)

1.2.1. General Information of mangosteen

Garcinia mangostana or mangosteen, often known as the “Queen of Fruits”, is an important tropical fruit desired for its distinctive appearance and unique taste. Mangosteen is divided into 3 main parts such as peel, flesh/aril, and apomictic seed parts (Figure 2). Mangosteen has a distinct peel that cannot be consumed and must be separated from the pulp. The flesh part is usually consumed has a unique flavor and distinctive taste³⁵⁻³⁷.

Mangosteen peel is generally the smooth, globe-shaped berry with a persistent calyx with thick and purple (during maturation process) color³⁷. Mangosteen peel also contains several antioxidant and antimicrobial compounds that already established to be consumed as a health supplement. Mangosteen as the antimicrobial and antioxidant compounds in mangosteen pericarp was successfully isolated in 1987 for the first time³⁸⁻⁴².

The flesh/aril part usually has 4-8 segments including 1 or 2 segments that are contained apomictic seeds ^{43,44}. The milky white flesh part usually consumed fresh as a dessert. As processed food, mangosteen fruits were further applied as heavy syrup, jam, syrup puree and flavor for ice-cream or juice. The flesh is sweet, slightly acid, and mild to distinctly acid in flavor and is acclaimed as exquisitely luscious and delicious ³⁶.

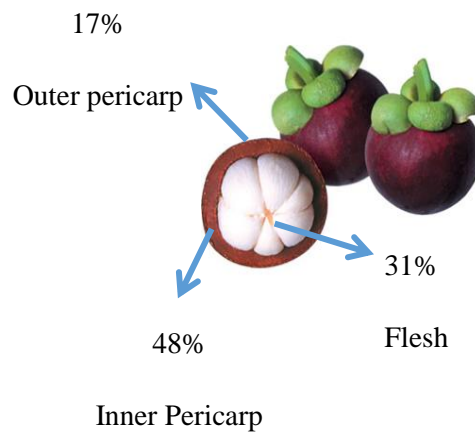


Figure 2. Mangosteen part

Several problems occur in mangosteen, including yellow gamboge disorder. The yellow gamboge, a disorder caused by the accumulation of yellow latex inside the fruit, is a major problem in mangosteen. This disorder occurs and generates the bitter taste of the fruit at the beginning of the ripening stage ^{44,45}. Consequently, this disorder has downgraded the fruit quality which affects its marketability and price both domestic and export market as well. The cause of this disorder remains unclear. However, previous studies suggest that the destruction of the epithelial cells that surround the yellow latex secretory ducts, and effect of excess water in nine weeks after bloom might cause this disorder ^{46,47}. Evaluation on reducing this disorder had been reported in the previous

research such as regulate the irrigation and application of calcium spray during on-tree ripening process ⁴⁸⁻⁵⁰.

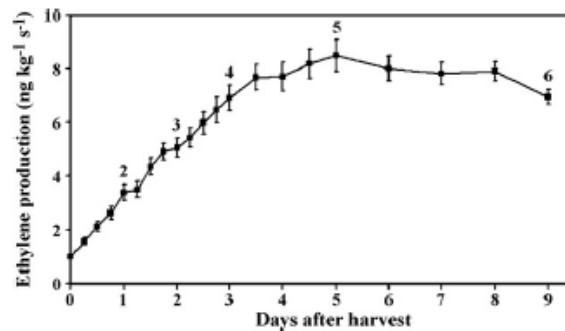


Figure 3. Ethylene production during mangosteen ripening stages (Palapol *et al*, 2009)

Mangosteen is one of climacteric fruit which changes its appearance due to the existences of ethylene around fruit. The mangosteen ripening process is affected by the ethylene existence around the fruit (Figure 3). Ethylene will change the mangosteen color from yellow-green to purple blackish color. Several researchers classified the mangosteen ripening stages by the color ^{27,51,52}. Consequently, previous study determined mangosteen ripening stages from measurement of several physical parameters such as the total soluble solids (TSS, %brix), titratable acidity (TA, pH), pericarp hardening, fresh weight (gram), fruit diameter (cm) ^{27,48,53}.



Figure 4. Mangosteen ripening stages. A photograph of typical mangosteen fruits during ripening stages as described by previous study (30) and CENTROHS, IPB.

Mangosteen ripening stages are generally determined by the color changes from yellow-green color to purple-blackish color (figure 4) ^{27,51}. Stage 2 of mangosteen ripening stages is described as 51 to 100% scattered pink spot. Stage 2 of mangosteen ripening stages is selected to be a standard qualification for export procedure to reach the final stage (stage five or six) for consumption when it arrived to export destination country which stated by CODEX, SNI (SNI 01-3211-1992), Thai Agricultural Standard (TAS 2-2013) and ASEAN Standard for mangosteen (ASEAN Stan 10, 2008). Stage 2 of mangosteen ripening stages is also selected as an appropriate stage to be exported because the ethylene production increases after stage 2 (Figure 4).

Color development during mangosteen ripening stages based on visual observation had been reported in the previous studies ^{27,51,54}. The detailed description of color changes during mangosteen ripening stages was explained as follows,

Table 1. Mangosteen ripening stages physical description

Stage	Description
0 (zero)	Yellowish white or yellowish white with light green. The yellow latex is contained and not ready for harvesting process
1	Light greenish yellow with 5-50% scattered pink spots. The flesh part cannot be separated and the yellow latex still remains inside of the fruit.
2	Light greenish yellow with 51-100% scattered pink spots. Yellow latex accumulation already reduced a little bit but the flesh part still cannot be separated. This stages, fruits ready to be exported to destination country.
3	Spots are not as distinct as in stage 2 or reddish pink. The flesh part can be separated from the pericarp part. The yellow gamboge still remains in pericarp part the fruit but as not much as previous stages. Fruits are ready to be exported to destination country.
4	Red to reddish purple. Pericarp still contains yellow latex. Fruits are ready to be exported to destination country.

5	Dark purple. Fruits start to ripen and ready to be consumed. The yellow latex is disappeared and the flesh /aril part is easy to be separated from the pericarp. Fruits ready to be consumed for domestic market
6	Purple-black. Fruit already ripens. Fruits are ready for domestic market and ready to be consumed.

Mangosteen also recognized as an important export commodity for Southeast Asian countries. In particular, mangosteen is the top commodity for export in Indonesia (table 2). In Indonesia, mangosteen is exported to several destination countries such as China, Hongkong, Saudi Arabia, Malaysia, Middle-east countries, Netherland, France, and Singapore ⁵⁵⁻⁵⁹. To achieve consumer needs, Indonesian government has prioritize mangosteen improvement to be an excellent export commodity.

Table 2. Export production of annual important fruits Indonesia (net weight in million Kg)

Commodity	Year				
	2013	2014	2015	2016	2017
Mangosteen	7.65	10.08	38.18	34.96	8.52
Banana	0.10	26.10	19.78	19.02	14.52
Mango	1.09	1.15	1.24	0.47	0.72
Pineapple	0.11	0.07	0.87	1.90	0.20

Mangosteen tree is claimed to be originated from South-east Asia. Several references reported that mangosteen is a native fruit to peninsular Malaya and Indonesia. *G. mangostana* is usually cultivated around South – East Asian region. It was believed that South East Asian is the origin country of *G. mangostana*. Several *Garcinia* genus were cultivated nearby South East Asian region containing Indonesia, Malaysia, Thailand, and Philippines ^{60,61}.

The distribution of mangosteen tree is limited in South-East Asian regions. Several difficulties had been reported and aided by using several alternatives such as micro-propagation and adventitious shoot formation to increase water intake of mangosteen tree ⁶²⁻⁶⁶. Mangosteen tree is very sensitive to inappropriate environment conditions especially drought condition ³⁵. Therefore, South East Asian region meet the optimized growth condition for mangosteen. Mangosteen requires high humidity and optimum temperature (around 25 to 35°C) ⁴³.

The mangosteen trees usually need 8 – 15 years to begin flowering due to the rootstock deficiency. This condition makes the photosynthesis rate mangosteen tree is lower. Mangosteen rootstock problem needs to be solved to improve mangosteen production. Grafting method was used to increase the number of roots in mangosteen. Mangosteen juvenile trees should be planted in the condition of the shade to boost the mangosteen growth rate ⁶⁷.

Additionally, the yield of a mangosteen tree also depends on environmental factors, especially climatic variability. A large crop of mangosteen will be produced with a suitable weather condition. Furthermore, the harvest season of mangosteen in Indonesia is short at about 1.5 – 2 months, only from January to February.

Mangosteen cultivation in Indonesia has several cultivars including mangosteen Raya cultivar. Mangosteen Raya / Manggis Raya is one of superior quality mangosteens that was selected by Indonesian Ministry of Agriculture (no: 2046/Kpts/SR.120/5/2010). Mangosteen (Raya cultivar) fruit was described as spherical fruit, with 4.5 – 5 cm diameter. The peel part of Raya mangosteen has purple blackish color at the end of ripening process. The flesh part (31.8% - 36.4% from the total portion of the fruit) is

edible for consumption. The flesh part contains 18.65% Brix of sugar. Mangosteen (Raya cultivar) is suggested as mangosteen with superior quality by Center of Tropical Horticultural Studies, Bogor Agricultural University, Indonesia in 2010.

1.3. Color measurements

Color is the characteristic of human visual perception described through color categories with names red, orange, yellow, green, blue or purple. Human eyes perceive stimulation of eye cone cells by electromagnetic radiation in the visible spectrum. The ability of the human eye to distinguish color differences are based upon the varying sensitivity of different cells in the retina to light of different wavelengths⁶⁸. Despite this reason, color perception is becoming a very subjective parameter to be applied as a standard for scientist⁶⁹⁻⁷¹.

Color science was introduced from a famous experiment conducted in 1666 by Isaac Newton. In his research, he performed visualization of the visible spectrum (rainbow color) after it was separated by a prism from white light⁷². Since this founding, the importance of color information is increased together with the increasing requirement in a scientific context. In 1931, Commission International d'Eclairage (CIE) or commonly known as International Commission of Illumination set a standard for a colorimetric observer with the angular substance from 1 to 4 as a representative color-matching properties. Recently, several color parameter standard had been established by CIE to uniformed color determination into value.

The first color specification was introduced by CIE, namely CIE1931. It defines the three essential components for perceiving a color: light source, object, and observer. Any

color thus can be measured and described by a set of tristimulus values, explained in XYZ, which indicate the amount of red, green, and blue lights (known as RGB values), respectively. The method allows the exchange of color information by numbers ^{73,74}.

In 1976, CIE recommended two standard color difference formulae: CIELAB and CIELUV for the colorant and lighting industries, respectively. Although several changes occurred over the years, the principle has remained unchanged. In the last decade, CIELAB space is mostly used for presenting colors.

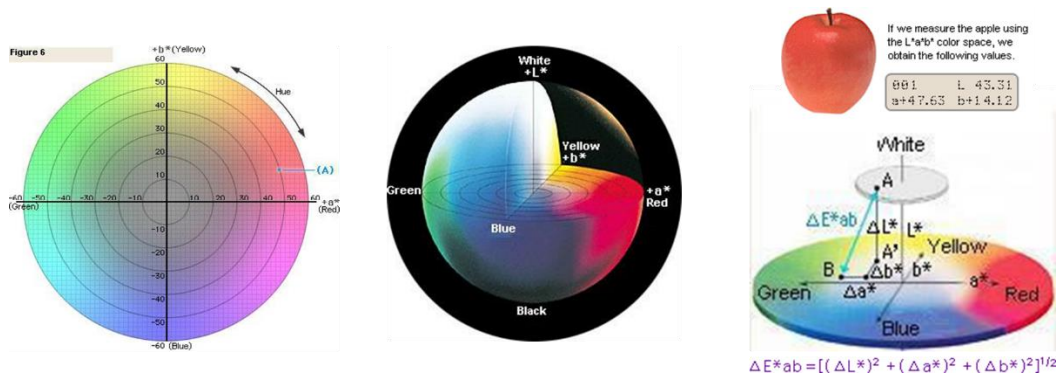


Figure 5. CIELAB color wheel.

As the most utilized color standard, CIELAB describes color circle based on three attributes as explained in lightness (L), and chromaticity coordinates (a and b value). Lightness dimensional can be explained from the white spectrum until the black spectrum. The range value of lightness was described from 0 (zero) as black spectrum and 100 (hundred) as a white spectrum. In figure 5, the a and b value indicate color direction: +a* indicates red direction and -a* indicates a green direction, +b* indicates yellow direction and -b* indicates blue direction. The value of a* and b* value points will move from the center of the color wheel (Figure 5) or achromatic, indicate the saturation of the color increases.

Furthermore, color difference can be expressed in a single numerical value in CIELAB color space. dE or $dLAB$ value indicates the size of the color difference between target and specimen (Figure 5). dE or $dLAB$ value is defined by the following equation:

$$dE^*_{ab} = \sqrt{(dL^*)^2 + (da^*)^2 + (db^*)^2}$$

The equation above explained dL^* , da^* and db^* value as a difference value between the specimen color and the target color were used in the object. By using the equation mentioned above, the color can be quantified and be used as a reference to characterize the color based on the number. Several applications had been applied in the agricultural product using CIELAB method. In the last decade, CIELAB method was used to classified the maturity index of peach, starfruit, mango, persimmon, apple, mango, banana, date palm fruit, peach, chili, paprika, and pepper⁷⁵⁻⁸⁶.

1.4. Metabolomics

1.4.1. General concept

In the last decade, metabolomics is the latest omics technology developed after genomics, transcriptomics, and proteomics (Figure 6). Metabolomics is also referred to as an interdisciplinary analysis that combines biology, analytical chemistry, and bioinformatics studies. Metabolomics is one of the omics applications that define the total metabolome profile of a biological system. Metabolomics is a field of study that encompasses the comprehensive, quantitative profiling of metabolites, which are subsequently analyzed using multivariate pattern recognition and statistical analysis⁸⁷⁻⁹⁰. As a consequence, metabolomics is now used widely in many applications including

microbiology, diagnostic biomarker discovery, toxicological testing, food and beverage analysis, plant and animal phenotyping, and drug discovery and development ^{91,92}.

Based on metabolites detection, metabolomics studies can be divided into two different approaches, including non-targeted and targeted metabolomics. Non-targeted approach is where the obtained data may be only semi-quantitative. The aim of this approach is to simultaneously measure as many metabolites as possible (including analyzing the identification of unknown metabolites signals) without having prior knowledge of the nature and the identity of assessed metabolites. This approach enables novel areas of metabolism to be identified and is therefore often hypothesis generating ^{90,92}.

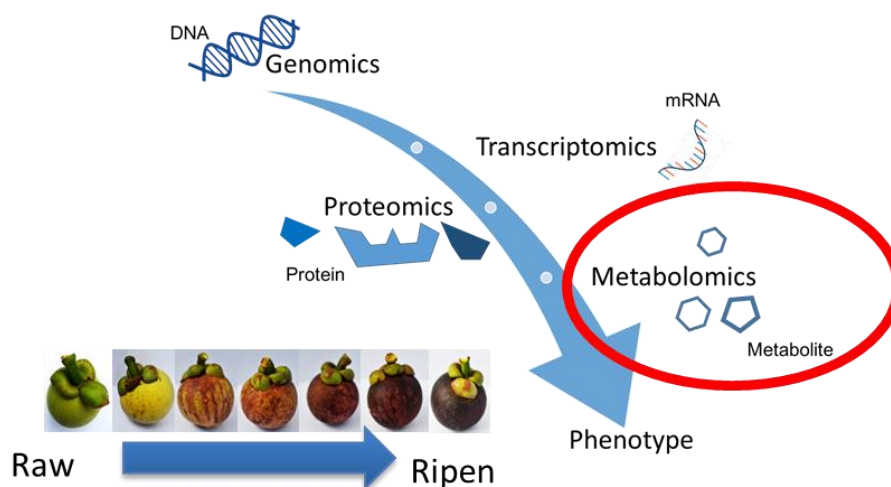


Figure 6. Recent omics technology

In contrast to non-targeted metabolomics, targeted metabolomics is driven by the specific hypothesis that motivates the investigation of particular biochemical pathways. A targeted approach, where the obtained data is aiming at quantitative data by using more

internal standards and reference compounds, ultimately resulting in absolute concentrations. In this strategy, predefined metabolite-specific signals are used to quantify, precisely, and accurately, concentrations of a limited number of metabolites.

These strategies have been used either separately or together for the following approaches:

- Metabolite profiling is the measurement of the levels of a metabolite set in the sample that useful to establish the complete composition in terms of metabolites. This approach usually is used as a high-throughput measurement of the levels of a large number of metabolites, including unknown metabolite. ^{88,93}
- Metabolite fingerprinting explains the total profile of metabolites, or so-called fingerprint, as a unique pattern characterizing a snapshot of the metabolism in the samples. Metabolite fingerprinting approach is particularly useful in combination with pattern recognition and discriminant analysis techniques ⁹⁴.

1.4.2. Metabolomics Workflow

Metabolomics workflow consists of sample preparation, separation and detection, and data transformation and data mining (Figure 7).

- Sample preparation

Sample preparation has a direct influence on the resulting metabolomics experiments and is, therefore, an especially critical step. Sample preparation includes samples collection and extraction process that are followed by analysis. Changes in the plant's metabolism occur from seconds up to few minutes, proper and fast sample collection is needed to catch the specific metabolite profile in one phenomenon. One of

the methods is the freezing of plant material in liquid nitrogen. Additionally, homogenization needs to be performed to homogenize all of the samples will be analyzed and can explain all of the samples by using a metabolomics approach. The homogenization process also can minimize experimental variation and improve reproducibility^{95,96}.

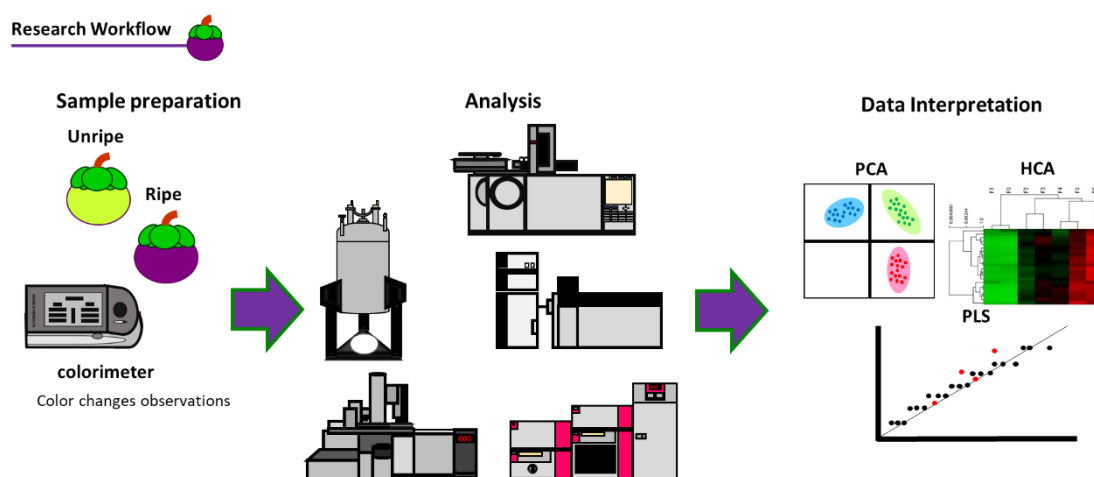


Figure 7. Common metabolomics research workflow

Extraction process is the following step after sample collection. Extraction method should be simple and as fast as possible. As one of the crucial steps for metabolomics experiment, extraction method should be considered properly based on the aim of research including the selection of solvent. A mixture of organic solvents with water is common because they reduce the extraction of non-polar compounds. Chloroform/methanol/water (2:1:1v/v) is a common mixture for the extraction of non-polar and polar compounds. The selection of extraction solvent also depends on the analytical platform will be used for the experiment⁹⁵⁻⁹⁸.

- Analysis

Analysis of metabolomics platform usually is divided into two processes such as separation and detection process. The separation and detection process usually use different types of analytical instruments either as a stand-alone instrument or in combination depending on the purpose of research. The analytical instruments commonly used in metabolomics research include gas chromatography (GC), liquid chromatography (LC), Inductively Coupled Plasma (ICP) for the separation process and paired using mass spectrometer (MS), flame induction detector (FID) as a detector. Data transformation and data mining (data acquisition) is the final step in the workflow of the metabolomics analysis ^{88,89,93,99,100}.

The separation principle in metabolomics is metabolite separation based on the interaction of stationary phase that is used during analysis. The stationary phases will interact with compounds and separate based on the elution time of compounds. For metabolomics research, a highly sensitive detector is desired to detect the separation of the metabolites. Mass spectrometry is one type of detectors which ionize and detect the compounds as an ion intensity. The ionized compounds will be detected based on m/z value ^{88,96,101}.

- Data interpretation

Subsequently, data mining is performed for interpreting the data of metabolomics as the end of the workflow. Finally, metabolomics results in big data (multivariate data). Various data mining is used during metabolomics processing data such as Principal Component Analysis (PCA), Partial Least Squares (PLS), and Hierarchical Cluster Analysis (HCA) to treat multivariate and megavariate data. The utilization of particular multivariate analysis depends on the aim of the research ^{91,102}.

1.4.3. Application to agricultural and food science

Over the past decade, the application of non-targeted high-throughput metabolomics analysis has gained ever-increasing interest and has truly established itself as a valuable tool for the study of biochemical composition⁹⁹. Metabolomics has been successfully employed to analyze various kind of samples such as food, animal, and plant using several metabolomics platforms for separation and detection such as GC/MS and LC/MS.

Metabolites profiling analysis was successfully conducted for determining the differences between *Angelicae radix* that originated from several places using GC-MS for separation and detection process and OPLS-DA (Orthogonal Projections to Latent Structure-Discriminant analysis). Mass spectrometry-based metabolomics analysis was useful to classify the geographical origin of *Angelicae radix* and establish the bio-markers responsible for this classification. Subsequently, upon identification of the biomarkers, another instrument such as GC-FID (Gas Chromatograph-Flame Ion Detection) may be employed to perform routine classification based on the known discriminant marker¹⁰³.

Metabolomics study is also applied to kopi luwak biomarker authentication. The authentication of kopi luwak (Arabica coffee that was digested by the Asian palm civet, one of the highest price of coffees in the world) is needed to verify the coffee from the adulteration. Metabolomics was used to find the biomarker that allows discrimination between Kopi luwak and adulterated coffee. The kopi luwak authentication study was

conducted using GC/MS as a separation and detection platform and analyzed using OPLS-DA as data mining platform ^{104,105}.

Metabolomics analysis of climacteric fruit and non-climacteric fruit were performed in tomato (*Solanum lycopersicum*), pepper (*Capsicum chilense*), Peach (*Prunus persica*), and strawberry (*Fragaria x ananassa*). Both ethylene-dependent and independent fruits revealed different patterns when it was analyzed using GC-MS. Non-climacteric fruits undergo less dramatic changes across the ripening process compared to climacteric fruits. Several metabolites abundance occurred during the ripening process of climacteric fruits are including sugar compounds, alcohol compounds, organic acids, and amino acids changes ^{4,5,28,106,107}. In recent years, metabolomics approach is widely used as an important tool to support postharvest fruit development and ripening studies including melon, strawberry, apples, grape, sapodilla, litchi, and peach ^{108–117}.

1.4.4. Recent research and objectives in this study

Despite economically important tropical fruit desired for its distinctive appearance and unique taste, there is a lack of scientific information on mangosteen, also well known as an exotic fruit. The reported studies mainly focused on color changes during mangosteen ripening has been conducted, but the study only focused on the identification of specific pigmentation metabolite. However, it is still not clear how these metabolic changes contribute to the qualities of fruit that are related to sensory attributes (sweet-acid taste, aroma, color changes, firmness).

In this study, metabolomics technology is applied as an important tool to support postharvest fruit development and ripening studies. Monitoring the changes in the metabolome during fruit ripening is important to obtain insight into the mechanisms involved and improve postharvest management strategies. To thoroughly identify and investigate metabolic changes and to select ripening-associated metabolites, two types of metabolomics strategies, informative, and predictive are applied, represented by the utilization of multivariate analyses such as Principal Component Analysis (PCA), Hierarchical Cluster Analysis (HCA), and Partial Least Square (PLS) analysis.

1.5. Research Objectives

The availability of genome sequence and genetic tools in fruits have made the technology for developing postharvest studies. Existing studies on mangosteen have been focused on transcriptome-level changes or targeting only a few metabolites in peel part. Therefore, this study aimed to gain insight into the metabolic changes that affect mangosteen quality during the ripening process and after postharvest treatment by using metabolomics approaches.

- First, non-targeted GC/MS-based metabolic profiling methods were applied to obtain a general view on the metabolic changes during ripening process throughout mangosteen color changes.
- The effects of different cultivation area, different tree, year of harvesting, and ripening condition were examined to confirm the metabolic changes during the mangosteen ripening process.

- Finally, these approaches were applied to evaluate the effect of different postharvest treatment in mangosteen.

1.6. Thesis outline

This thesis includes five chapters that provide the importance of metabolic changes to the quality of *Garcinia mangostana* (mangosteen). The developed methods focused on the metabolic changes, whose information throughout the mangosteen ripening process was explored and further proven to be effective to study the quality of mangosteen after postharvest process. Chapter 1 provides a general introduction concerning mangosteen as an important export commodity in Indonesia and how metabolomics can be an effective tool for mangosteen researches. In chapter 2, GC/MS-based metabolic profiling method was employed to gain insight into the metabolic changes based on mangosteen ripening stages. In chapter 3, in order to investigate the similarities of metabolic changes in different condition of preharvest (year, different cultivation area, different tree) and different preharvest mangosteen ripening stages were examined. In these experiments, all samples were evaluated based on their color changes and metabolic changes during ripening process. In chapter 4, several postharvest treatments were applied and evaluated using metabolomics approach. Finally, in chapter 5, the conclusions revealed from this study were summarized and the future perspectives were proposed.

Chapter 2

Metabolomics-based approach for the study of *Garcinia mangostana* (mangosteen) ripening stages

2.1. Introduction

Fruit ripening process is one of the factors that should be focused during postharvest handling. Fruit ripening process occurs in every fruit including mango, banana, guava, and papaya. Fruit ripening process affected by ethylene activities. The changes of fruit ripening process including color changes, aroma changes, sugar accumulation, and fruit softening ¹¹⁸.

Fruit ripening increases fruit palatability through changes in metabolite composition across ripening stages. Ripening in climacteric fruits (e.g., banana, papaya, mango, and mangosteen) depends on ethylene bursts that trigger metabolite production or breakdown to influence fruit color, taste, and firmness ^{30,119–121}. Ethylene production in several climacteric fruits commences in the early ripening stages, which is characterized by an immediate increase followed by a rapid decrease in ethylene levels ^{121–124}. Because excessive ethylene production during ripening process can drastically drop fruit quality, understanding the chemical mechanisms during ethylene production of fruit ripening stages is important for quality control and postharvest treatment of commercial fruits. Fruit quality is greatly affected by both pre-harvest (e.g. genetic origin, cultivation area, physicochemical properties of growing environment) and post-harvest processes (e.g. storage method, logistic condition, etc). The complex,

synergistic, non-linear interactions between many components define the sensory characteristics of food products. Therefore, the elucidation and scientific manipulation of these characteristics by targeting a single or just a few components become a very complex task^{88,98}.

Mangosteen has black-purple peel color when they reach their mature stage. The peel color formation is due to anthocyanins which are important antioxidants. Peel color is the major criterion used to judge maturity index of mangosteen^{27,51,52,54,125}. The earliest stage was selected to be harvested before it exported to several export-destination countries. The earliest stages were treated with several conditions were applied to prolong the shelf-life, avoid mangosteen pathology during shipping, and several potentials that make the quality of mangosteen were degraded^{43,44,54,66,125-129}. These qualities have resulted in considerable efforts to control mangosteen fruit ripening so as to achieve optimal fruit maturity for harvesting, as well as to devise appropriate postharvest packaging and handling strategies. However, the complex, synergistic, non-linear interactions between many components define the sensory characteristics of food products. Therefore, the elucidation and scientific manipulation of these characteristics by targeting a single or just a few components become a very complex task. Existing studies on mangosteen fruit ripening have been focused on transcriptome-level changes or targeting only a few metabolites in the pericarp. Previous study reported that there are several metabolites are dynamically changed during ripening stages in every part of mangosteen using color changes as its physical parameter²⁷.

Existing studies on mangosteen fruit ripening have been focused on

transcriptome-level changes or targeting only a few metabolites in the pericarp^{27,125,130–133}. In recent years, non-targeted metabolomics is a powerful approach to monitor global metabolite changes that occur during fruit development and ripening. Through the use of metabolic profiling approach, metabolic changes during ripening stages can be determined to aid in the development of postharvest packaging technologies and handling strategies.

In this chapter, gas chromatography-mass spectrometry (GC-MS)-based metabolite profiling was performed in peel, flesh and seed parts of mangosteen to gain insight on metabolic changes during mangosteen ripening stages. In addition, multivariate analysis was performed to correlate specific metabolites with color changes that occur during the ripening process.

2.2. Experimental section

2.2.1. Plant materials

Mangosteen samples were used are Raya cultivar as one of the superior commercialized cultivars in Indonesia. Mangosteen fruit was freshly harvested in February 2018 in Center of Tropical Horticultural Studies, Bogor Agricultural University, Bogor, Indonesia. Mangosteen plants were grown in an open field (6°38'S x 106°49'E) as a part of experiment field located in Southeast Asian Regional Center for Tropical Biology (SEAMEO BIOTROP), Bogor, Indonesia. For all samples, cultivation, irrigation, watering, fertilization and pathogen-pest control were performed according to the respective local commercial practices.

Mangosteen fruit from Indonesia corresponding to 7 different ripening stages (stages 0 to 6) were used in this study. Five samples (replicates) from 3 different trees were collected for each stage from the period of January – March 2016 in Center of Tropical Horticulture Studies, Bogor Agricultural University (CENTROHS, IPB), Bogor, Indonesia. Color changes in fruit peels were measured using Konica Minolta CM-2500d before homogenization and extraction of mangosteen.

2.2.2. Color changes measurement

Measurement of color changes was calculated using the previously established CIELAB method with illuminant D65, observer angle 10° ^{86,133}. The measured data was proceed using Spectramagic NX software (Konica Minolta, Tokyo, Japan). dLAB color space value (CIELAB method) was used as color solid representatives value to represent mangosteen color changes in ripening process. L^* indicates the lightness of the samples that were measured. a^* and b^* values are chromaticity diagram that describes red-green color for a^* values and yellow-blue color for b^* values.

2.2.3. Samples extraction

Three different parts of mangosteen, namely flesh, peel, and seed were separated and homogenized. Homogenized mangosteen samples were mixed with methanol (Wako Pure Chemical Industries, Osaka, Japan), chloroform (Kishida Chemical Co.Ltd, Osaka, Japan), ultrapure water (Wako Pure Chemical Industries, Osaka, Japan); 2.5/1/1 (v/v/v) together with an internal standard (Ribitol 100 $\mu\text{g/ml}$). Samples were sonicated for 1 minute and incubated at 37°C , 1200 rpm for 30 min. Incubated samples were centrifuged for 3 min at 4°C , 16000 rcf. Four hundred microliters (μL) of supernatant was transferred

to a new 1.5 mL microtube and added with 200 μ L of water. The mixture was centrifuged for 3 min at 4°C, 16000 ref. Four hundred microliters (μ L) of the polar phase was transferred to a new tube and vacuum evaporated for 2 hours at room temperature before lyophilization overnight.

2.2.4. Derivatization

One hundred microliters of methoxyamine hydrochloride (20 mg/ml in pyridine) were added and incubated for 90 min, 1200 rpm, 30°C into lyophilized samples. Subsequently, 50 μ l *N*-methyl-*N*-trimethylsilyl-trifluoroacetamide (MSTFA) (GL Sciences) were added and incubated for 30 min, 1200 rpm, 37°C to incubated samples before analyzed using GC-MS.

2.2.5. Gas chromatography-mass spectrometry analysis

Intracellular metabolites were measured by Shimadzu Ultra QP-2010 gas chromatography-mass spectrometry (GC-MS) with an InertCap 5 MS/NP (30 m, 0.25 mm i.d., 0.25 μ m film thickness, GL Sciences, Japan). Tuning and calibration of the mass spectrometer were done prior to analysis. The derivatized samples were injected to GC-MS. GC and MS conditions were performed by following the procedure as described in Supplementary Table S1.

2.2.6. Data analysis

The raw chromatographic data were converted into ANDI files (Analytical Data Interchange Protocol, *.cdf) using the GC-MS solution software package (Shimadzu, Kyoto, Japan) for GC-MS analysis. Peak detection, baseline correction, and peak

alignment of retention times were performed on the ANDI files using MetAlign (Wageningen; can be downloaded freely at <http://www.wageningenur.nl/>). All of the detailed metAlign parameter information had been explained in Supplementary Table S2. All of the converted data was aligned together with QC (Quality Control) samples as a reference. The peak intensity of each metabolite was normalized based on the ribitol internal standard.

The detected peaks were tentatively identified by comparing the retention indices and unique mass spectra with our in-house library database, AIOutput2 (version 1.30) annotation software^{134,135}. All of the detailed AIOutput parameter information had been explained in Supplementary Table S3. Retention indices of all detected metabolites were calculated based on standard alkane mixture (C10-C40). Additionally, the retention time of each tentatively identified metabolites was compared with the National Institute of Standards and Technology (NIST) library. All of the metabolites were tentatively identified refers to Metabolites Standard Initiatives (MSI) level 2 identification procedures¹³⁶.

2.3. Results and discussions

2.3.1. Assessment of mangosteen ripening stages

The seven mangosteen fruit ripening stages were classified following previous studies²⁷ and were based on color changes from yellow-green (unripe) to purple-black (fully ripe) (Figure 8). These changes occur due to ethylene production, which begins from stage 1 (9 weeks post-blooming) and reaches maximum levels at stage 5 (12 weeks post-blooming), before decreasing slightly^{27,52}. Ethylene signaling networks increase

plant pigments such as anthocyanin, which is associated with red, purple, and blue fruit colors. Therefore, we expected that anthocyanin levels would also vary with ripening of mangosteen.



Figure 8. Mangosteen ripening stages. A photograph of typical mangosteen fruits during ripening stages as described by previous study (30) and CENTROHS, IPB.

Mangosteen samples were collected from mature fruit that had reached maximum weight and volume but was at different ripening stages. A color-change index was used for sample classification: stage 0 and 1 are yellow-green, contain yellow gamboge, and have flesh inseparable from the rest of the peels. Stage 2-4 exhibit a gradual color change to purple-black, decreasing yellow gamboge, and eventual separation of the flesh from the other peels portions. Finally, stages 5 and 6 are fully purple-black, considered ready for consumption and distributed to domestic markets.

Mangosteen color changes (including depth, vividness, and hue variation) per stages were measured with a colorimeter, then calculated using the non-destructive CIELAB method, which generates a dLAB value useful as a quantitative phenotype for describing fruit ripening stages^{86,133,137}. CIELAB has been applied to other fruits (e.g, strawberry, mango, and apple) to ascertain ripeness, typically after an edible coating treatment to prolong the shelf-life of the fruits^{79,138,139}. We observed increasing dLAB as fruit color shifted from green to purple-black (Table 3 and Supplementary Table S4). We

also noted a significant decrease in hue as the fruit ripened, corroborating previous studies ²⁷.

Table 3. Postharvest physiological quality indices of mangosteen fruit during ripening process. Stage zero was used as a reference samples for color measurement

Ripening stages	Lightness (dL)	Vivid color (da)	Hue color (db)	dlab value
I	3.59a	3.16a	2.59a	10.76a
II	-14.25b	15.49b	-15.69b	26.56b
III	-26.79bc	17.25b	-25.19c	41.37c
IV	-27.67c	17.71b	-28.66c	43.80c
V	-32.58c	12.82b	-30.34c	46.42c
VI	-35.29c	7.38ab	-32.59d	48.78c

2.3.2. Elucidation of metabolic changes during mangosteen ripening stages

Metabolic changes during mangosteen ripening stages were assessed with GC/MS for the first time. Three fruits per ripening stage were used and the analysis was performed separately for each part of mangosteen. A total of 70 metabolites from flesh, 62 metabolites from peels, and 69 metabolites from seeds were tentatively identified using the National Institute of Standards and Technology and our laboratory in-house library (Supplementary Table S5).

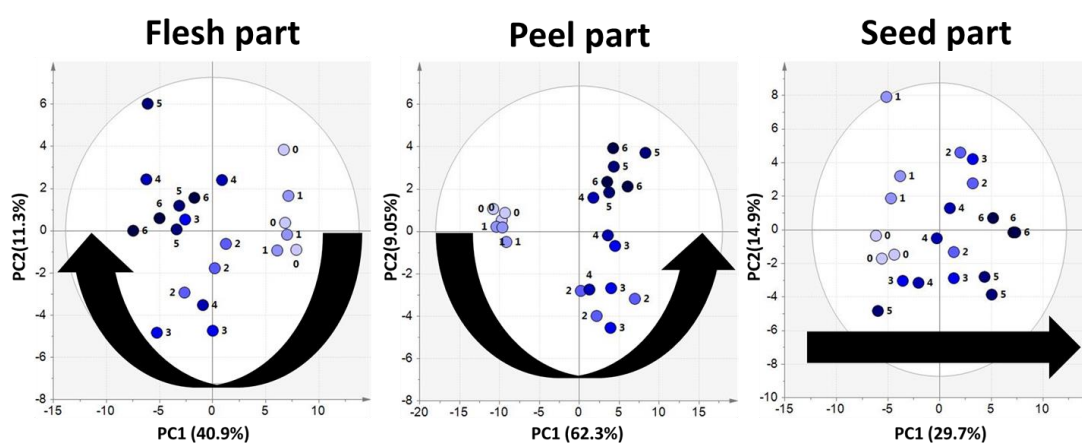


Figure 9. Metabolites abundances during mangosteen ripening process in flesh part, peel part, and seed part. The number showed in PCA showed the ripening stages. PCA showed the separation

between each stages during mangosteen ripening process in each mangosteen parts. Scaling method: UVscale, transformation: none, $n = 3$.

Principal component analysis (PCA) of the GC-MS derived dataset revealed two principal components explaining 71.35%, 52.2% and 44.6% of metabolite variation in flesh, peels, and seeds, respectively (Figure 9). The results clustered mangosteen ripening stages into three phases (early, middle, and late) based on metabolite distributions. Metabolite quantification was normalized with ribitol as the internal standard, which allowed us to determine relative metabolite intensity in each ripening stage and correct for potential errors during sample preparation or analysis.

Hierarchical cluster analysis (HCA) was performed to further clarify metabolite distribution during mangosteen ripening, hierarchically clustering each stage based on metabolite abundance per fruit part. Pearson's coefficients were calculated to look for significant correlations between metabolites and ripening stage. The resultant heat-map revealed that metabolite intensities significantly increased from stage 2 in the peel and flesh part (Figure 10a,b). Seeds differed from the other mangosteen parts in exhibiting a larger metabolite-abundance gap between stage 4 and other stages (Figure 10c). Despite this result, HCA classified stage 4 as part of early ripening stages. It is presently unknown why the metabolite intensities in stage 4 of seed part show more similarities with metabolites in early ripening stage. It is possible that the metabolite dynamics during ripening stage in the seed part do not follow the same trend as other parts of mangosteen.

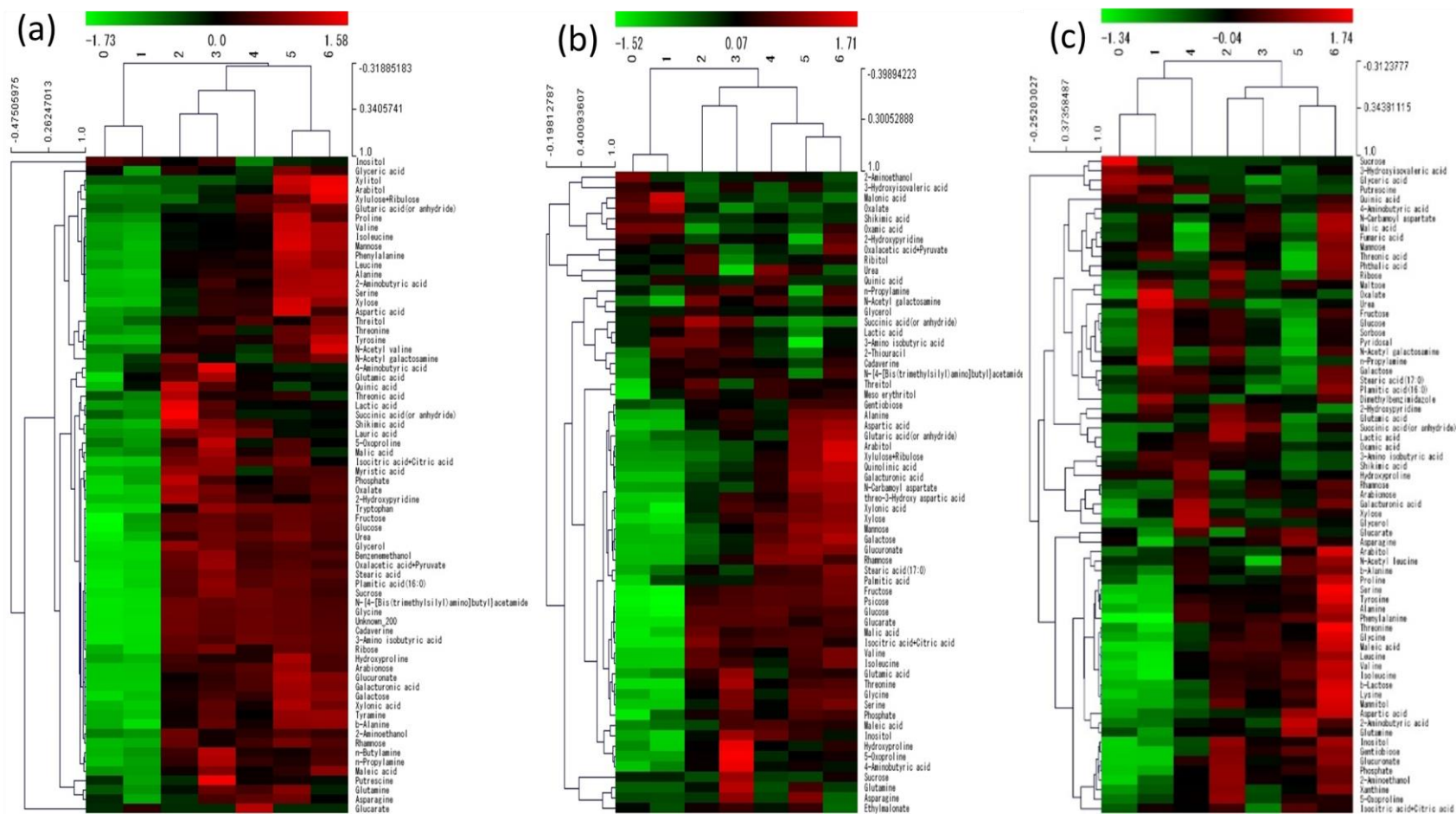


Figure 10. Distribution of metabolites analyzed using GC-MS during mangosteen ripening stages in the (a) flesh part, (b) peel part, (c) seeds part. HCA clearly clustered early (stage 0-1), mid (stage 2-4), and late (5-6) stage ripening stages based on metabolites abundance during mangosteen ripening process. The significant metabolites changes during mangosteen ripening stages also shown in the HCA. The color scale is plotted at the top of the figures.

2.3.3. Color changes based exploratory analysis of mangosteen ripening stages

A partial least square (PLS) analysis was used to regress PCA variables (metabolite intensity) on color change values, allowing us to verify whether color predicted metabolite-based ripening stages. This is the first report of the use of PLS analysis to correlate metabolite intensity and color changes as a physical parameter for predicting ripening process of mangosteen.

PLS analysis was conducted using data from color changes as the response variable (y-variable) and metabolite peak intensity values as the predictor variables (x-variables)¹⁴⁰. Representative samples of three major ripening stages (stage 0, 2, 4, and 6) were selected as a training set, and the remaining stages were used as a data set to validate the prediction model (Figure 11). The constructed model has linear coefficient (R^2) and prediction ability (Q^2) greater than 0.5, both thresholds for a valid model with good fit.

The results of the PLS indicated that different metabolites were giving a large contributors to color change depending on mangosteen part. Contributing metabolites were selected based on the five highest Variable Importance in the Projection (VIP) scores (Table 4). Primary metabolites were: fructose, psicose, glucose, galacturonic acid in the peel; xylose, glucuronate, 2-aminoisobutyric acid, tryptophan, and xylulose in the flesh; and phenylalanine, valine, tyrosine, isoleucine, and serine in the seed.

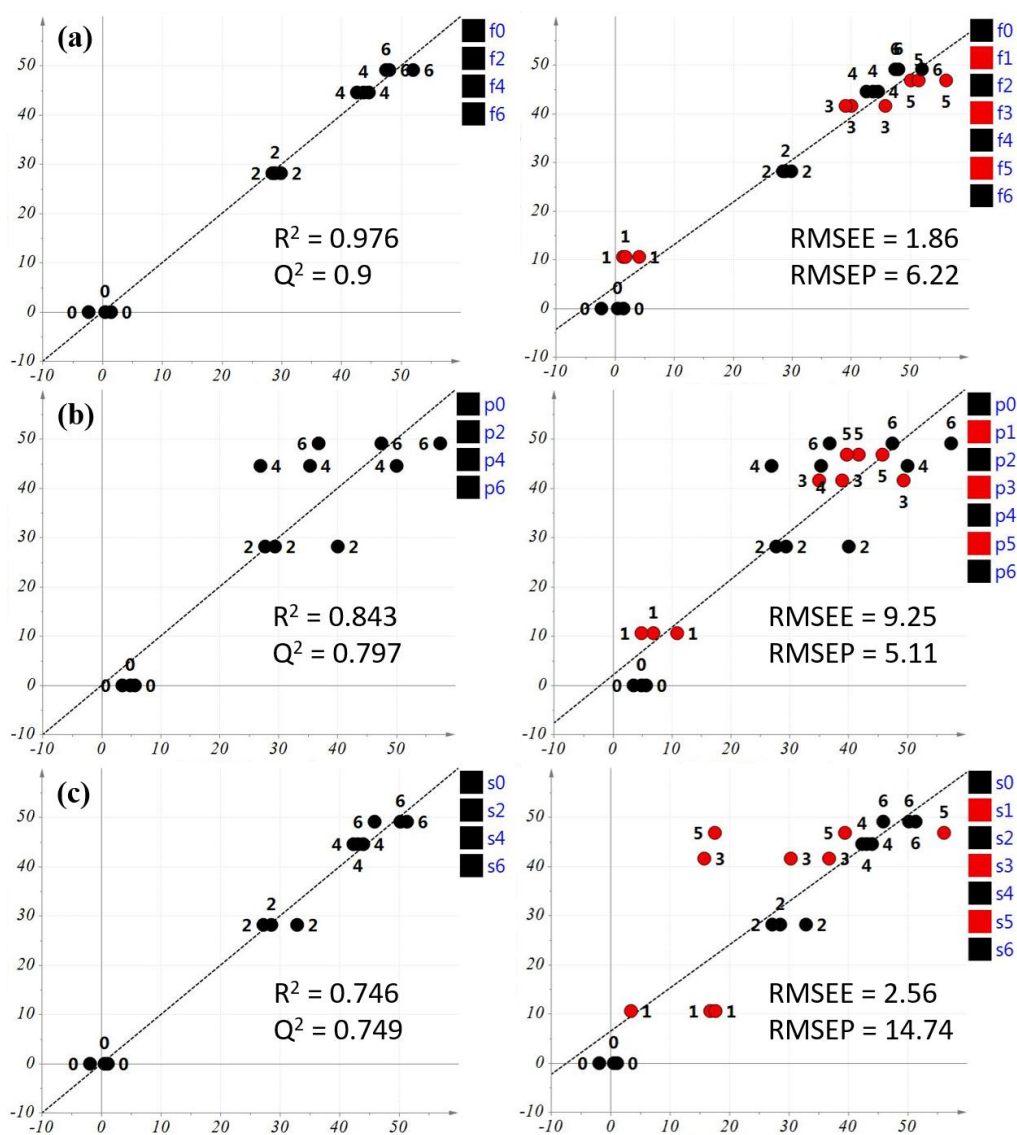


Figure 11. Prediction model of mangosteen ripening stages using Projection to Latent Squares (PLS) analysis (f represents flesh part, p represents peels part, and s represent seeds part; numbers in each mangosteen part represent the ripening stages). The observed parameter that was used is color changes of the ripening stages classified by previous studies²⁷. Scaling method: UV scale, transformation: none. (a). The prediction model of flesh part during mangosteen ripening stages; (b) the prediction model of peel part during mangosteen ripening stages; (c) the prediction model of seed during mangosteen ripening stages. All prediction models of mangosteen parts (flesh, peel, seed) were built using stage 0,2,4, and 6 as a training set and stage 1,3, and 5 were used as a test set. The prediction model was validated by using root mean square error estimation (RMSEE) and root mean square error prediction (RMSEP) value to evaluate accuracy, prediction and model robustness

2.3.4. Important metabolites change in mangosteen during ripening are related to color changes

The relative intensity (normalized with ribitol) of major metabolites elevated during mangosteen ripening were compared using a boxplot to examine metabolite fluctuation. Top metabolites (based on VIP scores, Table 4) from individual mangosteen parts were analyzed separately. Xylose, xylulose + ribulose, glucuronate, 2-aminoisobutyric acid, and tryptophan were compared in the flesh. Psicose, fructose, xylose, galacturonic acid, and glucose were compared in the peel. Phenylalanine, valine, isoleucine, serine, and tyrosine were compared in the seed. The boxplot (Figure 12) showed that the relative intensities of top metabolites were correlated with ripening stages, increasing as ripening progressed.

Table 4. VIP Score and coefficient of fifth highest metabolites for each mangosteen part

Mangosteen part	Metabolites	VIP score	Coefficient
Peel	Psicose	1.549	0.0328
	Fructose	1.534	0.0325
	Xylose	1.484	0.0314
	Galacturonic acid	1.429	0.0303
	Glucose	1.408	0.0298
Flesh	Xylose	1.356	0.0502
	Xylulose+Ribulose	1.346	0.0635
	Glucuronate	1.254	0.0371
	2-Aminobutyric acid	1.247	0.0391
	Tryptophan	1.246	0.0404
Seed	Phenylalanine	1.729	0.0868
	Valine	1.491	0.0539
	Tyrosine	1.459	0.0557

Isoleucine	1.456	0.0632
Serine	1.324	0.0339

The metabolites found in this study accord with an existing understanding of fruit ripening. For example, an aspect of ripening involves ethylene-triggered breakdown of pectin, hemicellulose in cell walls to form simple metabolites such as galactose, xylose and galacturonic acid ^{23,141}. This cell-wall breakdown causes a drastic decrease in firmness when fruit is ripe. Here, we found that galacturonic acid and xylose abundance increased considerably during mangosteen ripening, implying the same process occurs in this fruit.

In mangosteen flesh, we identified 2-aminoisobutyric acid as an abundant metabolite in mangosteen flesh (Figure 12). The metabolite has been previously reported to inhibit ethylene production and postponed the peak of respiration rate in treated longan fruit ¹⁴². Additionally, psicose and several amino acids (phenylalanine, valine, isoleucine, serine, and tyrosine) have strong correlation with mangosteen ripening based on VIP score of PLS model in peel and seed of mangosteen, respectively. Previous research has indicated the involvement of psicose in transpiration inhibition mechanisms in tomato ¹⁴³, whereas amino acids such as phenylalanine, valine, isoleucine, serine, and tyrosine were reported to play a role in cacao seed development ¹⁴⁴.

In our analysis, psicose was considered as one of the important metabolites in peels during ripening stages. It is suggested to have a role as a supportive mechanism to decrease the respiration in order to produce more water as product and uncontrolled release of water content during ripening stage.

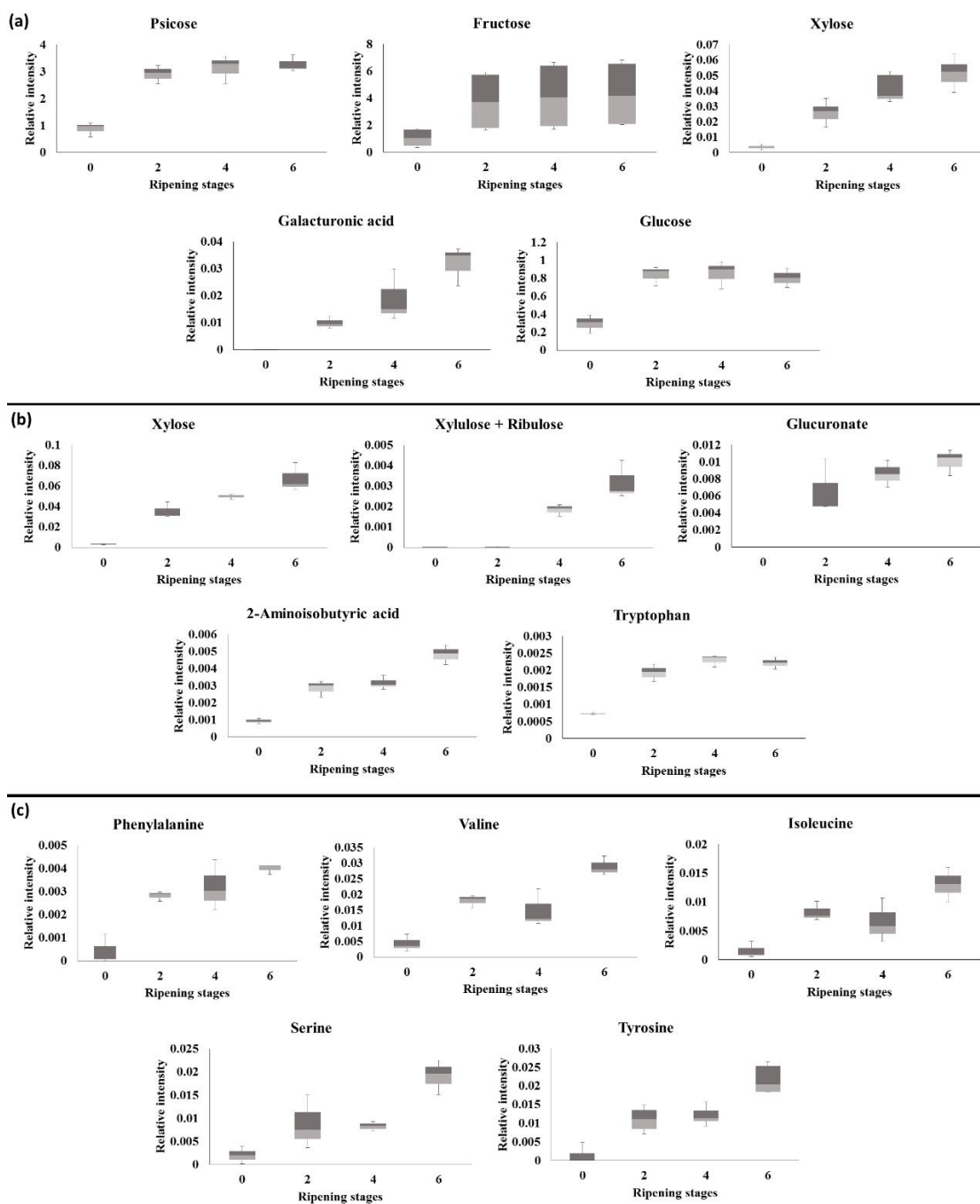


Figure 12. Box-plot of highly contributing five metabolites that are related to mangosteen (*Garcinia mangostana*) ripening stages of (a) peel part; (b) flesh part; (c) seeds part. The relative intensity of metabolites that are important during mangosteen ripening stages was explained using boxplot were dominated by saccharides, organic acids and amino acids. The peak intensity of each metabolite was normalized based on ribitol internal standard

2.3.5. Metabolites changes related to the quality of mangosteen during ripening process in flesh part

Organoleptic properties, such as fruit firmness, sweet-acid taste, and aroma, were dynamically changed during fruit ripening process especially in the flesh part. These qualities have resulted in considerable efforts to control mangosteen fruit ripening so as to achieve optimal fruit maturity for harvesting. The behavior observation in fruit firmness and color in mangosteen were explained in the previous section. In this section, metabolic changes related to quality of mangosteen during ripening process will be deeply discussed in the flesh part and peel part.

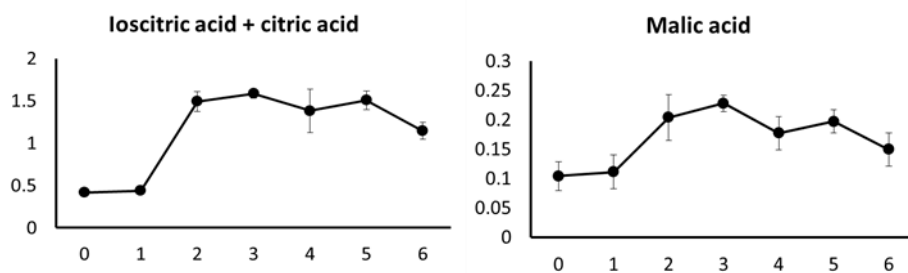


Figure 13. Relative intensity of isocitric acid + citric acid and malic acid during mangosteen ripening stages. The X-axis represents the ripening stages and Y-axis represents the relative intensity towards ribitol as an internal standard

The result shown in Figure 13 indicates that during ripening process, the relative intensity of isocitric acid, malic acid, are increased in stage 2 and remain stable until the end of ripening stages in the flesh part. These metabolites are intermediates in the tricarboxylic acid (TCA) cycle. In addition, similar trend was shown in several cell-walls modification-related metabolites (galacturonic acid, fructose, sucrose, galactose, and glucose). This founding suggested there is a mechanism of separation between peel and flesh part that has relation to cell-wall modification between the layer

between peel and flesh during stage two of mangosteen ripening. Furthermore, the stability of these metabolites indicated that the accumulation process remains until the end of ripening stages.

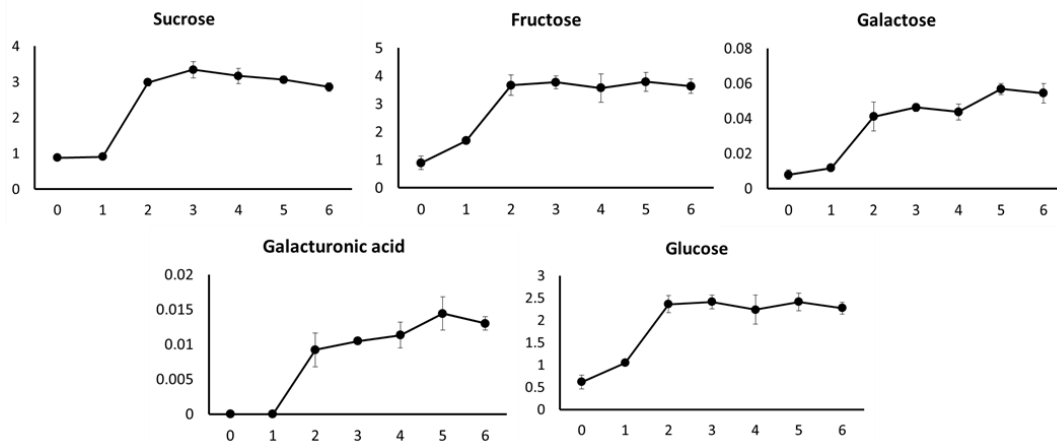


Figure 14. Relative intensity of saccharides during mangosteen ripening stages. The X-axis represents the ripening stages and Y-axis represents the relative intensity towards ribitol as an internal standard

The stability of metabolites intensity from stage two might cause by nutrition intake as a result of translocation process still occurs during attached/intact/on-tree ripening process. Fruit as a non-photosynthetic organ is known as sink from photosynthetic organ such as leaves. The results of sugar accumulation indicate (Figure 14) there is an association with photo assimilate metabolism occurs during intact/on-tree mangosteen ripening process^{145,146}. The sugar accumulation in intact fruits after stage two ripening means carbon storage for further used during postharvest showed an optimum number to be selected for postharvest storage. This result in agreement with the previous study mentioned the detached/off-tree fruit, markedly restricts or terminate photosynthesis, leaving them with the extremely low reserves that can be used for maintenance.

The amino acids intensity also gradually accumulated at the end of ripening stages of flesh part (Figure 15). Amino acids were reported as an important precursor of aroma/flavor volatiles in fruits. The accumulation of amino acids during mangosteen ripening process showed that the biosynthesis of aroma/flavor might occur. Additionally, the accumulation of amino acids indicates indirect effect after hypoxic condition during fruit ripening process due to ROS activity^{147–153}.

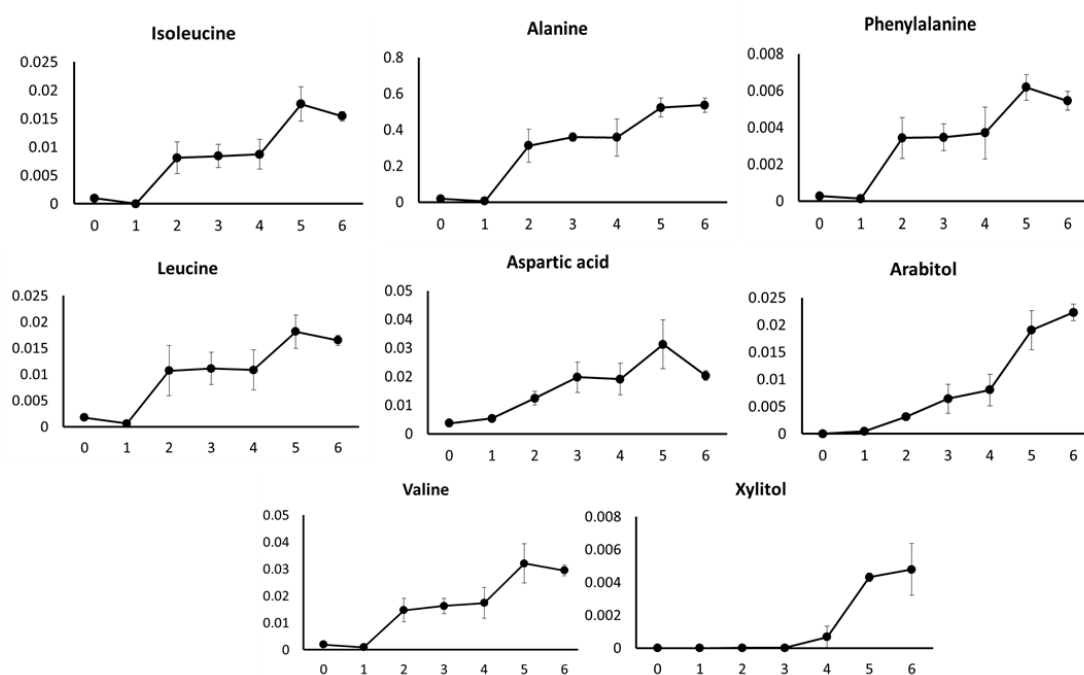


Figure 15. The relative intensity of sugar alcohols and amino acids during mangosteen ripening stages. The X-axis represents the ripening stages and Y-axis represents the relative intensity towards ribitol as an internal standard

Phenylalanine as a precursor metabolites in phenylpropanoid metabolic processes represent the pathways of flavonoid synthesis. The previous study reported a large number of genes in this pathway linked with cytochrome P450 were up-regulated during

fruit senescence or ripening process, which lead to the accumulation of polyphenol metabolites. The increased polyphenol metabolites could then be oxidized by ROS¹¹⁷.

The confirmation of low oxygen gradient condition by using line chart was generated to observe the metabolic changes during mangosteen ripening process (Figure 16). Several metabolites (4-aminoisobutyric acid, lactic acid, and proline) was reported as a metabolic response after stress conditions^{154,155}. Line chart was generated using the information of relative intensity of each metabolite in each ripening stages. Lactic acid and 4-aminoisobutyric acid showed a significant increase during stage two and three. This results indicated that there is a stress response during ripening stages. The increase of these metabolites in accordance with the increase of proline intensity until the end of ripening stages. This results supported the previous statement regarding the accumulation of the amino acids due to low oxygen gradient condition.

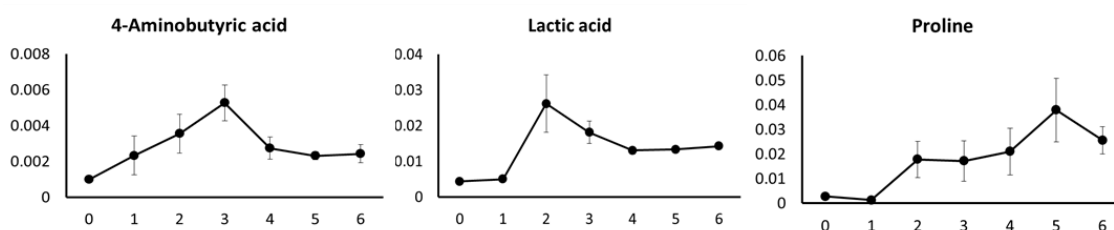


Figure 16. Relative intensity of stress-related metabolites during mangosteen ripening stages. The X-axis represents the ripening stages and Y-axis represents the relative intensity towards ribitol as an internal standard

2.3.6. Metabolites changes related to the quality of mangosteen during ripening process in peel part

The metabolic changes occurred in the peel part were deeply discussed since the firmness, and color changes are a common indicator for mangosteen maturity before it is

consumed. In HCA plot, the increased metabolites were selected and visualized using line charts. Similar with flesh part, several metabolites in peel part (malic acid, isocitric acid+citric acid, glucose, xylulose+ribulose, xylonic acid, and galactose) were observed in each stage during ripening stages (Figure 17). These metabolites were significantly increased starts from stage two and remain stable until the end of ripening process. The metabolites listed above is related to the degradation of the polysaccharides as reported in the previous study. Furthermore, these metabolites also reported has a role in fruit firmness during ripening process.

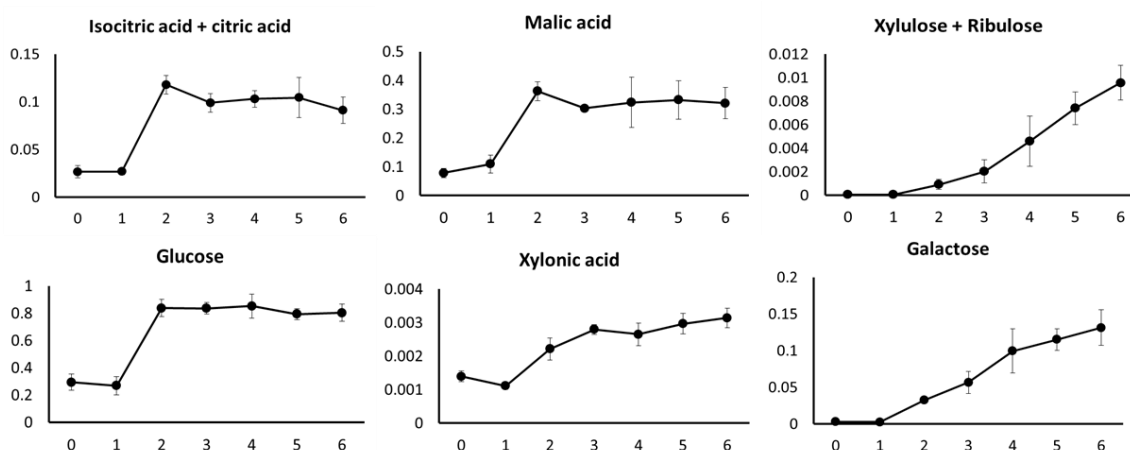


Figure 17. Relative intensity of firmness and TCA cycle metabolites during mangosteen ripening stages. The X-axis represents the ripening stages and Y-axis represents the relative intensity towards ribitol as an internal standard

Similar to the flesh part, the ripening process behavior was observed from the accumulation of metabolites. The significant increase of TCA-related metabolites (malic acid, and isocitric acid+citric acid) indicates there is a respiration process which resulted in the color changes from yellow-green to black-purple color. The respiration process was observed also give an effect to fruit firmness which showed in the relative intensity of galactose, glucose, and xylulose+ribulose metabolites.

2.4. Conclusions

Comparing the huge information about bioactive compounds in mangosteen, information from metabolomics studies during mangosteen ripening studies are still very limited. Finally, the study of mangosteen ripening using metabolomics approach provide further information about the chemical mechanisms of the rapid decrease in ethylene production during the mangosteen ripening stage. Metabolomics approach offers a great advantage compared to the traditional conventional appearance-based diagnosis as it can provide a quantitative and objective measurement of metabolites that contribute to the phenotypic traits of fruit, such as color, texture, and flavor.

This study marked the first investigation of mangosteen ripening using metabolic profiling and this study resulted in new insights on important metabolite changes that occur during ripening and suggested several important metabolites for mangosteen ripening. The approaches established from this study can provide a better understanding of the mangosteen ripening and aid the development of postharvest strategies and quality control of mangosteen by controlling changes in metabolites involved in ripening.

Chapter 3

Metabolomics-based approach for the evaluation of different mangosteen ripening condition

3.1. Introduction

Mangosteen is a climacteric fruit which color changes were changed by the existences of ethylene around the fruits. Mangosteen peel color is the major criterion used to judge its ripening index. Fruit ripening stage variation occurs from the different trees every harvesting year. It might cause by maturity and ripening process of each fruit cannot be done uniformly even it occurs in the same tree ⁶⁷.

Furthermore, fruit developmental process also depends on the weather condition. The fruiting season can occasionally begin four until six weeks earlier than typical. The fluctuation of rainfall, shades, location of the fruits in the tree might have different physiological condition for each mangosteen fruit. These climatic conditions cause uncertain phenology including fruit ripening behavior ^{75,156–159}.

The ripening behavior deviation can be observed between plant-attached and plant-detached. The ripening physiology between “on-tree” or attached fruit and “off-tree” or detached fruit has different pattern of genes, until biochemical changes as reported in several cultivars of detached chili and cut-off flower ^{13,160,161}. The inhibition of intracellular metabolites transport process in “off-tree” condition might affect the accumulation of starch during fruit development process.

Postharvest development always used fruits in their ethylene peak and allowed to ripen during storage treatment. During storage, the fruit quality reached at the end of the “on-tree” ripening condition needs to be maintained. To date, the application of metabolomics approach offers the possibility to better understand of biochemical changes occur in different ripening condition. Therefore, the comparison between “on-tree” and “off-tree” ripening condition using metabolomics approach is proposed in this study.

3.2. Experimental section

3.2.1. Plant materials

Mangosteen fruit from Bogor, Indonesia corresponding to 7 different ripening stages (stages 0 to 6) were used in this study⁵¹. Mangosteen fruits from each ripening stage with three biological replicates were collected from different trees and different cultivation area in random. Sample collection was done in one day on February, 19th 2018 in Center of Tropical Horticultural Studies, Bogor Agricultural University, Bogor, Indonesia. These samples were obtained at the optimum moment for harvest, always in the morning. These samples were obtained to imitate postharvest condition (“off-tree” ripening condition). These samples were analyzed together with natural (further will be mentioned as “on-tree”) ripening condition which is described in chapter 2. All mangosteen samples were fast quenched in the liquid nitrogen and stored in -20 °C prior to extraction and homogenization process.

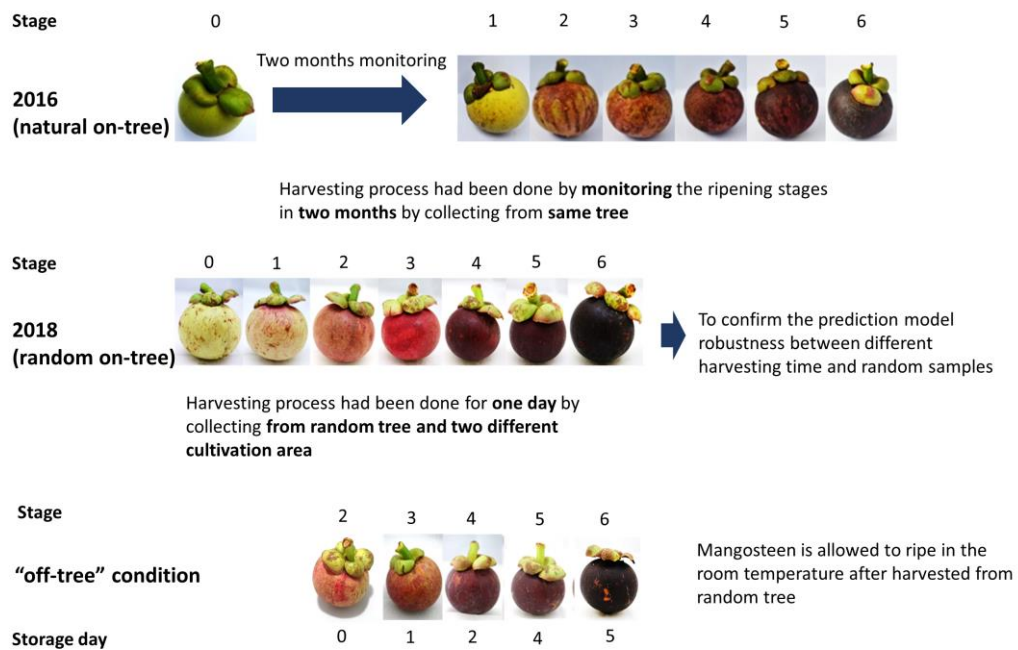


Figure 18. Samples information of this study. Seven ripening stages were collected from different ripening condition. “Natural on-tree” condition samples were collected from 2016 as described in chapter 2. “Random on-tree” samples were randomly collected from different tree and different cultivation area in 2018. The number shown in the figures represent the ripening stage. Both ripening condition samples were analyzed together using GC-MS. The “off-tree” condition was performed by using stage two as an initial stage which allows ripening in the room temperature until reach stage six of ripening. “Off-tree” samples will further be used as a control in postharvest treatment. Stage two was randomly collected and treated with several postharvest treatments.

3.2.2. Color changes measurement

Same as section 2.2.2

3.2.3. Samples extraction

Same as section 2.2.3

3.2.4. Derivatization

Same as section 2.2.4

3.2.5. Gas chromatography-mass spectrometry analysis

Same as section 2.2.5

3.2.6. Data analysis

Same as section 2.2.6

3.3. Results and discussions

3.3.1. Elucidation of metabolic changes during mangosteen ripening stages in different ripening conditions

The seven mangosteen fruit ripening stages were randomly collected in one day from different trees and from two different plantations. The mangosteen ripening stages were classified explained in the previous chapter. These samples (“random on-tree”) were compared with natural ripening condition (“natural on-tree”) (Figure 18) to evaluate whether the same ripening trend occurs in different harvesting year, different collection method and different plantations.

Colorimetric analysis revealed increasing color solid representative (dLAB value) as peel color shifted in both ripening stages from green to purple-black in both ripening conditions (Table 5). We also noted there is no significant difference in dLAB value between “random on-tree” ripening condition and “natural on-tree” ripening condition, corroborating previous studies which also described in chapter 2.

Table 5. Solid color representative values of on-tree and off-tree ripening condition. CIELAB was used to calculate the color representative values during mangosteen ripening condition. Stage 0 was used as a reference sample. dL indicates the different of lightness between the samples and reference that were measured. da and db values are chromaticity diagram that describes red-green color for da values and yellow-blue color for db values different between the samples and reference. dLab value is the total color of difference value between samples and reference.

Ripening condition	Ripening stages	Lightness (dL)	Vivid color (da)	Hue color (db)	dLab value
“Natural on-tree”	I	3.588a	3.158a	2.599a	10.759a
	II	-14.250b	15.493b	-15.693b	26.560b
	III	-26.789bc	17.248b	-25.189c	41.373c
	IV	-27.668c	17.711b	-28.659c	43.797c
	V	-32.580c	12.822b	-30.343c	46.421c
	VI	-35.293cd	7.377ab	-32.594d	48.778c
“Random on-tree”	I	2.207a	2.939a	-1.3292a	11.247a
	II	-11.627b	16.961b	-13.308b	25.100b
	III	-17.502bc	20.892b	-16.816b	33.077bc
	IV	-27.009c	7.625a	-26.029c	39.332bcd
	V	-31.741d	4.838a	-28.241c	42.905d
	VI	-32.289e	-0.884d	-30.468c	44.447d

Metabolic changes between “random on-tree” and “natural on-tree” ripening condition were further compared with GC-MS analysis. Three fruits from all ripening stages in “random on-tree” and “natural on-tree” ripening condition were used and the analysis was performed separately for peel and flesh part of mangosteen. A total of 70 metabolites from flesh and 60 metabolites from peel part were tentatively identified in both ripening conditions using the National Institute of Standards and Technology (NIST) and our laboratory in-house library (Supplementary Tables S6 and S7).

Two Principal component analysis (PCA) models of the GC-MS-derived dataset were generated, the first based upon the fruit peel samples and second based upon the

fruit flesh samples, the first two PCs within each model provided a total explained variance (TEV) of 49.8%, and 49.47%, respectively (Figure 19). The results showed the trend of PC1 describes the metabolite changes trends during mangosteen between “random on-tree” and “natural on-tree” ripening process from raw to ripen stages. PCA results also clustered based on metabolites distribution as explained in the previous chapter.

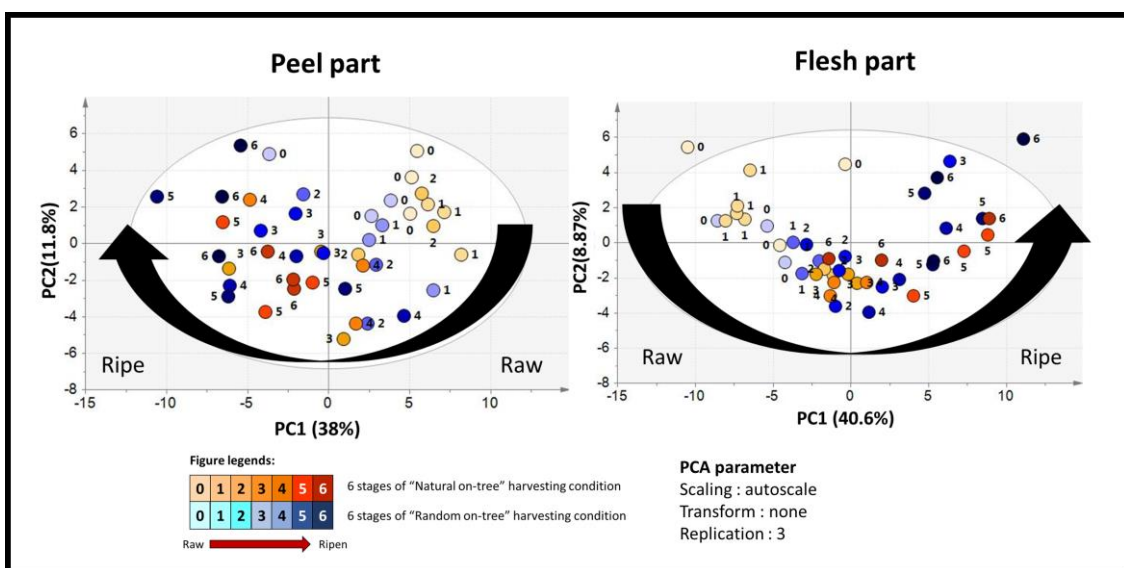


Figure 19. Metabolites abundances during mangosteen ripening process in peel part and flesh part using PCA. PCA results showed the trend of PC1 describes the metabolite changes trends during mangosteen between “natural on-tree” and “random on-tree” ripening process. Scaling method, UV scale; transformation, none; $n = 3$.

Hierarchical cluster analysis (HCA) was performed to further clarify metabolite distribution between “random on-tree” and “natural on-tree” ripening process. HCA resulted in clustering of metabolite intensity showing identical or highly similar patterns of intensities throughout all GC-MS datasets of different ripening condition. In accordance with PCA results, HCA results (Figure 21) showed a clear clustering based on its ripening stages in both ripening conditions. These results also successfully reproduced

the results from chapter 2 which describes heat-map results in “natural on-tree” ripening process. Therefore, we used the “random on-tree” samples as they are collected in the same harvesting time in 2018 with “off-tree” samples for the next comparison between “on-tree” and “off-tree” ripening stages. In “off-tree” samples, stage two mangosteen was allowed to ripen in room temperature over the course of 10 days observation. Based on color changes parameter, we assigned the ripening stage of mangosteen from stage 2 to stage 6. The progression of ripening was much faster in “off tree” samples compared to the ripening that occurred naturally “on-tree”. When harvested in stage 2, the peel color was light-greenish yellow scattered with a pinkish spot. At day one after harvest, the fruits ripened to stage 3, then reached stage 4 at day two, stage 5 at day four and reached fully ripen stage 6 at day five. The peel color then remained constant until day 10 (Figure 18).

Metabolic changes between “on-tree” and “off-tree” ripening condition were further compared with GC-MS analysis. Three fruits from different ripening stages in “on-tree” and “off-tree” ripening condition were used and the analysis was performed separately for peel and flesh part of mangosteen. A total of 57 metabolites from flesh and 72 metabolites from peel part were tentatively identified in both ripening conditions using the NIST and our laboratory in-house library (Supplementary Table S9). Two PCA models were generated, the first based upon the peel samples and second based upon the flesh samples, the first two PCs within each model provided a total explained variance (TEV) of 41.5%, and 56.3%, respectively (Figure 20). The results showed the trend of PC1 describes the metabolite changes trends during mangosteen between “on-tree” and “off-tree” ripening process from raw to ripen stages. The ripening progression in “on-tree”

ripening condition shown in Figure 20 is consistent with the previous PCA model (Figure 19).

In the comparison between “on-tree” and “off-tree”, the trend is different in samples of stage 4, 5 and 6 of peel part. Meanwhile, the trend of ripening progression in the flesh part is similar between the two ripening conditions (Figure 20). For detailed investigation on metabolite changes that are associated with ripening in these two conditions, PLS regression was performed.

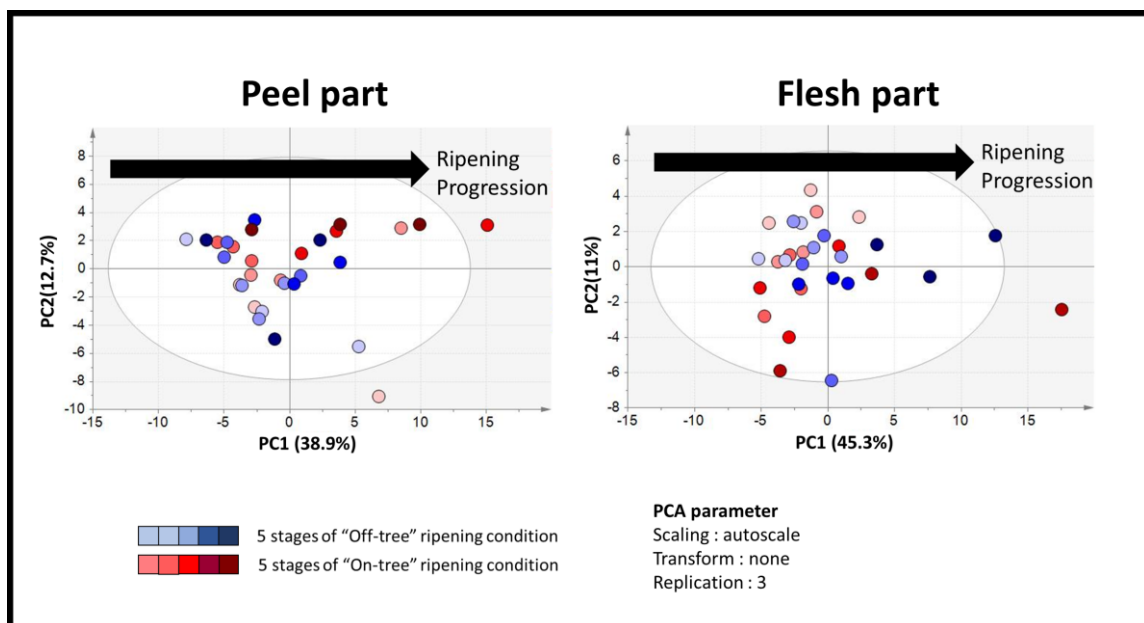


Figure 20. Metabolites abundances during mangosteen ripening process in peel part and flesh part using PCA. PCA results showed the trend of PC1 describes the metabolite changes trends during mangosteen between “on-tree” and “off-tree” condition. Scaling method, UV scale; transformation, none; $n = 3$.

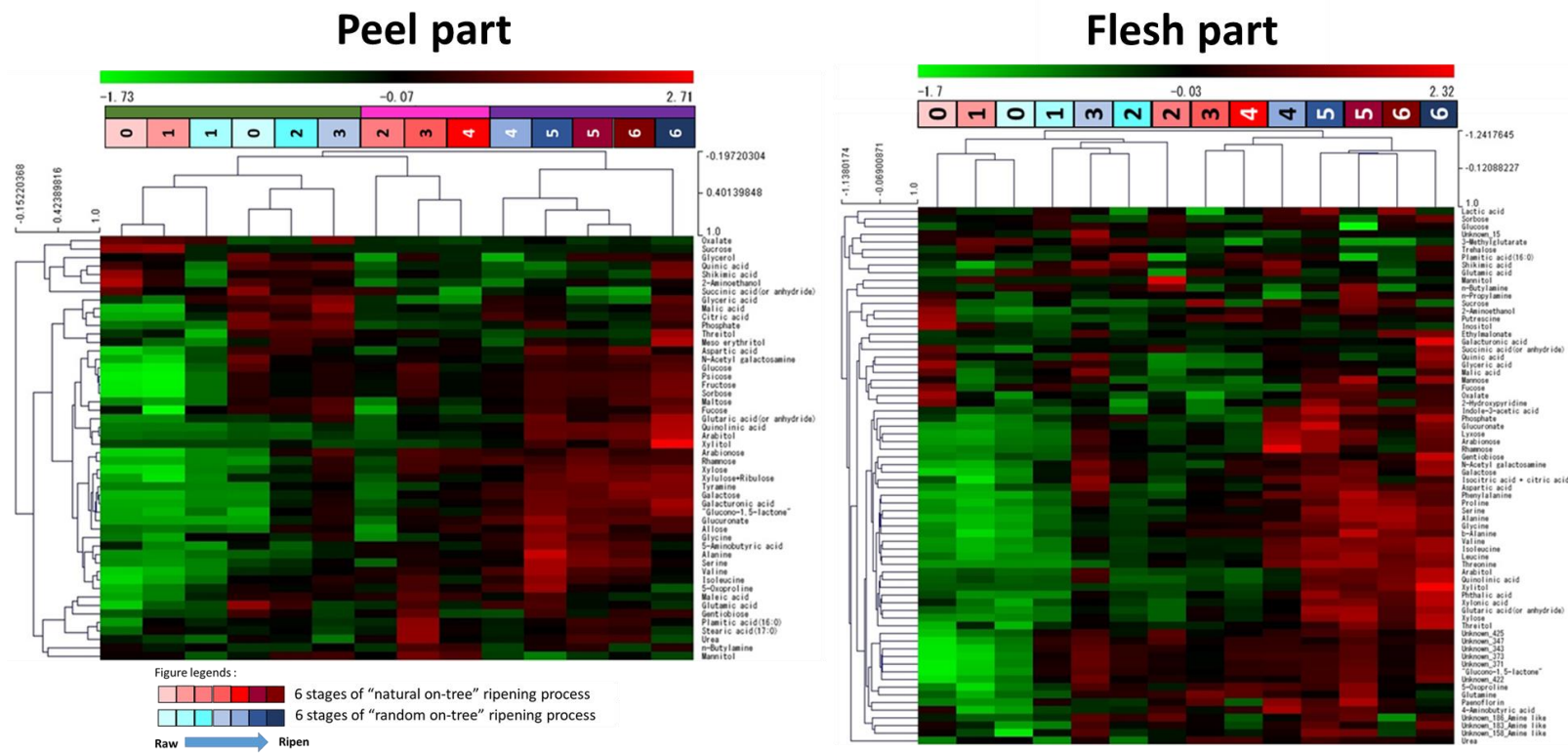


Figure 21. Metabolite distribution between two harvesting conditions was employed and analyzed using Hierarchical Cluster Analysis. HCA parameter * correlation: Pearson correlation, average linked cluster analysis. Up-regulated metabolites are presented in red and down-regulated metabolites in green. Red color represents on-tree ripening condition and blue color represents the off-tree ripening condition.

3.3.2. Prediction model of mangosteen ripening process in two different harvesting condition

PLS analysis was used to regress PCA variables (metabolite intensity) on color change values, allowing us to verify whether color changes can well predict metabolite-based ripening stages. PLS analysis was conducted using data from color changes as the response variable (y-variable) and metabolite peak intensity values as the predictor variables (x-variables). Representative samples of three major ripening stages (stage 0, 2, 4, and 6), referring to the previous chapter, were selected as a training set, and the remaining stages were used as a data set to validate the prediction model. PLS analysis was performed in both harvesting conditions to confirm their contributing metabolite differences.

Table 6. PLS model criteria and list of fifth highest VIP score metabolites from peel part and flesh part of mangosteen obtained from each harvesting conditions.

Fruit part	Criteria	Ripening condition	
		“Natural on-tree”	“Random on-tree”
	R²	0.994	0.982
	Q²	0.879	0.705
	RMSEE	1.883	2.998
	RMSEP	13.819	7.72
Peel part	5th highest VIP score Metabolites (VIP Score; Correlation coefficient)	Glycine (1.36; (+))	Galactose (1.72; (+))
		Galacturonic acid (1.36; (+))	Fructose (1.70; (+))
		Galactose (1.35; (+))	Glucuronate (1.65; (+))
		2-aminoethanol (1.33; (-))	Rhamnose (1.48; (+))
		Shikimic acid (1.32; (-))	Galacturonic acid(1.47; (+))
Flesh part	R²	0.863	0.958
	Q²	0.627	0.874

RMSEE	8.209	4.064
RMSEP	7.515	5.454
5th highest VIP score Metabolites (VIP Score; Correlation coefficient)	β -alanine (1.70; (+))	Phenylalanine (1.39; (+))
	Alanine (1.60; (+))	Threonine (1.38; (+))
	Lyxose (1.54; (+))	2-aminoethanol (1.38; (+))
	Arabinose (1.51; (+))	Isoleucine (1.37; (+))
	Phenylalanine (1.50; (+))	Valine (1.36; (+))

The constructed models have linear coefficient (R^2) and prediction ability (Q^2) greater than 0.7, both thresholds for a valid model with a good fit (Table 6). The results of the PLS model indicated that different metabolites were giving large contributions to color change depending on the mangosteen part. Contributing metabolites were selected based on the five highest variable importance in projection (VIP) scores.

Primary metabolites were selected from both harvesting conditions in the peel part as ripening-associated metabolites (Table 6). Galactose and galacturonic acid were repeatedly reported in both harvesting conditions in peel part. These metabolites have been reported in the previous chapter. Galacturonic acid and galactose were reported to have a contribution to cell wall degradation which gives an effect to fruit softening during the ripening process. This cell-wall breakdown causes a drastic decrease in firmness when the fruit is ripe ¹²⁵. For example, an aspect of ripening involves an ethylene-triggered breakdown of pectin, hemicellulose in cell walls to form simple metabolites such as galactose, xylose and galacturonic acid ^{23,141}. Here, we found that galacturonic acid and galactose abundance increased considerably during mangosteen ripening, implying the same process occurs in this fruit between two different harvesting conditions. Interestingly, shikimic acid was shown to be one of the important metabolites in the peel part of “on-tree” condition.

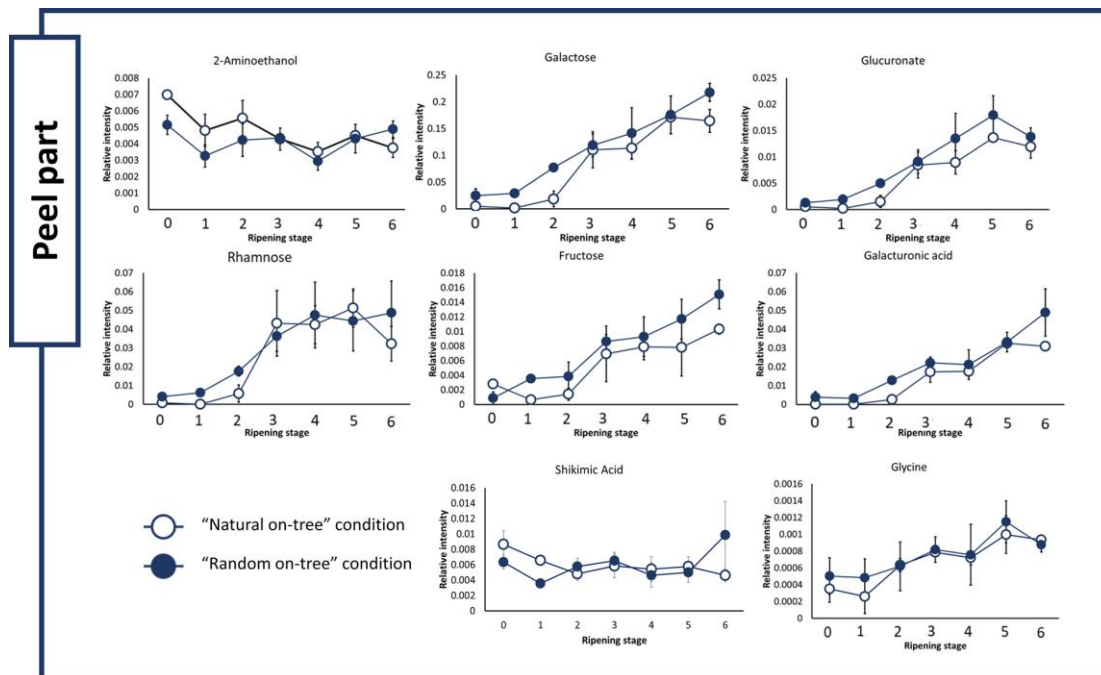


Figure 22. Line graph of important metabolites of peel part between “natural on-tree” ripening and “random on-tree” ripening.

Shikimic acid was repeatedly reported as a precursor metabolite for pigment and lignin production in transcriptomics studies of peach and pear fruit development ^{162,163}. Similar study in mangosteen reported that lignification was induced during “on-tree” fruit maturation upon hypoxic condition treatment using capillary water ¹⁶⁴. Lignification in mangosteen fruit affected peel hardness which increased fruit firmness and such phenomenon occurred under low oxygen conditions or upon physical damage ^{54,132,165}.

Additionally, primary metabolites were selected in the flesh part as ripening-associated metabolites in both “on-tree” conditions (Table 6). It is also mentioned that listed amino acids act as precursors for fruit aroma metabolites. Previous report mentioned several amino acids have a contribution to several volatile metabolites biosynthesis in melon ¹⁰⁹, These findings have a good agreement with the information of

several amino acids might have a role as a precursor metabolite for plant volatile metabolites that had been reported in the previous studies ^{109,166–168}. A number of flavor volatile metabolites were also found in abundance of mangosteen using headspace-solid phase microextraction (HS-SPME) which are related to specific aroma metabolites ¹⁶⁹. In addition to amino acids, metabolites such as quinic acid, lyxose, and arabionose that were previously reported as sweet-acid related metabolites in coffee and direct precursors of volatile metabolites in several fruits were also selected as ripening-associated metabolites ^{170–173}.

Furthermore, phenylalanine consistently appeared as the fifth highest VIP score obtained from the PLS model in both harvesting conditions in the flesh part. The metabolite has been previously reported to regulate reactive oxygen species (ROS) activity whilst also regulating pH, cell homeostasis, and structural integrity of membranes and cell walls ¹⁵³. The roles of ROS had also been reported in fruit development and ripening. ROS has an association with the increase in polygalacturonase activity, peroxidase activity and the concentration of peroxide during fruit softening process of papaya, and banana using proteomics approach ^{119,147,174,175}.

The increase of amino acids during ripening indicated that ROS activity was present during mangosteen ripening. Moreover, phenylalanine was reported as one of low oxygen stress response metabolite in the legume after waterlogging treatment ¹⁷⁶. The accumulation of several amino acids can also be caused by the hypoxia condition occurring in the flesh of mangosteen since the oxygen gradient in flesh might be lower than the peel part as previously reported in pear and apple ^{177,178}.

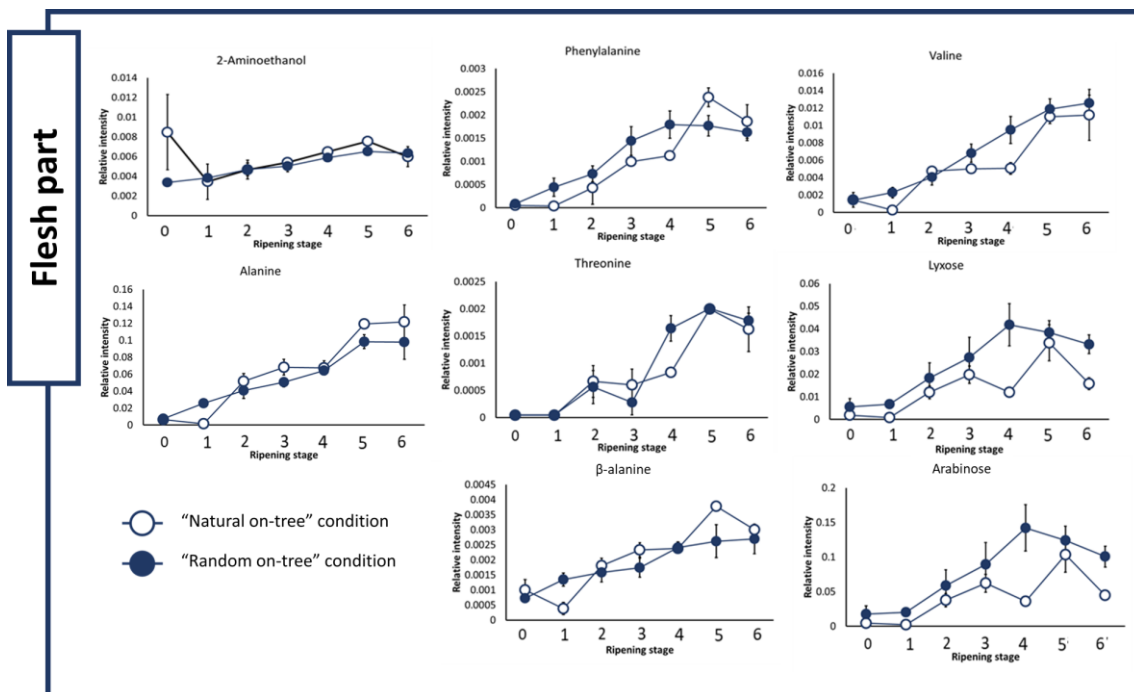


Figure 23. Line graph of important metabolites of flesh part between “natural on-tree” ripening and “random on-tree” ripening.

The additional PLS analysis was performed to confirm their robustness between different ripening condition. Samples of “natural on-tree” harvesting condition (stage 0 - 6) were selected as a training set, and the “random on-tree” samples were used as a data set to validate the prediction model. This model is herein referred to as “on tree” combined model. The constructed model has a linear coefficient (R^2) and prediction ability (Q^2) greater than 0.6 in both parts (peel and flesh part) (Table 6).

In order to verify our results, we added the test set into the model wherein they fit perfectly in the predicted regression line (Table 6). Moreover, the root means square error of estimation (RMSEE) was calculated to determine how well the observed color changes during ripening stages matched with the actual color changes during ripening stages of mangosteen. Result showed that the root mean square error of estimation (RMSEE = 6.90

and 5.89 in peel and flesh part, respectively) was considered as not significantly different from the root mean square error of prediction (RMSEP = 13.08 and 9.72 in peel and flesh part, respectively), thus indicating that the regression model was valid.

Table 7. PLS model criteria and list of 5th highest VIP score metabolites from peel part and flesh part of mangosteen obtained from both harvesting conditions

Fruit part	Criteria	VIP metabolites
	R²	0.873
	Q²	0.771
	RMSEE	6.909
	RMSEP	13.085
Peel part	5th highest VIP score Metabolites (VIP Score; Correlation coefficient)	Galactose (1.43;(+))
		Galacturonic acid (1.42;(+))
		Shikimic acid (1.40;(-))
		Xylose (1.40;(+))
		Glucuronate (1.39;(+))
	R²	0.926
	Q²	0.618
	RMSEE	5.897
	RMSEP	9.72
Flesh part	5th highest VIP score Metabolites (VIP Score; Correlation coefficient)	Alanine (1.52;(+))
		β-alanine (1.49;(+))
		Phenylalanine (1.41;(+))
		Quinic acid (1.39;(-))
		Glucuronate (1.36;(+))

In mangosteen peel, similar ripening-associated metabolites (galactose and galacturonic acid) with “natural on-tree” and “random on-tree” as contributing metabolites in combined prediction model (Table 7). In mangosteen flesh, we identified similar metabolites as “natural on-tree” and “random on-tree” as an abundant metabolite in “on-tree” combined prediction model.

The relative intensity of major metabolites between “natural on-tree” and “random on-tree” ripening condition was compared using a line chart. Top metabolites (based on VIP score from both ripening condition) individual mangosteen parts were analyzed separately (Tables 6, 7). The line chart shows that the relative intensities of top metabolites were correlated with ripening stages in both ripening conditions, in accordance with ripening progress (Figures 22, 23).

Major metabolites relative intensities are increased in accordance with ripening stages in all conditions. Contributed soluble sugars (galactose, fructose, glucuronate, rhamnose, lyxose, and arabinose) were accumulated at the end of the ripening process between both harvesting conditions. Additionally, contributed amino acids (phenylalanine, threonine, β -alanine, alanine, isoleucine, glycine, and valine) follow the same trends during the ripening process of both harvesting conditions. Meanwhile, 2-aminoethanol relative intensity is relatively constant between the stages in all mangosteen parts.

For comparative purpose, most significantly different metabolites in “natural on-tree” and “random on-tree” harvesting condition were shown in. Several metabolites in peel part (galactose, glucuronate, rhamnose, fructose, galacturonic acid) were significantly different in earlier ripening stage (stage 0, 1, and 2) between the two ripening conditions. Additionally, several metabolites (phenylalanine, valine, threonine, lyxose, isoleucine, and arabinose) in the flesh part were significantly different in mid-ripening stage (stage 4 and 5). These results showed the increasing of metabolites can be standards to determine the maturity that are not only related to color changes but also mangosteen firmness and aroma precursor metabolites during ripening process.

In conclusion, we successfully developed a robust prediction model of mangosteen ripening process based on metabolome data in two different harvesting conditions with data taken in different harvesting year, sample collection and plantations.

3.3.3. Prediction model of different ripening condition in mangosteen

Additional PLS analysis was performed to confirm the robustness of “on tree” ripening prediction model using “off-tree” samples as test set. Samples of “random on-tree” ripening condition (stages 2 - 6) were selected as a training set, and the “off-tree” samples (stage 2 - 6) were used as a test set to validate the prediction model. This model is herein referred to as “on tree” and “off-tree” combined model (Table 8).

Table 8. PLS model criteria from peel part and flesh part of mangosteen obtained from both ripening conditions

Criteria	Mangosteen part	
	peel	flesh
R²	0.984	0.842
Q²	0.625	0.48
RMSEE	1.12	1.159
RMSEP	227.272	5.84

The constructed model has a linear coefficient (R^2) and prediction ability (Q^2) greater than 0.6 in peel part (Table 8). However, validation using RMSEE and RMSEP value of peel part prediction model was not successfully performed since the result showed a significant difference ($RMSEE = 1.12$, $RMSEP = 227.272$) between two different ripening conditions. Furthermore, the constructed model of flesh part has the prediction ability (Q^2) lower than 0.5. This indicated that different metabolites were not giving large contributions to color change depending on the mangosteen part. In two

ripening conditions, significant difference may be observed if the comparison was performed using all metabolites. Such observation is understandable due to very different physiological conditions between “on-tree” and “off-tree” conditions.

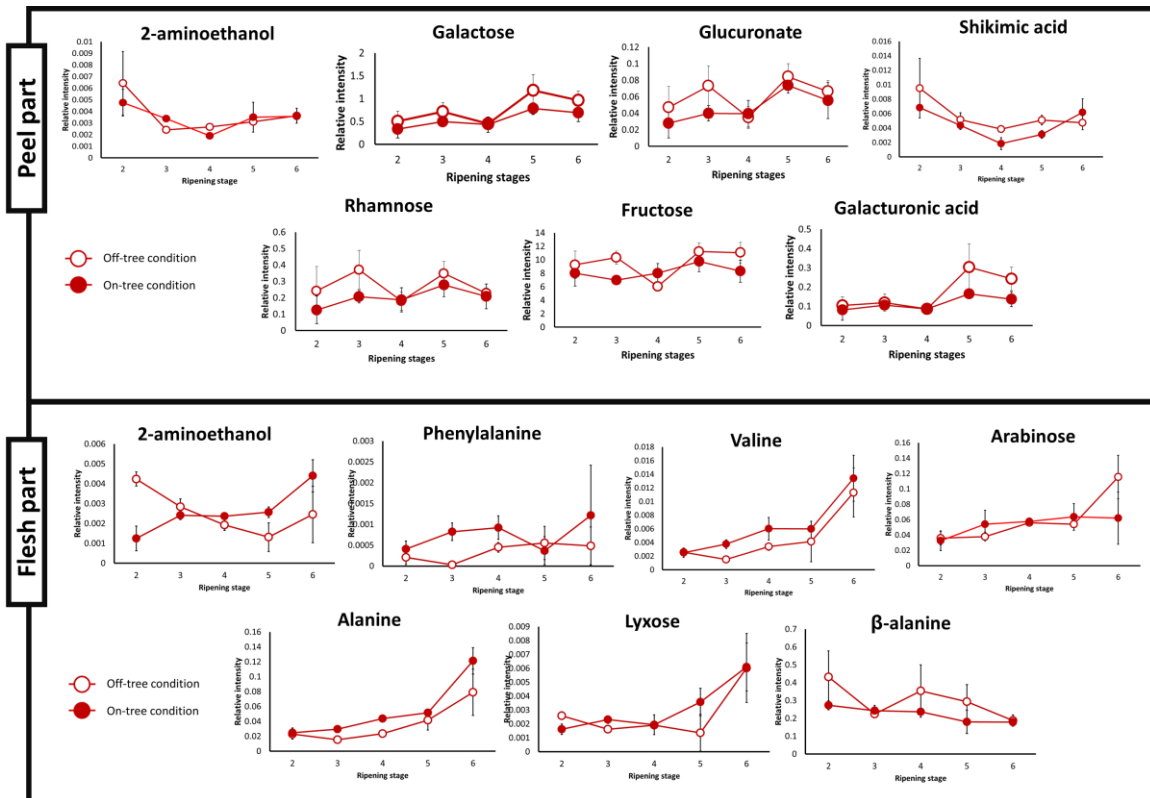


Figure 24. Line graph of metabolite relative intensity changes analysis using GC-MS between two ripening conditions of mangosteen ripening process in peel part and flesh part. The relative intensity of metabolites that are important between “on-tree” ripening condition and “off-tree” ripening condition was explained using a line chart. The peak intensity of each metabolite was normalized based on ribitol internal standard. Y-axis represents metabolites relative intensity and X-axis represents ripening stage. Black circle represents “on-tree” ripening condition and white circle represents “off-tree” ripening condition.

Despite low robustness between the two ripening conditions in PLS model, we examined the trends of ripening-associated metabolites in “on-tree” and “off-tree” ripening condition as shown in Figure 24. Interestingly, all of general ripening-associated

metabolites are increased in accordance with ripening stages in all ripening conditions. Degradation of cell-wall component to galactose and galacturonic acid in peel part during mangosteen ripening stages did not show any difference between “on-tree” and “off-tree” ripening conditions of mangosteen. Additionally, amino acids that were listed in the previous section also accumulated in flesh part. The accumulation of amino acids indicates similar low oxygen gradient condition occurs in the flesh part of two different ripening conditions.

3.4. Conclusions

The results suggest that rapid progression of ripening that occurred in “off-tree” samples did not result in any significant difference with regards to the changes in ripening-associated metabolites. This is the first report that mentions the “on-tree” and “off-tree” ripening conditions of mangosteen. These results can also be used as a basis to indicate the metabolite changes in different ripening conditions in mangosteen and can act as useful feedback for postharvest technology study as a basis to select the most suitable treatment for prolonging mangosteen shelf-life.

Chapter 4

Metabolomics-based approach for the evaluation of different mangosteen postharvest technologies

4.1. Introduction

Postharvest technology development is one of the most important processes which greatly affects fresh food quality including fresh fruit products. Several postharvest technologies (low temperature, edible coating) have been extensively developed to reach the most-favorable condition either for quality improvement or shelf-life improvement in several climacteric fruits such as banana, plum, and peach^{111,179–183}. Temperature and humidity control has been repeatedly reported as the most important factor to maintain product quality throughout the period between harvest and consumption since its lowering respiration rate, decreasing sensitivity to ethylene gas and reducing water loss through transpiration process. However, repeated cooling and warming of horticultural products cause deterioration which causes serious problem such as chilling injuries and affect the organoleptic quality^{111,184,185}. These deteriorative changes include enzymatic and non-enzymatic browning, off-flavor, discoloration, shrinking, peel hardening, and some other chemical, thermo-physical, and rheological alteration that modify the nutritive value and original taste, color, and appearance of fruits. Understanding the changes that occur during postharvest technology is necessary in order to assess optimal harvest maturity and the quality of fruit as it is marketed to the consumer as well as to devise appropriate postharvest packaging and handling strategies.

Existing studies on mangosteen postharvest technologies have been focused on a physio-chemical parameter or targeting only a few processes related to color changes, texture, and enzymatic assay in the peel part^{52,54,125,186-188}. In recent years, metabolomics approach is widely used as an important tool to support postharvest fruit development and ripening studies including melon, strawberry, apple, grape, sapodilla, litchi, and peach^{5,108-117}.

In order to better elucidate the complex mechanism of metabolic response during postharvest technologies in mangosteen, gas chromatography-mass spectrometry (GC-MS)-based metabolite profiling of mangosteen from different ripening stages was performed in postharvest condition (herein referred to as “off-tree” condition) in comparison with different postharvest treatments to ripening process of mangosteen. The postharvest treatments used were low-temperature treatment and stress inducer treatment using methyl jasmonate and salicylic acid. Multivariate analysis was then performed to correlate specific metabolites with color changes that occur during mangosteen postharvest treatment.

4.2. Experimental section

4.2.1. Plant materials

Fruits were selected at green-purple maturity (stage two) by using color changes parameter and were treated with several postharvest treatments. Stage two was selected as an initial stage for postharvest treatment samples to imitate the fresh fruit market condition (Figure 25). All stage two mangosteen samples were obtained at the optimum time for harvest, from 9-12 am in the morning. Four sets of experimental treatments were

adopted during this experiment: low temperature (LT; 12.3 ± 1.4 °C); methyl jasmonate (MeJa) 0.5 mM, and 5.0 mM of salicylic acid (SA) treatment. Room temperature (RT; 27 ± 3.4 °C) storage was performed as a control treatment. These postharvest treatments were previously reported as an effective treatment to prolong mangosteen shelf life ^{125,189}. For stress inducer (SI), MeJa and SA were selected to enhance the production of psicose and 2-aminoisobutyric acid as reported in the previous chapter. For temperature treatment, the fruits were stored at RT and LT for 10 days and fruits were randomly collected for each treatment every day. For stress inducer treatment, treated and untreated fruit (control) were allowed to dry at room temperature after treatment and was stored at room temperature for 10 days. Similarly, with temperature treatment, sample collection was performed daily for each treatment. All mangosteen samples were fast quenched in the liquid nitrogen and stored in -20 °C prior to extraction and homogenization process.

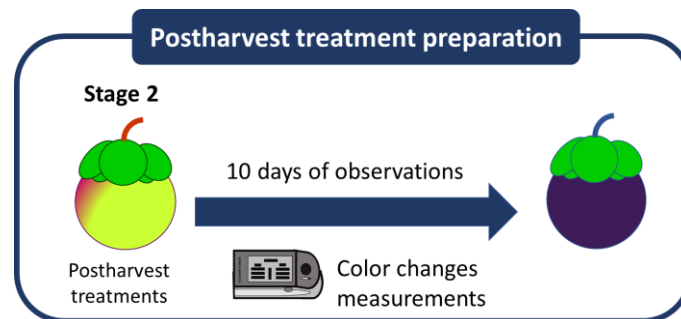


Figure 25. Samples information of this study. Stage two was randomly collected and treated with several postharvest treatments.

4.2.2. Color changes measurement

Same as section 2.2.2

4.2.3. Samples extraction

Same as section 2.2.3

4.2.4. Derivatization

Same as section 2.2.4

4.2.5. Gas chromatography-mass spectrometry analysis

Same as section 2.2.5

4.2.6. Data analysis

Same as section 2.2.6

4.3. Results and discussions

4.3.1. Physical appearance assessment of mangosteen postharvest technology

Physical appearance (color changes) of all treated-mangosteen was evaluated during the treatment period for ten days. Mangosteen color changes were selected based on the determination of ripening index as explained in chapter 2 and chapter 3. Peel color is also reported as an important marketing attribute of mangosteen and influences both consumer acceptance and sales. Different mangosteen samples sets were used for postharvest treatment. Stage two of mangosteen ripening was used as an initial stage before it is treated with several postharvest treatments, namely low temperature and stress inducer treatment using either salicylic acid or methyl jasmonate. All treated samples were allowed to ripe and evaluated for 10 days of storage.

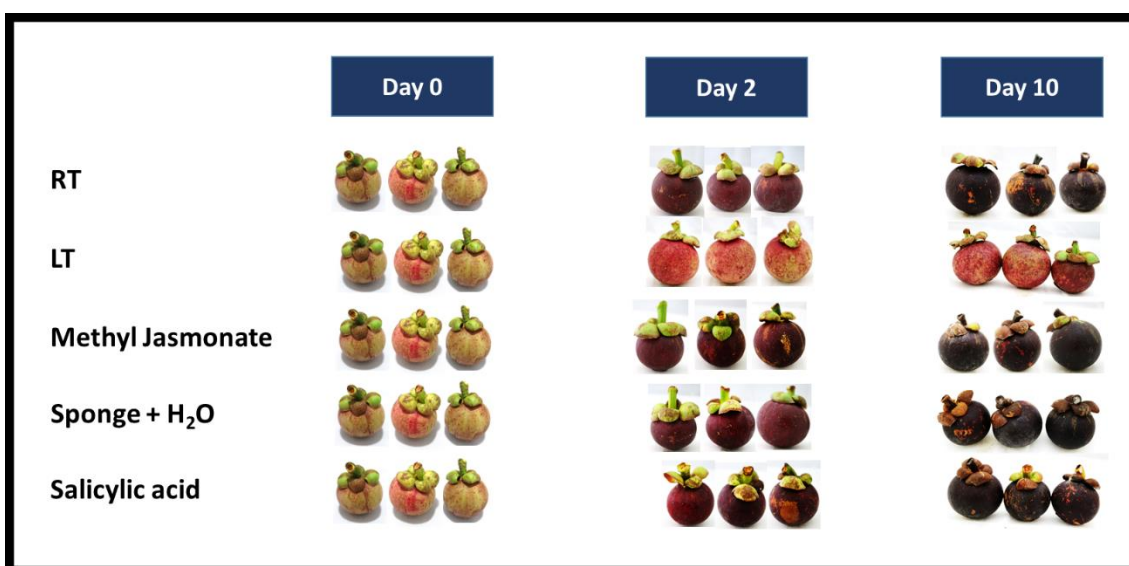


Figure 26. A photograph of physical appearance comparison between room temperature and several temperature treatments after ten days of observation. Fruits were selected at green-purple maturity (stage two) by using color changes parameter as an initial stage and were treated with several postharvest treatments. The fruits were then stored inside the containers at room temperature and low temperature (12.3 ± 1.4 °C) for 10 days.

The peel color during treatment is shown in Figure 26 and appendix Figure S1. When harvested in stage 2 (herein defined as day 0 after harvest), the color was light-greenish yellow scattered with a pinkish spot. On day 2 after harvest, control sample (storage in room temperature (RT) at 27 ± 3.4 °C) showed rapid change of peel color to red and purple. By day 5, it reached blackish-purple color and the color remained constant until day 10. Among all postharvest treatment, low temperature (LT) showed the most significant effect to delay ripening based on the peel color, whereas stress inducer (SI) treatment did not show any significant effect compared to control. Similar physical parameter changes after LT treatment have been reported in the previous study with similar treatment ^{125,186} and is considered as a suitable treatment for prolonging mangosteen shelf-life based on peel color with good reproducibility.

LT treatment effects in the peel part were furtherly evaluated by using a metabolomics approach to confirm its metabolite changes, especially for the fifth highest VIP score metabolites. We did not further analyze the metabolite changes data of peel part after SI treatment because it did not show any effect to prolong mangosteen shelf life based on color changes. However, we analyzed the metabolite data on flesh part for all postharvest treatments to confirm the detailed effect in fruit metabolite changes.

4.3.2. Elucidation of metabolic changes during mangosteen postharvest technology in peel part

A total of 71 metabolites were annotated in peel part of mangosteen samples treated with LT versus control (Supporting Information, Table S10). After GC-MS analysis, the data set of LT treatments and control were subjected to multivariate statistical analysis. PCA model was generated, with each explaining an accumulated TEV for the first two PCs of 42.7% (Figure 27), attributable to the metabolite variation in the peel of the fruits stored under the two different temperature regimes. PC1 describes the difference of metabolite changes trends between LT treatment and control from raw to ripen stages in the peel part.

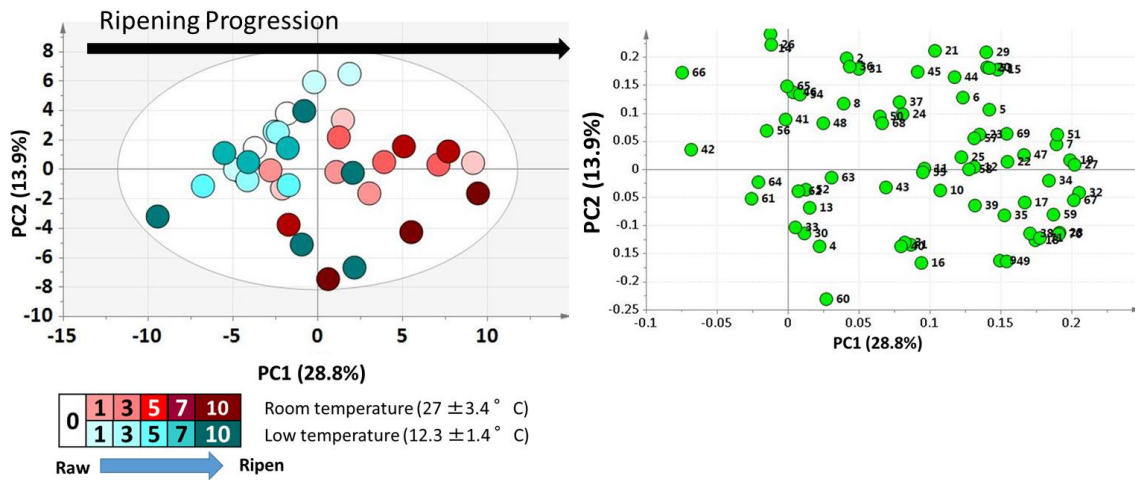


Figure 27. Metabolites abundances during mangosteen LT treatment in peel part. PCA score plot results showed the trend of PC1 describes the metabolite changes trends during mangosteen between room temperature and low-temperature storage condition. PCA loading plot shows the contributions of each metabolite on the changes during treatment in score plot according to the distance to the origin. PCA parameter is described as follows, scaling method, UV scale; transformation, none; $n = 3$.

As can be seen in the PCA score plot of peel part, LT treatment showed markedly different metabolite changes with that of control. HCA analysis results (Figure 28) in the peel part allows the classification of two treatment into three major groups that explained raw to ripen stage after storage treatment. HCA resulted in clustering of low-temperature treatment together with day 1 and 3 in room temperature. Low-temperature treatment seems to delay the ripening process based on HCA result of peels part.

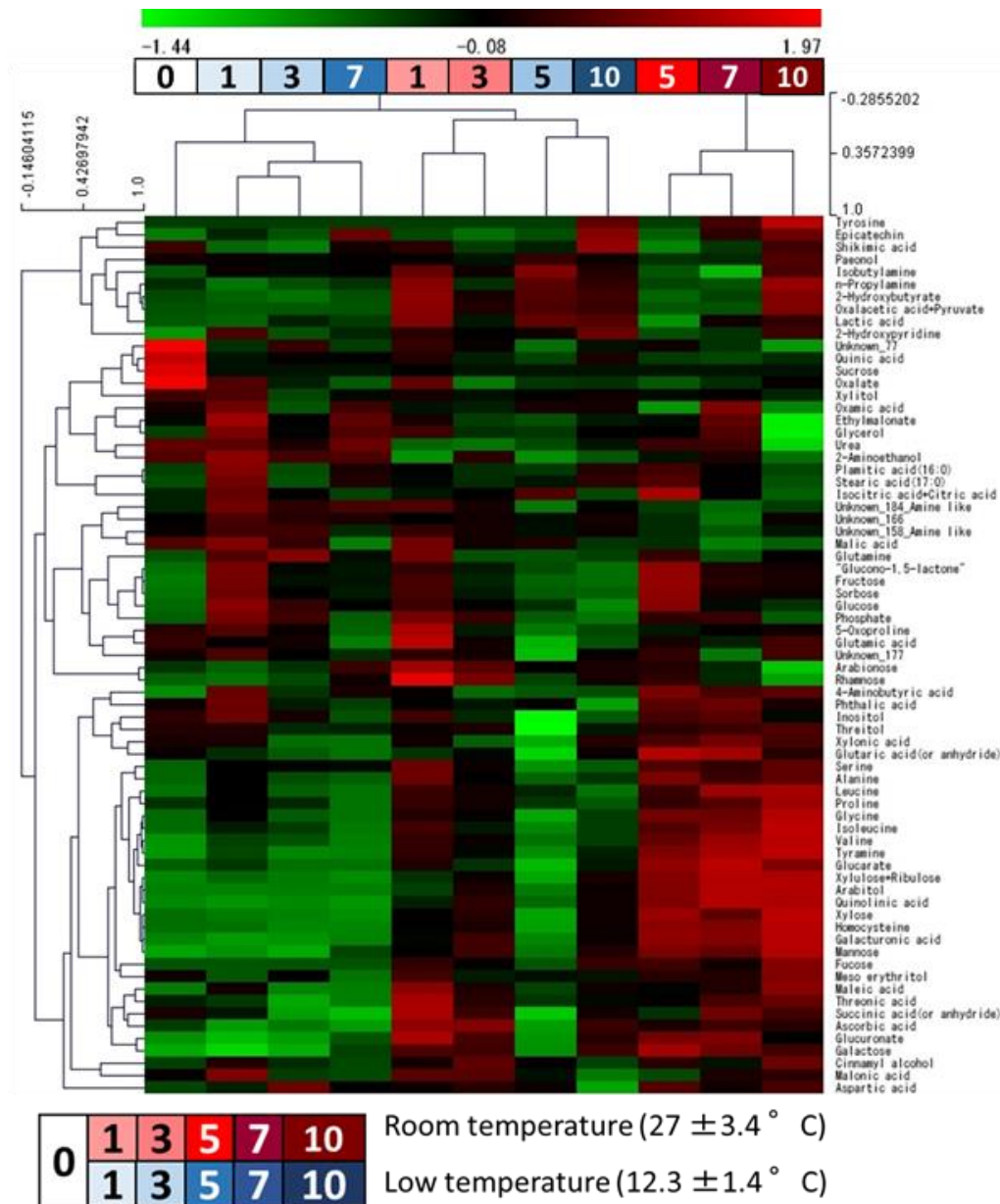


Figure 28. Distribution of metabolites analyzed using GC-MS during mangosteen LT storage treatment in peel part. Stored-mangosteen was observed for 10 days. Metabolite distribution during storage was employed and analyzed using Hierarchical Cluster Analysis. HCA parameter * correlation: Pearson correlation, average linked cluster analysis. Red color represents control treatment. Blue color represents low-temperature treatment. The number shown in the figures represent the storage day of each treatment. Both treatments were analyzed together using GC-MS.

The relative intensity of metabolites with highest VIP score obtained from all PLS models during LT and control were compared using a line chart in a time course manner for 10 days. Top metabolites and flavor-related metabolites from individual mangosteen parts were analyzed separately. Relative intensities of important metabolites in LT treatments and control were shown in Figure 29. These metabolites all had lower relative intensity in LT treatment compared to control treatment in both parts of mangosteen.

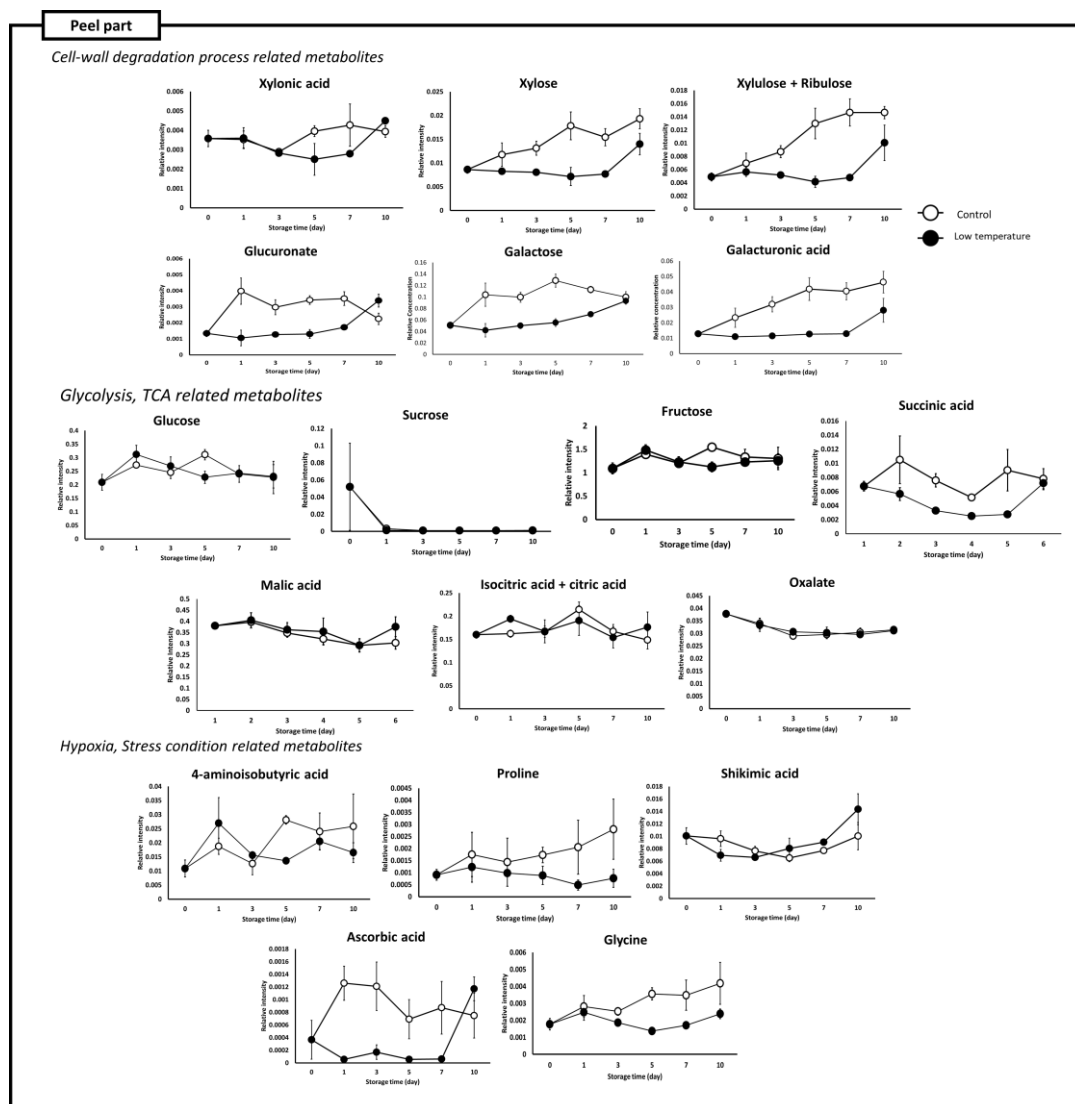


Figure 29. Line graph of metabolite changes analysis using GC-MS during mangosteen LT treatment in peel part. The relative intensity of metabolites that are important during mangosteen

postharvest treatment at low temperature and room temperature were explained using a line chart. The metabolites were dominated by saccharides, organic acids, and amino acids. The peak intensity of each metabolite was normalized based on ribitol internal standard. Y-axis represents metabolites relative intensity and X-axis represents day after storage. White circle represents room temperature treatment and black circle represents low-temperature treatment. The metabolites were marked with an asterisk are listed as ripening-associated metabolites.

In mangosteen peel part, we identified several metabolites related with citric acid cycle (oxalacetic acid, isocitric acid + citric acid, and succinic acid) were decreased together with the storage time (Figure 29). The metabolites have a strong correlation with the respiration process. It is suggested that LT treatment decreased the respiration process in mangosteen, implying the same process occurs in other fruit such as banana, tomato, sapodilla, litchi, and peach ^{111,112,117,173,183,190}. Previous research has indicated the reduction of ACO activity during 15°C storage of mangosteen which related to anoxia condition during storage treatment ^{54,125,165}. In conclusion, this study suggests that LT treatment is the most effective treatment to prolong mangosteen shelf-life based on color appearances and metabolites changes in the peel part.

In order to evaluate the effect of postharvest treatment in the flesh part, metabolomics approach was performed in LT and SI treatment separately. Two PCA models were generated, with each explaining an accumulated TEV for the first two PCs of 40.1% and 42.6% (Figure 30), attributable to the metabolite variation in the flesh of the fruits stored under the two different temperature and stress inducer regimes, respectively.

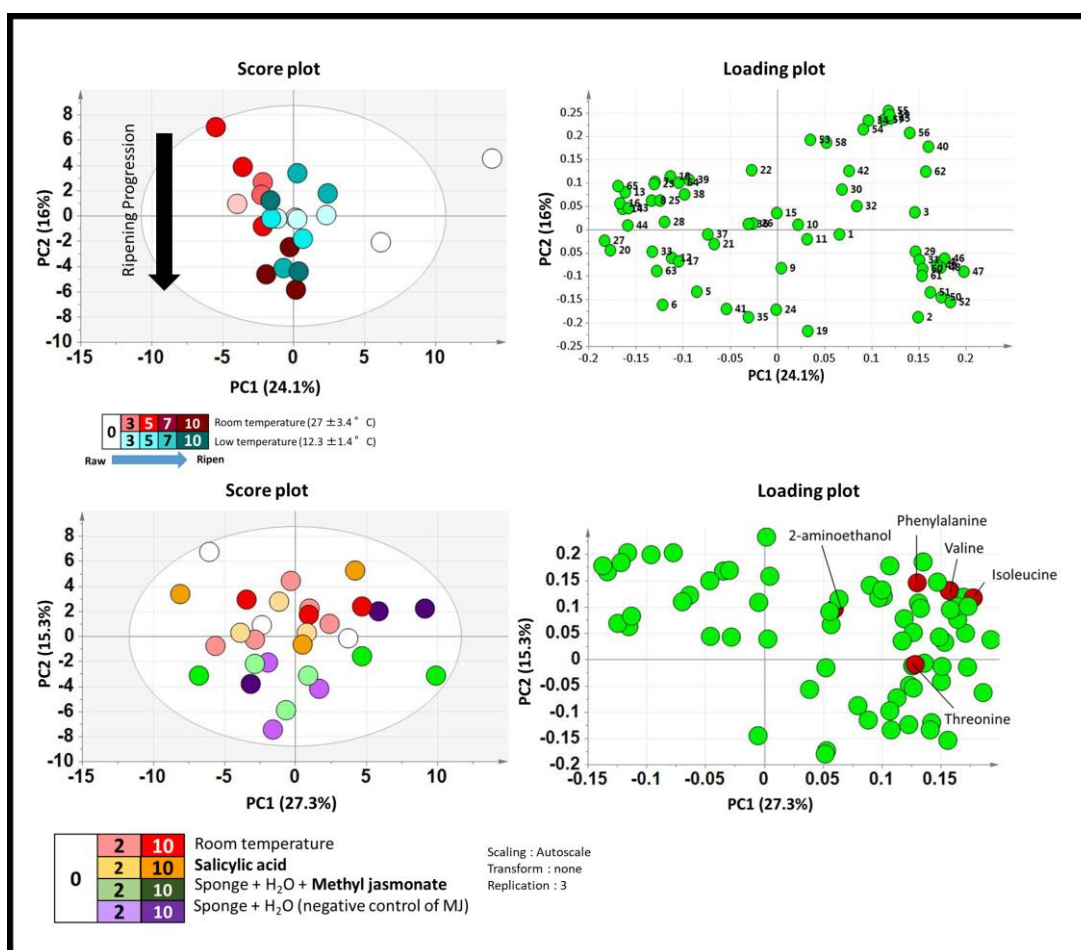


Figure 30. Metabolites abundances during mangosteen postharvest treatment in flesh part. PCA score plot results showed the trend of PC1 describes the metabolite changes trends during mangosteen between room temperature and low-temperature storage condition. However, there is no trend showed in PCA score plot. PCA loading plot shows the contributions of each metabolite on the changes during treatment in score plot according to the distance to the origin. Metabolites marked in red color showed ripening associated metabolites distribution in loading plot after stress inducer treatment. PCA parameter is described as follows, scaling method, UV scale; transformation, none; $n = 3$.

Similarly with PCA result, HCA result also confirmed all postharvest treatment was not effective to halt ripening-associated metabolite increase in the flesh part (Figure 31). Since the flesh part is the consuming part in mangosteen and might affect the organoleptic properties such as fruit firmness and taste-aroma. Therefore, more detailed investigation of the metabolites associated with organoleptic properties was also performed.

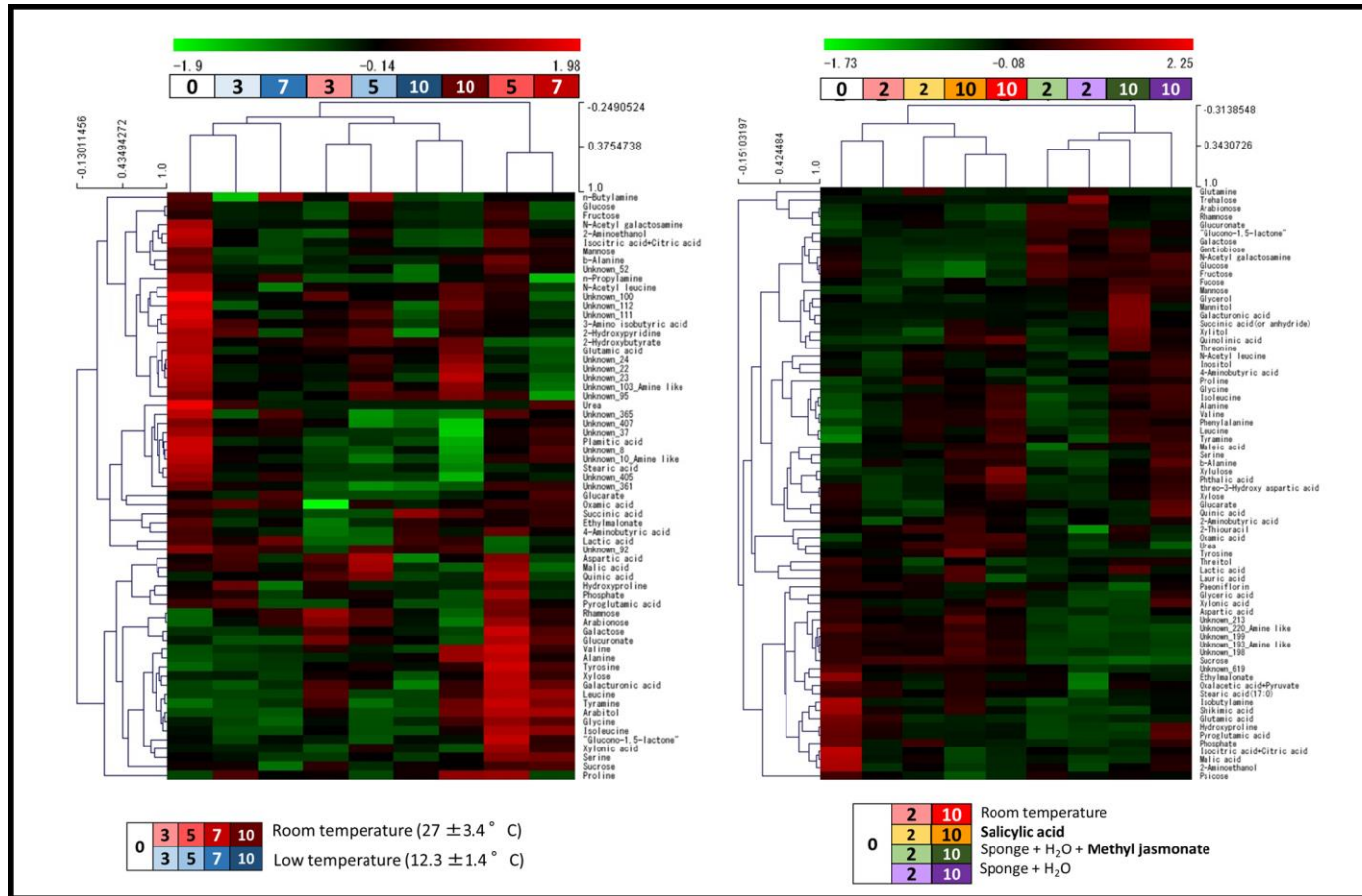


Figure 31. Distribution of metabolites analyzed using GC-MS during mangosteen LT and SI storage treatment in flesh part. Stored-mangosteen was observed for 10 days. Metabolite distribution during storage was employed and analyzed using Hierarchical Cluster Analysis. HCA parameter * correlation: Pearson correlation, average linked cluster analysis. Color boxes represent each postharvest treatment. All treatments were analyzed together using GC-MS.

In mangosteen flesh part, glucuronate and several amino acids that are reported to be aroma metabolites precursors (β -alanine, isoleucine, valine, alanine) seem to be inhibited in LT treatment (Figure 32). The inhibition of amino acid biosynthesis was presumably caused by hypoxia condition that was more profound in flesh part after LT treatment. Previous research indicated the decrease of oxygen concentration in flesh part compared to peel part as reported in apple and pear^{177,178,191}. Meanwhile, most of metabolites relative intensity related to sweet-acidic taste quality (glucose, sucrose, fructose, citric acid, malic acid, quinic acid, and lactic acid) did not show any significant differences between LT treatment and control during mangosteen storage.

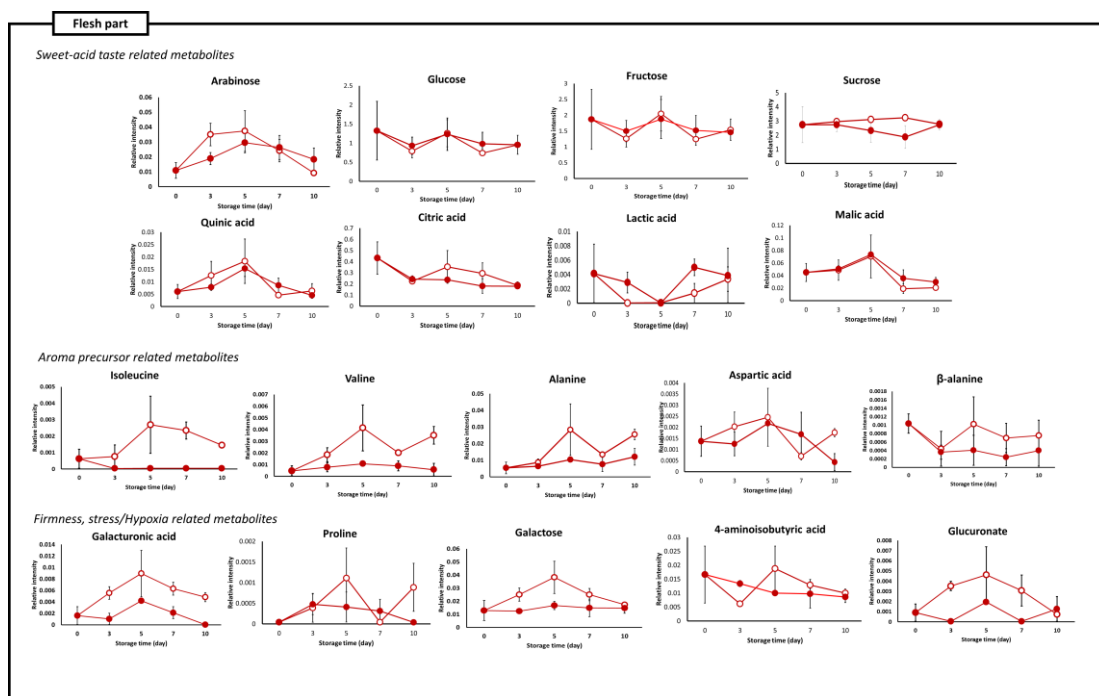


Figure 32. Line graph of metabolite changes analysis using GC-MS during mangosteen LT treatment in flesh part. The relative intensity of metabolites that are important during mangosteen postharvest treatment at low temperature and room time temperature were explained using a line chart. Y-axis represents metabolites relative intensity and X-axis represents day after storage. White circle represents room temperature treatment and black circle represents low-temperature treatment. Day 1 sample of flesh was removed from analysis because it is an outlier.

Moreover, the relative intensity of important metabolites between SI and control were compared using a line chart in a time course manner between day 0, 2, and 10. Most of the important metabolites relative intensity were not affected by SI treatment (Figure 33). This finding further strengthens that stress inducer treatments did not show any effect to prolong mangosteen shelf-life based on metabolite abundance. Based on the results, the LT treatment showed the most effective method to prolong mangosteen shelf-life and further development of postharvest technology in mangosteen should be introduced in the future.

Although previous reports mentioned that a combination of several postharvest treatments (1-MCP, methyl jasmonate (MeJa), and salicylic acid, edible coating) was effective to prolong mangosteen shelf life ^{125,186,189}, our results showed that when tested individually, only LT treatment showed a profound effect. Further studies to assess the effect of postharvest treatment on sensory attributes such as flavor, taste, and aroma should be investigated to confirm consumer acceptance. In addition, application of other omics approaches may validate and strengthen the results obtained in this study.

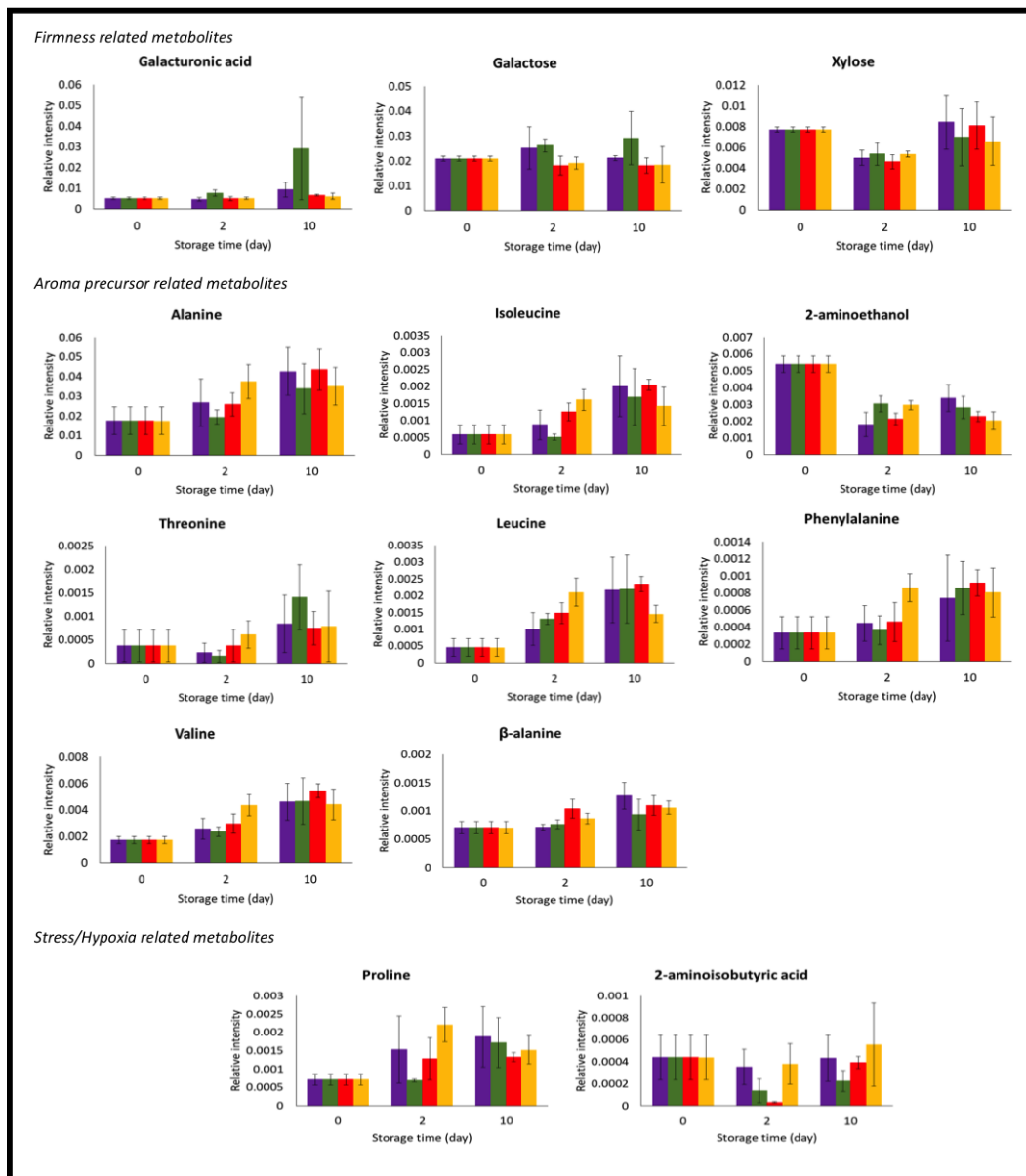


Figure 33. Bar graph of metabolite changes analysis using GC-MS during mangosteen SI treatment in flesh part. The relative intensity of metabolites that are important during mangosteen postharvest treatment at stress inducer treatment and room temperature were explained using a line chart. The metabolites were dominated by saccharides, organic acids, and amino acids. The peak intensity of each metabolite was normalized based on ribitol internal standard. Y-axis represents metabolites relative intensity and X-axis represents day after storage. The colored bar graph represented each of the SI treatments.

4.4. Conclusions

Finally, the study of mangosteen postharvest technology using a metabolomics approach provides further information about the chemical mechanism of several physio-chemical results such as pericarp hardening during mangosteen storage treatment. Metabolomics approach offers a great advantage to discover metabolites and metabolic associations correlated with fruit quality traits such as color, texture, and flavor. The present study marked the first investigation using GC-MS based metabolomics approach to evaluate the effect of different harvesting and ripening conditions as well as postharvest technology in mangosteen. In addition, this is the first report of the use of PLS analysis to correlate metabolite intensity and color changes as a physical parameter for maturity indices of mangosteen in different ripening process conditions. The results from this study can provide a better understanding of mangosteen postharvest strategies and quality control by controlling changes in metabolites involved in ripening.

In conclusions, the combination of several postharvest treatments (1-MCP, methyl jasmonate (MeJa), and salicylic acid, edible coating (alginate, chitosan)) that are performed in the previous studies^{125,186,189} using mangosteen did not have any significant effect regardless the treatment in low temperature to reach the flesh part. Furthermore, the better validation method such as sensory attributes that are related to flavor, taste, and aroma should be furtherly investigated to confirm the acceptance of after-storage mangosteen among mangosteen consumer. In addition, another platform of omics approaches need to be performed to validate and strengthen the results obtained in this study

Chapter 5

Conclusions and perspectives

Advances in fruit metabolomics in recent time have allowed the precise selection of desirable traits along with offering the opportunity to better understand the mechanism of ripening process in mangosteen. The shift of technology from targeted single metabolite analysis to high throughput assays generating footprints of a variety of metabolites in one go has paved the way for discovery or construction of better postharvest technology and identification of contributed metabolites during ripening process. In the last decade, the implementation of metabolomics has allowed determining their specific contribution toward improving key plant attributes such as quality, yield, shelf-life, etc. This study was performed to anticipate that the integration of metabolomics and the other omics tools greatly improve the ability of plant breeder that adequately meet the challenges of 21st-century agriculture.

Fruit ripening process is a process that involves several changes as a result of dynamic process of molecular and biochemical changes caused by genetic and/or environmental condition around fruits. Banana, mango, tomato, and papaya are several examples of climacteric fruits that are dependently affected by the concomitant burst of ethylene. The changes in fruit characteristics during ripening stages contribute to fruit sensory quality. Mangosteen (*Garcinia mangostana*) is one of climacteric fruits that are often referred to as “Queen of Fruits” due to its distinctive appearance and unique taste. Mangosteen is a rich source of vitamin C and has numerous nutritional benefits for

humans, which makes it an attractive nutraceutical. Understanding the changes that occur during ripening is necessary in order to assess optimal harvest maturity and the quality of fruit as it is marketed to the consumer as well as to devise appropriate postharvest packaging and handling strategies. In this study, Gas Chromatography-Mass Spectrometry (GC-MS)-based metabolite profiling was performed in peel, flesh and seed parts of mangosteen to gain insight on metabolic changes during mangosteen ripening stages. In addition, multivariate analysis was performed to correlate specific metabolites with color changes that occur during the ripening process. The obtained data showed that there are metabolic changes throughout ripening stages. By using multivariate analysis, elucidation of the metabolic changes related to cell-wall degradation related metabolites (galacturonic acid, xylose, xylulose+ribulose galactose), a flavor and aroma precursor metabolites (sucrose, glucose, fructose, several organic acids) quality that strongly correlated with the color changes of each ripening stages were successfully performed.

Further investigation of fruit ripening processes was explained in the second part. The application of metabolomics approach offers the possibility to give better understanding of biochemical changes occur in different ripening condition. In this part, the results showed a comparison between different ripening conditions was observed in the consistent metabolic profiles based on color changes of each ripening stages. Consequently, the quality-related metabolites did not show significant differences between “on-tree” and “off-tree” ripening condition. The results in this study also supported the experimental design for further metabolomics study, where the weather, the physiological condition did not give any significant effect as well as described in the color changes during ripening process.

Consequently, the information gained about mangosteen fruit ripening process was used as a basis to select the most-favorable postharvest treatment using metabolomics approach. Several postharvest technologies (low temperature, edible coating) have been extensively developed to reach the most-favorable condition either for quality improvement or shelf-life improvement especially in agricultural products such as fruits. Several postharvest treatments were reported as a successful treatment to prolong mangosteen shelf-life based on physicochemical parameter observation. Low temperature and stress inducer (methyl jasmonate, salicylic acid) were selected to be evaluated by using metabolomics approach. The metabolome data and color changes observation showed that low-temperature treatment could prolong mangosteen shelf-life among all treatments in all part. Several ripening-associated metabolites were affected after postharvest treatment. In contrast, stress inducer treatments did not show any significant changes and did not give effect to prolong mangosteen shelf-life based on color changes and metabolome analysis. In conclusion, the results of metabolomics analysis indicated a positive role of color changes as an indicator of maturity during mangosteen ripening process.

This thesis study showed the strength of metabolomics as an important tool to support postharvest fruit development and ripening studies. It is the first report on *Garcinia mangostana* metabolic profile focusing on the quality after postharvest treatment throughout its ripening stages. The results of this study proved the strong correlation between metabolic profiles and color changes can be an effective tool for further investigation of postharvest effect in *Garcinia mangostana*. As a high-throughput method, the presented method was able to focus on a global monitor of metabolites

changes in the samples at various stages, which can be used to aid postharvest technology development in the future.

References

1. Liu, M., Pirrello, J., Chervin, C., Roustan, J.-P. & Bouzayen, M. Update on Ethylene Control of Fruit Ripening Ethylene Control of Fruit Ripening: Revisiting the Complex Network of Transcriptional Regulation. *Plant Physiol.* **169**, 2380–2390 (2015).
2. Marriott, J. & Palmer, J. K. Bananas — physiology and biochemistry of storage and ripening for optimum quality. *CRC Crit. Rev. Food Sci. Nutr.* **13**, 41–88 (1980).
3. Pirrello, J. Regulation of tomato fruit ripening. *CAB Rev. Perspect. Agric. Vet. Sci. Nutr. Nat. Resour.* **4**, 1–14 (2009).
4. Klie, S. *et al.* Conserved changes in the dynamics of metabolic processes during fruit development and ripening across species. *Plant Physiol.* **164**, 55–68 (2014).
5. Osorio, S. *et al.* Integrative Comparative Analyses of Transcript and Metabolite Profiles from Pepper and Tomato Ripening and Development Stages Uncovers Species-Specific Patterns of Network Regulatory Behavior. *Plant Physiol.* **159**, 1713–1729 (2012).
6. Osorio, S. *et al.* Molecular regulation of fruit ripening. *Front. Plant Sci.* **4**, 198–206 (2013).
7. Bouzayen, M., Latché, A., Nath, P. & Pech, J. C. Mechanism of Fruit Ripening. in *Plant Developmental Biology-Biotechnological Perspectives* **1**, (Springer, 2010).
8. Guo, H. & Ecker, J. R. The ethylene signaling pathway: New insights. *Curr. Opin. Plant Biol.* **7**, 40–49 (2004).
9. Karlova, R. *et al.* Transcriptional control of fleshy fruit development and ripening. *J. Exp. Bot.* **65**, 4527–4541 (2014).
10. In, B. C., Strable, J., Binder, B. M., Falbel, T. G. & Patterson, S. E. Morphological and molecular characterization of ethylene binding inhibition in carnations. *Postharvest Biol. Technol.* **86**, 272–279 (2013).

11. Kim, J. Y. *et al.* Sound waves delay tomato fruit ripening by negatively regulating ethylene biosynthesis and signaling genes. *Postharvest Biol. Technol.* **110**, 43–50 (2015).
12. Gapper, N. E., Mcquinn, R. P. & Giovannoni, J. J. Molecular and genetic regulation of fruit ripening. *Plant Mol. Biol.* **82**, 575–591 (2013).
13. Paul, V., Pandey, R. & Srivastava, G. C. The fading distinctions between classical patterns of ripening in climacteric and non-climacteric fruit and the ubiquity of ethylene-An overview. *J. Food Sci. Technol.* **49**, 1–21 (2012).
14. Palma, J. M., Corpas, F. J. & del Rio, L. A. Proteomics as an approach to the understanding of the molecular physiology of fruit development and ripening. *J. Proteomics* **74**, 1230–1243 (2011).
15. D’Ambrosio, C. *et al.* Proteomic analysis of apricot fruit during ripening. *J. Proteomics* **78**, 39–57 (2013).
16. Seymour, G. B., Chapman, N. H., Chew, B. L. & Rose, J. K. C. Regulation of ripening and opportunities for control in tomato and other fruits. *Plant Biotechnol. J.* **11**, 269–278 (2013).
17. Wang, K. L., Li, H. & Ecker, J. R. Ethylene Biosynthesis and Signaling Networks. *Plant Cell* **14**, 131–152 (2002).
18. Nakatsuka, A., Shiomi, S., Kubo, Y. & Inaba, A. Expression and internal feedback regulation of ACC synthase and ACC oxidase genes in ripening tomato fruit. *Plant Cell Physiol.* **38**, 1103–1110 (1997).
19. Liu, M., Pirrello, J., Chervin, C., Roustan, J. P. & Bouzayen, M. Ethylene Control of Fruit Ripening: Revisiting the Complex Network of Transcriptional Regulation. *Plant Physiol.* **169**, 2380–90 (2015).
20. Xiao, Y. Y. *et al.* Banana ethylene response factors are involved in fruit ripening through their interactions with ethylene biosynthesis genes. *J. Exp. Bot.* **64**, 2499–2510 (2013).
21. Asif, M. H. *et al.* Transcriptome analysis of ripe and unripe fruit tissue of banana identifies major metabolic networks involved in fruit ripening process. *BMC Plant Biol.* **14**, 316 (2014).

22. Hayama, H., Shimada, T., Fujii, H., Ito, A. & Kashimura, Y. Ethylene-regulation of fruit softening and softening-related genes in peach. *J. Exp. Bot.* **57**, 4071–4077 (2006).
23. Hayama, H., Tatsuki, M., Ito, A. & Kashimura, Y. Ethylene and fruit softening in the stony hard mutation in peach. *Postharvest Biol. Technol.* **41**, 16–21 (2006).
24. Lewinsohn, E. *et al.* Not just colors—carotenoid degradation as a link between pigmentation and aroma in tomato and watermelon fruit. *Trends Food Sci. Technol.* **16**, 407–415 (2005).
25. Asensio, E., Sanvicente, I., Mallor, C. & Menal-Puey, S. Spanish traditional tomato. Effects of genotype, location and agronomic conditions on the nutritional quality and evaluation of consumer preferences. *Food Chem.* **270**, 452–458 (2019).
26. Campbell, A. D. & Labavitch, J. M. Induction and Regulation of Ethylene Biosynthesis and Ripening by Pectic Oligomers in Tomato Pericarp Discs. *Plant Physiol* **97**, 706–713 (1991).
27. Palapol, Y. *et al.* Colour development and quality of mangosteen (*Garcinia mangostana* L.) fruit during ripening and after harvest. *Postharvest Biol. Technol.* **51**, 349–353 (2009).
28. Lombardo, V. A. *et al.* Metabolic Profiling during Peach Fruit Development and Ripening Reveals the Metabolic Networks That Underpin Each Developmental Stage. *Plant Physiol.* **157**, 1696–1710 (2011).
29. Dave, R. K., Rao, T. V. R. & Nandane, A. S. Improvement of post-harvest quality of pear fruit with optimized composite edible coating formulations. *J. Food Sci. Technol.* **54**, 3917–3927 (2017).
30. Ali, A., Muhammad, M. T. M., Sijam, K. & Siddiqui, Y. Effect of chitosan coatings on the physicochemical characteristics of Eksotika II papaya (*Carica papaya* L.) fruit during cold storage. *Food Chem.* **124**, 620–626 (2011).
31. Díaz-Mula, H. M., Serrano, M. & Valero, D. Alginate Coatings Preserve Fruit Quality and Bioactive Compounds during Storage of Sweet Cherry Fruit. *Food Bioprocess Technol* **5**, 2990–2997 (2012).

32. Suseno, N., Savitri, E., Sapei, L. & Padmawijaya, K. S. Improving Shelf-life of Cavendish Banana Using Chitosan Edible Coating. *Procedia Chem.* **9**, 113–120 (2014).
33. Oms-Oliu, G., Soliva-Fortuny, R. & Martín-Belloso, O. Using polysaccharide-based edible coatings to enhance quality and antioxidant properties of fresh-cut melon. *LWT - Food Sci. Technol.* **41**, 1862–1870 (2008).
34. De Moraes, K. S., Fagundes, C., Melo, M. C., Andreani, P. & Monteiro, A. R. Conservation of Williams pear using edible coating with alginate and carrageenan. *Cienc. E Tecnol. Aliment.* **32**, 679–684 (2012).
35. Te-Chato, S. Floral and fruit morphology of some species in *Garcinia* spp. *Songklanakar J. Sci. Technol.* **29**, 245–252 (2007).
36. Palakawong, C. & Delaquis, P. Mangosteen processing: A review. *J. Food Process. Preserv.* **42**, 1–10 (2018).
37. Chaovanalikit, A. *et al.* Anthocyanin and total phenolics content of mangosteen and effect of processing on the quality of Mangosteen products. *Int. Food Res. J.* **19**, 1047–1053 (2012).
38. Mahabusarakam, W. & Wiriyachitra, P. Chemical constituents of *Garcinia mangostana*. *J. Nat. Prod.* **50**, 474–478 (1987).
39. Gutierrez-Orozco, F. & Failla, M. L. Biological activities and bioavailability of mangosteen xanthenes: A critical review of the current evidence. *Nutrients* **5**, 3163–3183 (2013).
40. Karthiga, P., Soranam, R. & Annadurai, G. Alpha-mangostin, the Major Compound from *Garcinia mangostana* Linn. Responsible for Synthesis of Ag Nanoparticles: Its Characterization and Evaluation Studies. *Research Journal of Nanoscience and Nanotechnology* **2**, 46–57 (2012).
41. Pedraza-Chaverri, J., Cárdenas-Rodríguez, N., Orozco-Ibarra, M. & Pérez-Rojas, J. M. Medicinal properties of mangosteen (*Garcinia mangostana*). *Food Chem. Toxicol.* **46**, 3227–3239 (2008).
42. Shibata, M., Matoba, Y., Tosa, H. & Iinuma, M. Effects of Mangosteen Pericarp Extracts Against Mammary Cancer. *Altern. Integr. Med.* **2**, 8–12 (2013).

43. Paull, R. E. & Ketsa, S. *Mangosteen. Agriculture Handbook No. 66. The commercial storage of fruits, vegetables, and florist and nursery stocks* (2002).
44. Paull, R. E. & Ketsa, S. Mangosteen: Postharvest Quality-Maintenance Guidelines. *Fruit, Nut, Beverage Crop*. 30–32 (2014).
45. Sukatta, U. *et al.* Distribution of Major Xanthones in the Pericarp, Aril, and Yellow Gum of Mangosteen (*Garcinia Mangostana* Linn.) Fruit and Their Contribution to Antioxidative Activity. *Biosci. Biotechnol. Biochem.* **77**, 984–987 (2013).
46. Mansyah, E., Sobir, Santosa, E., Sisharnin, A. & Sulassih. Polymorphic Marker Designed from Bioinformatics Sequences Related to Cell Wall Strength for Discrimination of Mangosteen (*Garcinia Mangostana* L.) Clones Resistant to Gamboge Disorder. *Int. J. Agric. Biosyst. Eng.* **6**, 1023–1028 (2012).
47. Sdoodee, S. & Chiarawipa, R. Regulating irrigation during pre-harvest to avoid the incidence of translucent flesh disorder and gamboge disorder of mangosteen fruits. *Songklanakarin J.Sci. Technol* **27**, 957–965 (2005).
48. Dorly, Tjitrosemito, S., Poerwanto, R. & Juliarni. Secretory Duct Structure and Phytochemistry Compounds of Yellow Latex in Mangosteen Fruit. *Hayati J. Biosci.* **15**, 99–104 (2008).
49. Rai, I., Wiraatmaja, I., Semarajaya, C., Arsana, D. & Astiari, A. Control of Yellow Latex on Mangosteen Fruit by Using Drip Irrigation and Chitosan Antitranspirant. *J.Hort* **24**, 307–315 (2014).
50. Pechkeo, S., Sdoodee, S. & Nilnond, C. The Effects of Calcium and Boron Sprays on the Incidence of Translucent Flesh Disorder and Gamboge Disorder in Mangosteen (*Garcinia mangostana* L.). *Kasetart J. (Nat. Sci.)* **41**, 621–632 (2007).
51. Tongdee, S. C. & Suwanagul, A. Postharvest Mechanical Damage in Mangosteens. *Asean Food J.* **4**, 151–155 (1989).
52. Lerslerwong, L., Rugkong, A., Imsabai, W. & Ketsa, S. The harvest period of mangosteen fruit can be extended by chemical control of ripening-A proof of concept study. *Sci. Hortic.* **157**, 13–18 (2013).

53. Kurniawati, A., Poerwanto, R., Efendi, D. & Cahyana, H. Character, Xanthone Content and Antioxidant Properties of Mangosteen Fruit's Hull (*Garcinia mangostana* L.) at Several Fruit Growth Stadia. *J. Agron. Indones.* **39**, 188–192 (2011).
54. Dangcham, S. & Ketsa, S. Relationship between Maturity Stages and Low Temperature Involved in the Pericarp Hardening of Mangosteen Fruit after Storage. *Thai J. Agric. Sci.* **40**, 3–4 (2007).
55. BPS-Statistics Indonesia. *Indonesia Statistics of Annual Fruit and Vegetable Plants 2013*. (2014).
56. BPS-Statistics Indonesia. *Indonesia Statistics of Annual Fruit and Vegetable Plants 2011*. (2012).
57. BPS-Statistics Indonesia. *Indonesia Statistics of Annual Fruit and Vegetable Plants 2012*. (2013).
58. BPS-Statistics Indonesia. *Indonesia Statistics of Annual Fruit and Vegetable Plants 2015*. (2016).
59. BPS-Statistics Indonesia. *Indonesia Statistics of Annual Fruit and Vegetable Plants 2016*. (2017).
60. Richards, A. J. Studies in *Garcinia*, dioecious tropical fruit trees: the origin of the mangosteen (*G. mangostana* L.). *Bot. J. Linn. Soc.* **103**, 301–308 (1990).
61. Othman Yaacob. & Tindall, H. D. *Mangosteen cultivation*. (Food and Agriculture Organization of the United Nations, 1995).
62. Harahap, F., Poerwanto, R., Suriani, C. & Rahayu, S. In Vitro Growth and Rooting of Mangosteen (*Garcinia mangostana* L.) on Medium with Different Concentrations of Plant Growth Regulator. *Hayati J. Biosci.* **21**, 151–158 (2014).
63. Poerwanto, R. *et al.* Study Peningkatan Kualitas Buah Manggis (Study on Mangosteen Fruit Quality Improvements). in *Prosiding Seminar Hasil-Hasil Penelitian IPB* (2011).

64. Akmal, A., Handayani, R. S., Yunus, I., Santosa, E. & Poerwanto, R. The Relationship between Transpiration and Calcium Fertilization on Mangosteen (*Garcinia mangostana* L.) Seedlings. *J. Trop. Hortic.* **1**, 15 (2018).
65. Hapsari, D. P., Poerwanto, R., Sopandie, D. & Santosa, E. Partial root-zone irrigation effects on growth, metabolism and calcium status of Mangosteen seedling (*Garcinia mangostana* L.). *Adv. Hortic. Sci.* **32**, 49–59 (2018).
66. Hidayati, I., Poerwanto, R. & Efendi, D. Study of Postharvest Quality Changes of Mangosteen Fruit (*Garcinia mangostana* L.) at Several Stage of Maturity and Storage Temperature. in *Kemandirian Produk Hortikultura untuk memenuhi pasar domestik dan ekspor* 932–942 (2011).
67. Setiawan, E., Poerwanto, R., Fukuda, F. & Kubota, N. Meteorological Conditions of Mangosteen Orchard in West Java, Indonesia and Seasonal Changes in C-N Ratio of Their Leaves as Affected by Sector (Position in Canopy) and Tree Age. (Faculty of Agriculture Okayama University, 2012).
68. Viviani, P. & Aymoz, C. Colour, form, and movement are not perceived simultaneously. *Vision Res.* **41**, 2909–2918 (2001).
69. Hanafy, I. M. & Sanad, R. Colour preferences according to educational background. *Procedia - Soc. Behav. Sci.* **205**, 437–444 (2015).
70. Gong, R., Wang, Q., Hai, Y. & Shao, X. Investigation on factors to influence color emotion and color preference responses. *Optik.* **136**, 71–78 (2017).
71. Nascimento, S. M. C. *et al.* The colors of paintings and viewers preferences. *Vision Res.* **130**, 76–84 (2017).
72. Platts, J. Newton, Goethe and the process of perception: an approach to design. *Opt. Laser Technol.* **38**, 205–209 (2006).
73. Luo, M. R. Applying colour science in colour design. *Opt. Laser Technol.* **38**, 392–398 (2006).
74. Harkness, N., Boyle, R., Da Vinci, L., Goethe, E. & Hering, A. M. The colour wheels of art, perception, science and physiology. *Opt. Laser Technol.* **38**, 219–229 (2006).

75. Soteriou, G. A., Kyriacou, M. C., Siomos, A. S. & Gerasopoulos, D. Evolution of watermelon fruit physicochemical and phytochemical composition during ripening as affected by grafting. *Food Chem.* **165**, 282–289 (2014).
76. Hashim, N. Determination of baseline qualities of malaysian export-grade starfruits. (Universiti Putra Malaysia, 2008).
77. Krajayklang, M., Klieber, A. & Dry, P. R. Colour at harvest and post-harvest behaviour influence paprika and chilli spice quality. *Postharvest Biol. Technol.* **20**, 269–278 (2000).
78. Tepić, A. N. & Vujičić, B. L. Colour change in pepper (*Capsicum annuum*) during storage. *Acta Period. Technol.* **35**, 59–64 (2004).
79. Kienzle, S. *et al.* Harvest maturity specification for mango fruit (*Mangifera indica* L. 'Chok Anan') in regard to long supply chains. *Postharvest Biol. Technol.* **61**, 41–55 (2011).
80. Liamnimitr, N. *et al.* Optimization of bulk modified atmosphere packaging for long-term storage of 'Fuyu' persimmon fruit. *Postharvest Biol. Technol.* **135**, 1–7 (2017).
81. Ghavidel, R. A. *et al.* Effect of selected edible coatings to extend shelf-life of fresh cut apples. *Int. J. Agric. Crop Sci.* **6**, 1171–1178 (2013).
82. Ibarra-Garza, I. P., Ramos-Parra, P. A., Hernandez-Brenes, C. & Jacobo-Velazquez, D. A. Effects of postharvest ripening on the nutraceutical and physicochemical properties of mango (*Mangifera indica* L. cv Keitt). *Postharvest Biol. Technol.* **103**, 45–54 (2015).
83. Alkarkhi, A. F. M., Ramli, S., Yong, Y. S. & Mat Easa, A. Comparing physicochemical properties of banana pulp and peel flours prepared from green and ripe fruits. *Food Chem.* **129**, 312–318 (2011).
84. Gomes, J. F. S., Vieira, R. R. & Leta, F. R. Colorimetric indicator for classification of bananas during ripening. *Sci. Hortic.* **150**, 201–205 (2013).
85. Abdul-Hamid, N. *et al.* Quality Evaluation of the Physical Properties, Phytochemicals, Biological Activities and Proximate Analysis of Nine Saudi Date

- Palm Fruit Varieties. *J. Saudi Soc. Agric. Sci.* (2018).
doi:10.1016/j.jssas.2018.08.004
86. Tosetti, R. *et al.* Molecular and biochemical responses to wounding in mesocarp of ripe peach (*Prunus persica* L. Batsch) fruit. *Postharvest Biol. Technol.* **90**, 40–51 (2014).
 87. Putri, S. P. *et al.* Current metabolomics: Practical applications. *J. Biosci. Bioeng.* **115**, 579–589 (2013).
 88. Putri, S. P., Yamamoto, S., Tsugawa, H. & Fukusaki, E. Current metabolomics: Technological advances. *J. Biosci. Bioeng.* **116**, 9–16 (2013).
 89. Fiehn, O. Metabolomics - the link between genotypes and phenotypes. *Plant Mol. Biol.* **48**, 155–171 (2002).
 90. Fiehn, O. *et al.* Mass-spectrometry-based metabolomics: limitations and recommendations for future progress with particular focus on nutrition research. *Metabolomics* **5**, 435–458 (2009).
 91. Sugimoto, M., Kawakami, M., Robert, M., Soga, T. & Tomita, M. Bioinformatics Tools for Mass Spectroscopy-Based Metabolomic Data Processing and Analysis. *Curr. Bioinform.* **7**, 96–108 (2012).
 92. Agin, A. *et al.* Metabolomics - an overview. From basic principles to potential biomarkers (part 1). *Med. Nucl.* **40**, 4–10 (2016).
 93. Liesenfeld, D. B., Habermann, N., Owen, R. W., Scalbert, A. & Ulrich, C. M. Review of mass spectrometry-based metabolomics in cancer research. *Cancer Epidemiol. Biomarkers Prev.* **22**, 2182–2201 (2013).
 94. Shulaev, V. Metabolomics technology and bioinformatics. *Brief. Bioinform.* **7**, 128–139 (2006).
 95. Ernst, M., Silva, D. B., Silva, R. R., Encio, R. Z. N. & Lopes, N. P. Mass spectrometry in plant metabolomics strategies: from analytical platforms to data acquisition and processing. *Nat. Prod. Rep.* **31**, 784–806 (2014).
 96. Verpoorte, R., Choi, Y. H. & Kim, H. K. Metabolomics: Will it stay? *Phytochem. Anal.* **21**, 2–3 (2010).

97. Kim, H. K. & Verpoorte, R. Sample preparation for plant metabolomics. *Phytochem. Anal.* **21**, 4–13 (2010).
98. Putri, S. P. *et al.* Current metabolomics: Practical applications. *J. Biosci. Bioeng.* **115**, 579–589 (2013).
99. Allwood, J. W. & Goodacre, R. An introduction to liquid chromatography-mass spectrometry instrumentation applied in plant metabolomic analyses. *Phytochem. Anal.* **21**, 33–47 (2010).
100. Dunn, W. B. *et al.* Mass appeal: metabolite identification in mass spectrometry-focused untargeted metabolomics. *Metabolomics* **9**, 44–66 (2012).
101. Lisec, J., Schauer, N., Kopka, J., Willmitzer, L. & Fernie, A. R. Gas chromatography mass spectrometry–based metabolite profiling in plants. *Nat. Protoc.* **1**, (2006).
102. Worley, B. & Powers, R. Multivariate Analysis in Metabolomics. *Curr Metabolomics* **1**, 92–107 (2013).
103. Kobayashi, S. *et al.* Gas chromatography-mass spectrometry based metabolic profiling for the identification of discrimination markers of *Angelicae radix* and its application to gas chromatography-flame ionization detector system. *J. Biosci. Bioeng.* **114**, 232–236 (2012).
104. Jumhawan, U., Putri, S. P., Yusianto, Bamba, T. & Fukusaki, E. Application of gas chromatography/flame ionization detector-based metabolite fingerprinting for authentication of Asian palm civet coffee (Kopi Luwak). *J. Biosci. Bioeng.* **120**, 555–561 (2015).
105. Jumhawan, U., Prama Putri, S., Bamba, T. & Fukusaki, E. Quantification of coffee blends for authentication of Asian palm civet coffee (Kopi Luwak) via metabolomics: A proof of concept. *J. Biosci. Bioeng.* **122**, 79–84 (2016).
106. Elo, K., Sasanelli, N., Maxia, A. & Caboni, P. Untargeted Metabolomics of Tomato Plants after Root-Knot Nematode Infestation. *J. Agric. Food Chem.* **64**, 5963–5968 (2016).

107. Fatima, T., Sobolev, A. P., Teasdale, J. & K., A. Fruit metabolite networks in engineered and non-engineered tomato genotypes reveal fluidity in a hormone and agroecosystem specific manner. *Metabolomics* **12**, (2016).
108. Ali, K. *et al.* Monitoring biochemical changes during grape berry development in Portuguese cultivars by NMR spectroscopy. *Food Chem.* **124**, 1760–1769 (2011).
109. Allwood, J. W. *et al.* Metabolomics in melon: A new opportunity for aroma analysis. *Phytochemistry* **99**, 61–72 (2014).
110. Biais, B. *et al.* Metabolic acclimation to hypoxia revealed by metabolite gradients in melon fruit. *J. Plant Physiol.* **167**, 242–245 (2010).
111. Bonghi, C. *et al.* Metabolic Responses to Low Temperature of Three Peach Fruit Cultivars Differently Sensitive to Cold Storage. *Front. Plant Sci.* **9**, 1–16 (2018).
112. Das, S. & De, B. Analyzing changes in metabolite profile during postharvest ripening in *Achras sapota* fruits: GC-MS based metabolomics approach. *Int. Food Res. J.* **22**, 2288–2293 (2015).
113. Hatoum, D., Annaratone, C., Hertog, M. L. A. T. M., Geeraerd, A. H. & Nicolai, B. M. Targeted metabolomics study of ‘Braeburn’ apples during long-term storage. *Postharvest Biol. Technol.* **96**, 33–41 (2014).
114. Kanellis, A. K. *et al.* Differential Metabolic Rearrangements after Cold Storage Are Correlated with Chilling Injury Resistance of Peach Fruits. *Front. Plant Sci.* **7**, 1–15 (2016).
115. Moing, A. *et al.* Extensive metabolic cross-talk in melon fruit revealed by spatial and developmental combinatorial metabolomics. *New Phytol.* **190**, 683–696 (2011).
116. Osorio, S. *et al.* Systems Biology of Tomato Fruit Development: Combined Transcript, Protein, and Metabolite Analysis of Tomato Transcription Factor (nor, rin) and Ethylene Receptor (Nr) Mutants Reveals Novel Regulatory Interactions. *Plant Physiol.* **157**, 405–425 (2011).
117. Yun, Z. *et al.* Comparative transcriptome and metabolome provides new insights into the regulatory mechanisms of accelerated senescence in litchi fruit after cold storage. *Sci. Rep.* **6**, 1–16 (2015).

118. Giovannoni, J. Genetic regulation of fruit development and ripening. *Plant Cell*. **16**, 170–181 (2004).
119. Du, L. *et al.* Proteome changes in banana fruit peel tissue in response to ethylene and high-temperature treatments. *Hortic. Res.* **3**, 16012 (2016).
120. Eccher Zerbini, P. *et al.* Optical properties, ethylene production and softening in mango fruit. *Postharvest Biol. Technol.* **101**, 58–65 (2015).
121. Alexander, L. & Grierson, D. Ethylene biosynthesis and action in tomato: a model for climacteric fruit ripening. *J. Exp. Bot.* **53**, 2039–2055 (2002).
122. Liu, X. *et al.* Characterization of Ethylene Biosynthesis Associated with Ripening in Banana Fruit. *Plant Physiol.* **121**, 1257–1265 (1999).
123. Eaks, I. L. Ripening, Respiration, and Ethylene Production of ‘Hass’ Avocado Fruits at 20° to 40°C. *J. Amer. Soc. Hort. Sci* **103**, 576–578 (1978).
124. Bron, I. U. *et al.* Temperature-related changes in respiration and Q10 coefficient of Guava. *Sci. Agric. Piracicaba* **62**, 458–463 (2005).
125. Piriyaivinit, P., Ketsa, S. & van Doorn, W. G. 1-MCP extends the storage and shelf life of mangosteen (*Garcinia mangostana* L.) fruit. *Postharvest Biol. Technol.* **61**, 15–20 (2011).
126. de Castro, M. F. P. P. M., Anjos, V. D. D., Rezende, A. C. B., Benato, E. A. & Valentini, S. R. D. Postharvest technologies for mangosteen (*Garcinia mangostana* L.) conservation. *Cienc. E Tecnol. Aliment.* **32**, 668–672 (2012).
127. Bunsiri, A., Ketsa, S. & Paull, R. E. Phenolic metabolism and lignin synthesis in damaged pericarp of mangosteen fruit after impact. *Postharvest Biol. Technol.* **29**, 61–71 (2003).
128. Astuti, R. *et al.* Risks and Risks Mitigations in the Supply Chain of Mangosteen : A Case Study. *Oper. Supply Chain Manag.* **6**, 11–25 (2013).
129. Poerwanto, R., Efendi, D., Bintang, M. & Muchtadi, D. *Fisiologi Pengerasan Perikarp Buah Manggis (Hardening Physiology of Mangosteen Pericarp)*. (2012).
130. Wittenauer, J., Falk, S., Schweiggert-Weisz, U. & Carle, R. Characterisation and quantification of xanthenes from the aril and pericarp of mangosteens (*Garcinia*

- mangostana* L.) and a mangosteen containing functional beverage by HPLC-DAD-MS n. *Food Chem.* **134**, 445–452 (2012).
131. Yodhnu, S., Sirikatitham, A. & Wattanapiromsakul, C. Validation of LC for the determination of alpha-mangostin in mangosteen peel extract: a tool for quality assessment of *Garcinia mangostana* L. *J. Chromatogr. Sci.* **47**, 185–189 (2009).
 132. Ketsa, S. & Atantee, S. Phenolics, lignin, peroxidase activity and increased firmness of damaged pericarp of mangosteen fruit after impact. *Postharvest Biol. Technol.* **14**, 117–124 (1998).
 133. Voss, D. H. Relating Colorimeter Measurement of Plant Color to the Royal Horticultural Society Colour Chart. *Hortic. Sci.* **27**, 1256–1260 (1992).
 134. Tsugawa, H., Tsujimoto, Y., Arita, M., Bamba, T. & Fukusaki, E. GC/MS based metabolomics: development of a data mining system for metabolite identification by using soft independent modeling of class analogy (SIMCA). *BMC Bioinformatics* **12**, 131 (2011).
 135. Tsugawa, H. Advances in computational metabolomics and databases deepen the understanding of metabolisms. *Curr. Opin. Biotechnol.* **54**, 10–17 (2018).
 136. Fiehn, O. *et al.* The metabolomics standards initiative (MSI). *Metabolomics* **3**, 175–178 (2007).
 137. Amal, S. H., El-Mogy, M. M., Aboul-Anean, H. E. & Alsanius, B. W. Improving Strawberry Fruit Storability by Edible Coating as a Carrier of Thymol or Calcium Chloride. *J. Hortic. Sci. Orn. Plants* **2**, 88–97 (2010).
 138. Haven, W. & River, H. Effect of Polysaccharide Coatings on Quality of Fresh Cut Mangoes (*Mangifera indica*). *Sci. Technol.* **117**, 382–388 (2004).
 139. Amal, S. H., El-Mogy, M. M., Aboul-Anean, H. E. & Alsanius, B. W. Improving Strawberry Fruit Storability by Edible Coating as a Carrier of Thymol or Calcium Chloride. *J. Hortic. Sci. Orn. Plants* **2**, 88–97 (2010).
 140. Abdi, H. E. Partial least squares regression and projection on latent structure regression (PLS Regression). *WIREs Comp Stat* **2**, 97–106 (2010).

141. Merchante, C. *et al.* Ethylene is involved in strawberry fruit ripening in an organ-specific manner. *J. Exp. Bot.* **64**, 4421–4439 (2013).
142. Wang, H., Zhi, W., Qu, H., Lin, H. & Yueming, J. Application of α -aminoisobutyric acid and β -aminoisobutyric acid inhibits pericarp browning of harvested longan fruit. *Chem. Cent. J.* **9**, 1–8 (2015).
143. Yamada, Y. *et al.* Effects of the Rare Sugars D-psicose and D-tagatose on the Sugar Content and Incidence of Blossom End Rot in Tomato Grown Hydroponically with Salinity Treatment. *Environ. Control Biol.* **52**, 155–160 (2014).
144. Wang, L. *et al.* System level analysis of cacao seed ripening reveals a sequential interplay of primary and secondary metabolism leading to polyphenol accumulation and preparation of stress resistance. *Plant J.* **87**, 318–332 (2016).
145. Gillaspay, G., Ben-David, H. & Gruissem', W. Fruits: A Developmental Perspective. *Plant Cell* **5**, 1439–1451 (1993).
146. William, J. Molecular regulation of seed and fruit set. *Trends Plant Sci.* **17**, 1360–1385 (2012).
147. Huan, C. *et al.* Potential role of reactive oxygen species and antioxidant genes in the regulation of peach fruit development and ripening. *Plant Physiol. Biochem.* **104**, 294–303 (2016).
148. Yeung, E., Bailey-Serres, J. & Sasidharan, R. After The Deluge: Plant Revival Post-Flooding. *Trends Plant Sci.* **24**, 443–454 (2019).
149. Ślesak, I., Libik, M., Karpinska, B., Karpinski, S. & Miszalski, Z. The role of hydrogen peroxide in regulation of plant metabolism and cellular signalling in response to environmental stresses. *Acta Biochim. Pol.* **54**, 39–50 (2007).
150. Rodrigues, R. B. *et al.* Total oxidant scavenging capacity of *Euterpe oleracea* Mart. (açai) seeds and identification of their polyphenolic compounds. *J. Agric. Food Chem.* **54**, 4162–4167 (2006).
151. Tian, S., Qin, G. & Li, B. Reactive oxygen species involved in regulating fruit senescence and fungal pathogenicity. *Plant Mol. Biol.* **82**, 593–602 (2013).

152. Kumar, V. *et al.* Fruit ripening mutants reveal cell metabolism and redox state during ripening. *Protoplasma* **253**, 581–594 (2016).
153. Schmidt, R., Kunkowska, A. B. & Schippers, J. H. M. Update on Reactive Oxygen Species Role of Reactive Oxygen Species during Cell Expansion in Leaves. *Plant Physiol.* **172**, 2098–2106 (2016).
154. Tsai, K. J., Lin, C. Y., Ting, C. Y. & Shih, M. C. Ethylene-Regulated Glutamate Dehydrogenase Fine-Tunes Metabolism during Anoxia-Reoxygenation. *Plant Physiol.* **172**, 1548–1562 (2016).
155. Lara, M. V *et al.* Peach (*Prunus Persica*) Fruit Response to Anoxia: Reversible Ripening Delay and Biochemical Changes. *Plant cell Physiol.* **52**, 392–403 (2011).
156. Magwaza, L. S., Opara, U. L., Cronje, P. J. R., Landahl, S. & Terry, L. A. Canopy position affects rind biochemical profile of ‘Nules Clementine’ mandarin fruit during postharvest storage. *Postharvest Biol. Technol.* **86**, 300–308 (2013).
157. Muhl, Q. E., Du Toit, E. S., Steyn, J. M. & Apostolides, Z. Bud development, flowering and fruit set of *Moringa oleifera* Lam. (Horseradish Tree) as affected by various irrigation levels. *J. Agric. Rural Dev. Trop. Subtrop.* **114**, 79–87 (2013).
158. Imada, S., Tako, Y., Tani, T., Takaku, Y. & Hisamatsu, S. Translocation and distribution of photosynthetically assimilated ¹³C to ‘Tsugaru’ apple fruits. *J. Agric. Meteorol.* **73**, 187–194 (2017).
159. Gucci, R., Lodolini, E. M. & Rapoport, H. F. Water deficit-induced changes in mesocarp cellular processes and the relationship between mesocarp and endocarp during olive fruit development. *Tree Physiol.* **29**, 1575–1585 (2009).
160. Thammawong, M. & Arakawa, O. Starch Degradation of Detached Apple Fruit in Relation to Ripening and Ethylene. *J. Japanese Soc. Hortic. Sci.* **76**, 345–350 (2007).
161. In, B. & Lim, J. H. Potential vase life of cut roses: Seasonal variation and relationships with growth conditions, phenotypes, and gene expressions. *Postharvest Biol. Technol.* **135**, 93–103 (2018).

162. Liu, J., Hu, X., Yu, J., Yang, A. & Liu, Y. Caffeoyl Shikimate Esterase has a Role in Endocarp Lignification in Peach (*Prunus persica* L.) Fruit. *Hortic. Sci. Technol.* **35**, 59–68 (2017).
163. Zhang, M. Y. *et al.* Distinct transcriptome profiles reveal gene expression patterns during fruit development and maturation in five main cultivated species of pear (*Pyrus* L.). *Sci. Rep.* **6**, 1–12 (2016).
164. Noichinda, S., Bodhipadma, K. & Kong-In, S. Capillary Water in Pericarp Enhances Hypoxic Condition during On-Tree Fruit Maturation That Induces Lignification and Triggers Translucent Flesh Disorder in Mangosteen (*Garcinia mangostana* L.). *J. Food Qual.* **2017**, 1–7 (2017).
165. Dangcham, S., Bowen, J., Ferguson, I. B. & Ketsa, S. Effect of temperature and low oxygen on pericarp hardening of mangosteen fruit stored at low temperature. *Postharvest Biol. Technol.* **50**, 37–44 (2008).
166. Ä Herna Ä Ndez-orte, P. N., Cacho, J. F. & Ferreira, V. Relationship between Varietal Amino Acid Profile of Grapes and Wine Aromatic Composition. Experiments with Model Solutions and Chemometric Study. *J. Agric. Food Chem.* **50**, 2891–2899 (2002).
167. Macleod, A. J. & Gonzalez de Troconis, N. Volatile flavour components of guava. *Phytochemistry* **21**, 1339–1342 (1982).
168. Tieman, D. *et al.* Tomato aromatic amino acid decarboxylases participate in synthesis of the flavor volatiles 2-phenylethanol and 2-phenylacetaldehyde. *Proc. Natl. Acad. Sci.* **103**, 8287–8292 (2006).
169. Laohakunjit, N., Kerdchoechuen, O., Matta, F. B., Silva, J. L. & Holmes, W. E. Postharvest survey of volatile compounds in five tropical fruits using headspace-solid phase microextraction (HS-SPME). *Hort Sci.* **42**, 309–314 (2007).
170. El Hadi, M. A. M., Zhang, F. J., Wu, F. F., Zhou, C. H. & Tao, J. Advances in fruit aroma volatile research. *Molecules* **18**, 8200–8229 (2013).
171. Jumhawan, U. *et al.* Selection of discriminant markers for authentication of asian palm civet coffee (Kopi Luwak): A metabolomics approach. *J. Agric. Food Chem.* **61**, 7994–8001 (2013).

172. Trinh, T., Woon, W., Yu, B., Curran, P. & Liu, S.Q. L-phenylalanine addition on aroma compound formation during longan juice fermentation by a co-culture of *Saccharomyces cerevisiae* and *Williopsis saturnus*. *South African J. Enol. Vitic.* **31**, 116–124 (2010).
173. Zou, J. *et al.* Transcriptome analysis of aroma volatile metabolism change in tomato (*Solanum lycopersicum*) fruit under different storage temperatures and 1-MCP treatment. *Postharvest Biol. Technol.* **135**, 57–67 (2018).
174. Pandey, V. P. *et al.* Papaya fruit ripening: ROS metabolism, gene cloning, characterization and molecular docking of peroxidase. *J. Mol. Catal. B Enzym.* **98**, 98–105 (2013).
175. Yang, S. *et al.* Oxidation and Peroxidation of Postharvest Banana Fruit during Softening. *Pak. J. Bot* **40**, 2023–2029 (2008).
176. António, C. *et al.* Regulation of Primary Metabolism in Response to Low Oxygen Availability as Revealed by Carbon and Nitrogen Isotope Redistribution. *Plant Physiol.* **170**, 43–56 (2016).
177. Ho, Q. T., Verlinden, B. E., Verboven, P., Vandewalle, S. & Nicolai, B. M. A permeation-diffusion-reaction model of gas transport in cellular tissue of plant materials. *J. Exp. Bot.* **57**, 4215–4224 (2006).
178. Ho, Q. T. *et al.* Genotype effects on internal gas gradients in apple fruit. *J. Exp. Bot.* **61**, 2745–2755 (2010).
179. García, M., Casariego, A., Díaz, R. & Roblejo, L. Effect of edible chitosan/zeolite coating on tomatoes quality during refrigerated storage. *Emirates J. Food Agric.* **26**, 238–246 (2014).
180. Raghav, P. K., Agarwal, N. & Saini, M. Edible Coating of Fruits and Vegetables : A Review. *Int. J. Sci. Res. Mod. Educ.* **1**, 2455–5630 (2016).
181. Ren Yinzhe, Y. Y. Effect of Chitosan Coating on Preserving Character of Post-Harvest Fruit and Vegetable: A Review. *J. Food Process. Technol.* **04**, 8–10 (2013).

182. Valero, D. *et al.* Effects of alginate edible coating on preserving fruit quality in four plum cultivars during postharvest storage. *Postharvest Biol. Technol.* **77**, 1–6 (2013).
183. Virginia De Vasconcelos Facundo, H. *et al.* Influence of different banana cultivars on volatile compounds during ripening in cold storage. *Food Res. Int.* **49**, 626–633 (2012).
184. Xi, W. peng *et al.* Intermittent warming alleviated the loss of peach fruit aroma-related esters by regulation of AAT during cold storage. *Postharvest Biol. Technol.* **74**, 42–48 (2012).
185. Cantín, C. M. *et al.* Chilling injury susceptibility in an intra-specific peach [*Prunus persica* (L.) Batsch] progeny. *Postharvest Biol. Technol.* **58**, 79–87 (2010).
186. de Castro, M. F. P., de Almeida Anjos, V. D., Bortolossi Rezende, A. C., Benato, E. A. & de Toledo Valentini, S. R. Postharvest technologies for mangosteen (*Garcinia mangostana* L.) conservation. *Cienc. E Tecnol. Aliment.* **32**, 668–672 (2012).
187. Kondo, S., Ponrod, W., Kanlayanarat, S. & Hirai, N. Relationship between ABA and chilling injury in mangosteen fruit treated with spermine. *Plant Growth Regul* **39**, 119–124 (2003).
188. Manurakchinakorn, S., Chainarong, Y. & Sawatpadungkit, C. Quality of mangosteen juice colored with mangosteen pericarp. *Int. Food Res. J.* **23**, 1033–1039 (2016).
189. Mustafa, M. A., Ali, A., Seymour, G. & Tucker, G. Delayed pericarp hardening of cold stored mangosteen (*Garcinia mangostana* L.) upon pre-treatment with the stress hormones methyl jasmonate and salicylic acid. *Sci. Hortic. (Amsterdam)*. **230**, 107–116 (2018).
190. Bustamante, C. A. *et al.* Heat treatment of peach fruit: Modifications in the extracellular compartment and identification of novel extracellular proteins. *Plant Physiol. Biochem.* **60**, 35–45 (2012).
191. Cukrov, D. Plants Progress toward Understanding the Molecular Basis of Fruit Response to Hypoxia. *Plants* **7**, 1–11 (2018).

Appendix

Table S1. Gas Chromatography instrument parameter

Instrument name	Shimadzu Ultra QP-2010 gas chromatography-mass spectrometry (GC-MS)
Column	InertCap 5 MS/NP (30 m , 0.25 mm i.d., 0.25 μ m film thickness)
Autosampler	AOC 20i/s autoinjector (Shimadzu, Kyoto, Japan)
Injection mode	Split
Split ratio	25
Injection temperature	230 °C
Carrier gas	Helium
Carrier gas flow	1.12 mL/min
Linear velocity	39 cm/sec
Column temperature	Hold at 80 °C for 2 min Raised by 15 °C/min to 330 °C hold for 6 min
Transfer line temperature	250 °C
Ion source temperature	200 °C
Ionization energy	0.93 kV (Electron Ionization (EI))
Mass range	85-500 m/z

Table S2. MetAlign parameter

Data Type		Nominal mass data
Mass Bin Parameter for Conversion to Nominal		0.6
Retention Begin (Scan nr)		1
Retention End (Scan nr)		28800
Maximum Amplitude		1000000000
Peak Slope Factor (x Noise)		2
Peak Threshold Factor (x noise)		4
Peak threshold (Abs. Value)		100
Average Peak Width at Half Height (Scans)		23
Scaling options		No scaling
Initial Peak	Begin of 1st region	Scan Nr. : 0; Max shift : 10
	End of 1st Region	Scan Nr. : 28800; Max shift : 10
Search Criteria	Begin on 2nd Region	Scan Nr. : 0; Max shift : 0
	End of 2nd Region	Scan Nr. : 0; Max shift : 0
Tuning alignment option and criteria		Pre-align Processing (Iterative)
Maximum shift per 100 scan		35
Mass peak selection	Min. Factor (x Noise)	1st Iteration: 7; Last Iteration: 7
	Min. Nr. Of Masses	1st Iteration: 5; Last Iteration: 5

Table S3. AIOutput (ver 1.30) parameter

1. Peak Making	Table	Height Threshold	1000
		RT Bining	2
2. Peak Identification and Annotation		Available index	Retention Index
		Analysis Type	Non Targeted
		Match Threshold	0.7
		RI Tolerance	10
3. Filtering			Accurate
		Height Filter	10000
		RSD (CV) Filter	10

Table S4. Solid color representative values of on-tree and off-tree ripening condition.

CIELAB was used to calculate the color representative values during mangosteen ripening condition.

Ripening stage	Solid color representative value (D65)						
	L*	a*	b*	dL*	da*	db*	dE*ab
1	55.84	4.32	39.36	2.15	7.48	4.61	9.05
1	61.25	4.15	39.56	7.57	7.32	4.81	11.58
1	57.85	2.07	39.93	4.17	5.24	5.19	8.47
1	34.65	-2.38	26.92	-19.03	0.79	-7.83	20.59
1	63.68	-0.76	40.12	10	2.41	5.37	11.61
1	59.54	-2.17	38.68	5.86	1	3.94	7.13
1	56.58	-4.66	36.9	2.9	-1.5	2.15	3.91
1	55.1	0.16	39.79	1.42	3.33	5.04	6.2
1	70.69	-1.4	33.98	17.01	1.77	-0.77	17.12
2	35.66	14.6	15.61	-18.02	17.77	-19.14	31.73
2	34.38	12.08	18.79	-19.31	15.25	-15.95	29.32
2	29.72	9.88	18.25	-23.97	13.05	-16.5	31.89
2	37.34	15.33	16.9	-16.35	18.49	-17.85	30.46
2	40.36	12.99	16.09	-13.33	16.15	-18.66	28.05
2	46.44	6.23	27.2	-7.24	9.39	-7.54	14.06
2	44.25	9.22	23.53	-9.43	12.39	-11.22	19.19
2	43.75	14.46	16.61	-9.93	17.63	-18.13	27.17
2	42.22	15.5	17.96	-11.46	18.67	-16.79	27.6
3	29.54	18.69	7.99	-24.14	21.86	-26.76	42.15
3	30.7	9	9.04	-22.98	12.17	-25.71	36.57
3	27.2	10.89	5.78	-26.49	14.06	-28.97	41.7
3	38.24	20.95	18.06	-15.44	24.12	-16.69	33.15
3	21.84	14.22	7.44	-31.85	17.39	-27.3	45.41
3	26.71	12.47	7.16	-26.97	15.64	-27.59	41.63
3	29.53	19.68	8.63	-24.15	22.85	-26.12	42.28
3	30.55	18.18	10.58	-23.13	21.35	-24.17	39.69
3	10.54	5.3	8.5	-43.15	8.47	-26.25	51.21

3	21.75	10.98	10.92	-31.93	14.14	-23.83	42.28
4	28.99	13.45	5.14	-24.7	16.62	-29.61	41.98
4	24.05	16.56	6.93	-29.63	19.73	-27.82	45.18
4	27.92	15	6.89	-25.77	18.17	-27.85	42.07
4	24.92	18.05	8.37	-28.77	21.22	-26.38	44.42
4	23.3	18.67	9.09	-30.38	21.83	-25.66	45.37
4	29.6	16.52	7.73	-24.08	19.69	-27.02	41.2
4	23.75	10.55	3.2	-29.94	13.71	-31.55	45.6
4	25.88	12.53	3.87	-27.81	15.69	-30.88	44.42
4	23.17	9.42	2.79	-30.51	12.59	-31.95	45.94
5	22.05	11.33	4.27	-31.63	14.49	-30.48	46.26
5	19.62	12.93	4.66	-34.06	16.1	-30.09	48.22
5	22.16	13.19	4.91	-31.52	16.35	-29.84	46.38
5	22.38	6.3	1.38	-31.31	9.46	-33.37	46.72
5	22.78	9.71	5.33	-30.9	12.88	-29.42	44.57
5	18.09	6.99	2.19	-35.59	10.16	-32.56	49.3
5	19.81	8.92	4.65	-33.88	12.08	-30.1	46.9
5	16.8	8.32	4.48	-36.88	11.49	-30.27	49.08
5	22.81	8.33	6.15	-30.88	11.5	-28.6	43.63
6	16.67	3.88	1.64	-37.01	7.04	-33.11	50.15
6	9.63	3.59	5.46	-44.06	6.76	-29.28	53.33
6	16.36	4.18	0.56	-37.32	7.35	-34.19	51.14
6	22.7	2.13	0.05	-30.98	5.29	-34.7	46.82
6	25.2	2.47	1.71	-28.49	5.64	-33.04	43.99
6	15.97	2.6	0.22	-37.72	5.77	-34.52	51.46
6	22.08	6.01	3.16	-31.6	9.17	-31.58	45.61
6	20.04	6.72	2.61	-33.65	9.89	-32.14	47.57
6	14.05	5.52	2.4	-39.63	8.68	-32.35	51.89

Table S5. Annotated metabolites of mangosteen fruit during ripening

	Peel		Flesh		Seeds	
	RT (min)	Metabolites	RT (min)	Metabolites	RT (min)	Metabolites
1	4.70	n-Propylamine	4.70	n-Propylamine	4.71	n-Propylamine
2	4.82	2-Hydroxypyridine	4.82	2-Hydroxypyridine	4.83	2-Hydroxypyridine
3	5.04	Oxalacetic acid+Pyruvate	5.04	Oxalacetic acid+Pyruvate	5.12	Lactic acid
4	5.11	Lactic acid	5.11	Lactic acid	5.61	Alanine
5	5.60	Alanine	5.60	Alanine	5.92	Oxalate
6	5.89	Oxalate	5.66	n-Butylamine	6.17	Leucine
7	6.69	Malonic acid	5.91	Oxalate	6.38	2-Aminobutyric acid
8	6.82	3-Hydroxyisovaleric acid	6.37	2-Aminobutyric acid	6.41	Isoleucine
9	6.85	Valine	6.85	Valine	6.83	3-Hydroxyisovaleric acid
10	6.98	Urea	6.98	Urea	6.86	Valine
11	7.12	Oxamic acid	7.38	2-Aminoethanol	7.05	Urea
12	7.25	Serine	7.42	Leucine	7.13	Oxamic acid
13	7.38	2-Aminoethanol	7.44	Phosphate	7.40	2-Aminoethanol
14	7.38	Ethylmalonate	7.45	Glycerol	7.45	Phosphate
15	7.44	Phosphate	7.64	Threonine	7.46	Glycerol
16	7.45	Glycerol	7.64	Maleic acid	7.70	Proline

17	7.64	Threonine	7.64	Isoleucine	7.72	Maleic acid
18	7.64	Isoleucine	7.68	Proline	7.79	Succinic acid(or anhydride)
19	7.71	Maleic acid	7.77	Succinic acid(or anhydride)	7.80	Glycine
20	7.78	Succinic acid(or anhydride)	8.00	Glyceric acid	8.02	Glyceric acid
21	7.78	Glycine	8.28	Serine	8.10	Fumaric acid
22	8.64	Glutaric acid(or anhydride)	8.31	N-Acetyl valine	8.30	Serine
23	8.95	Cadaverine	8.64	Glutaric acid(or anhydride)	8.57	Threonine
24	9.23	3-Amino isobutyric acid	8.89	b-Alanine	8.91	b-Alanine
25	9.42	Malic acid	8.95	Cadaverine	8.91	N-Acetyl leucine
26	9.50	N-{4-[Bis(trimethylsilyl)amino]butyl}acetamide	9.18	Unknown_200	9.25	3-Amino isobutyric acid
27	9.57	Threitol	9.23	3-Amino isobutyric acid	9.44	Malic acid
28	9.62	2-Thiouracil	9.37	Glycine	9.71	Aspartic acid
29	9.63	Meso erythritol	9.42	Malic acid	9.74	5-Oxoproline
30	9.69	Aspartic acid	9.50	N-{4-[Bis(trimethylsilyl)amino]butyl}acetamide	9.76	4-Aminobutyric acid
31	9.71	5-Oxoproline	9.57	Threitol	9.79	Hydroxyproline
32	9.72	Hydroxyproline	9.69	Aspartic acid	10.10	Threonic acid

33	9.73	4-Aminobutyric acid	9.71	5-Oxoproline	10.51	Glutamic acid
34	10.49	Glutamic acid	9.74	4-Aminobutyric acid	10.61	Phenylalanine
35	10.82	threo-3-Hydroxy aspartic acid	9.76	Hydroxyproline	10.90	Xylose
36	10.82	Xylose	10.07	Threonic acid	10.93	Asparagine
37	10.90	Asparagine	10.49	Glutamic acid	10.95	Arabionose
38	11.04	Xylulose+Ribulose	10.59	Phenylalanine	11.07	Phthalic acid
39	11.37	Rhamnose	10.68	Lauric acid	11.07	Ribose
40	11.38	Quinolinic acid	10.88	Xylose	11.40	Rhamnose
41	11.38	Arabitol	10.90	Asparagine	11.41	Arabitol
42	11.66	Glutamine	10.93	Arabionose	11.50	Putrescine
43	11.72	Xylonic acid	11.04	Xylulose+Ribulose	11.69	Glutamine
44	11.91	Shikimic acid	11.04	Ribose	11.95	Shikimic acid
45	12.05	Isocitric acid+Citric acid	11.29	Xylitol	12.04	Dimethylbenzimidazole
46	12.41	Quinic acid	11.37	Rhamnose	12.08	Isocitric acid+Citric acid
47	12.50	Psicose	11.38	Arabitol	12.44	Quinic acid
48	12.57	Fructose	11.47	Putrescine	12.54	Pyridoxal
49	12.60	Mannose	11.66	Glutamine	12.54	Sorbose
50	12.65	Galactose	11.72	Xylonic acid	12.60	Fructose
51	12.69	Glucose	11.92	Shikimic acid	12.69	Galactose
52	12.73	N-Carbamoyl aspartate	12.05	Isocitric acid+Citric acid	12.73	Glucose
53	12.97	Glucuronate	12.12	Myristic acid	12.77	N-Carbamoyl aspartate

54	13.02	Galacturonic acid	12.41	Quinic acid	12.77	Mannose
55	13.43	Plamitic acid(16:0)	12.57	Fructose	12.77	Lysine
56	13.43	Palmitic acid	12.61	Mannose	12.89	Tyrosine
57	13.51	Glucarate	12.65	Galactose	12.96	Mannitol
58	13.92	N-Acetyl galactosamine	12.70	Glucose	13.00	Glucuronate
59	13.97	Inositol	12.74	Tyramine	13.05	Galacturonic acid
60	14.64	Stearic acid(17:0)	12.86	Tyrosine	13.07	Glucarate
61	17.10	Sucrose	12.97	Glucuronate	13.42	Xanthine
62	17.97	Gentiobiose	13.02	Galacturonic acid	13.47	Plamitic acid(16:0)
63			13.04	Glucarate	13.96	N-Acetyl galactosamine
64			13.44	Plamitic acid(16:0)	14.01	Inositol
65			13.92	N-Acetyl galactosamine	14.68	Stearic acid(17:0)
66			13.98	Inositol	17.15	Sucrose
67			14.64	Tryptophan	17.53	b-Lactose
68			14.64	Stearic acid	17.75	Maltose
69			17.11	Sucrose	18.15	Gentiobiose
70			18.51	Benzenemethanol		

Table S6. A list of tentatively identified metabolites GC-MS analysis in mangosteen peel part between two harvesting condition. All metabolites are detected in both harvesting condition after alignment process and tentatively identified using our laboratory in-house library.

No	Peel Part				
	Metabolites name	Retention time (min)	Retention index	QuantMS	Metabolite ID
1	n-Propylamine	4.57	1026.82	174	PubChem: 7852
2	2-Aminoethanol	7.23	1275.21	174	C00189
3	2-Aminoisobutyrate	5.87	1144.27	130	C03665
4	2-Hydroxypyridine	4.69	1037.38	152	C02502
5	4-Aminobutyric acid	9.63	1540.26	174	C00334
6	5-Oxoproline	9.55	1531.22	156	PubChem: 7405
7	Alanine	5.46	1106.56	116	C00041
8	Arabionose	10.77	1685.00	103	C00216
9	Arabitol	11.23	1746.24	217	C01904
10	Aspartic acid	9.54	1529.60	232	C00049
11	Epicatechin	17.81	2891.88	368	C09727(8)
12	Fructose	12.45	1919.39	103	C00085
13	Fucose	11.39	1768.10	117	C01018
14	Galactose	12.49	1926.59	147	C00124
15	Galacturonic acid	12.85	1981.26	333	C00333
16	Glucose	12.53	1932.78	319	C00031
17	Glucuronate	12.81	1974.07	160	C00191
18	Glutamic acid	10.34	1628.15	246	C00302
19	Glutamine	11.50	1783.36	156	C00064
20	Glutaric acid(or	8.48	1406.81	147	C00489

	anhydride)				
21	Glycerol	7.30	1281.80	147	C00116
22	Glycine	7.63	1315.10	174	C00037
23	Inositol	13.81	2132.43	217	C00137
24	Isocitric acid+Citric acid	11.89	1838.29	147	C00158+ C00311
25	Isoleucine	7.49	1300.62	158	C00407
26	Lactic acid	4.98	1063.42	147	C00186
27	Lyxose	10.72	1678.30	217	C00476
28	Malic acid	9.26	1496.24	147	C00149
29	Mannose	12.45	1919.65	319	C00159
30	Meso erythritol	9.50	1524.22	217	C00503
31	N-Acetyl galactosamine	13.76	2123.90	319	PubChem: 129680793
32	Oxalacetic acid+Pyruvate	4.90	1056.28	174	C00022+ C00036
33	Oxalate	5.64	1122.92	147	C00209
34	Phosphate	7.29	1280.32	299	C00009
35	Phthalic acid	11.01	1715.85	147	C01606
36	Quinic acid	12.25	1890.25	345	C00296
37	Quinolinic acid	11.22	1744.54	147	C03722
38	Rhamnose	11.21	1744.31	117	C01684
39	Ribose	10.89	1700.02	217	C00121
40	Serine	8.14	1369.30	204	C00065
41	Shikimic acid	11.76	1819.85	204	C00493
42	Sorbose	12.41	1914.47	217	C00764
43	Stearic acid(17:0)	14.47	2244.26	117	PubChem: 5281
44	Succinic acid(or anhydride)	7.63	1314.93	147	C00042
45	Sucrose	16.93	2705.11	361	C00089
46	Threitol	9.42	1514.68	217	C16884
47	threo-3-Hydroxy aspartic acid	10.72	1678.51	189	C03961

48	Tyrosine	12.69	1956.52	218	C00082
49	Unknown_103 Amine like	8.48	1406.62	174	
50	Unknown_110 Amine like	8.79	1441.80	174	
51	Unknown_115	9.02	1468.69	174	
52	Unknown_116	9.02	1468.78	86	
53	Unknown_127 Amine like	9.34	1505.24	174	
54	Unknown_129 Amine like	9.46	1519.35	174	
55	Unknown_131	9.46	1519.55	86	
56	Urea	6.89	1240.96	147	C00086
57	Valine	6.70	1222.51	144	C00183
58	Xylonic acid	11.57	1792.35	292	C05411
59	Xylose	10.72	1678.40	103	C00181
60	Xylulose+Ribulose	10.89	1699.70	147	C00310 + C00309

Table S7. A list of tentatively identified metabolites GC-MS analysis in mangosteen flesh part between two harvesting condition. All metabolites are detected in both harvesting condition after alignment process and tentatively identified using our laboratory in-house library. The metabolites were marked with * are tentatively identified using both NIST library and our laboratory in-house library.

No	Flesh Part				
	Metabolites name	Retention time (min)	Retention index	QuantMS	Metabolite ID
1	2-Aminoethanol	4.59	1027.03	174	C00189
2	2-Hydroxypyridine	4.71	1037.69	152	C02502
3	3-Methylglutarate	8.72	1432.82	147	PubChem: 12284
4	4-Aminobutyric acid	9.64	1540.36	174	C00334
5	5-Oxoproline	9.56	1531.09	156	PubChem: 7405
6	Alanine	8.16	1370.81	188	C00041
7	Arabionose	10.78	1685.02	103	C00216
8	Arabitol	11.24	1746.33	217	C01904
9	Aspartic acid	9.55	1529.67	232	C00049
10	b-Alanine	8.75	1435.78	174	C00099
11	Ethylmalonate	7.32	1281.80	147	PubChem: 11756
12	Fucose	11.41	1770.13	117	C01018
13	Galactose*	12.51	1927.33	147	C00124
14	Galacturonic acid	12.86	1981.42	333	C00333
15	Gentiobiose	17.82	2891.38	204	PubChem: 441422
16	Glucono-1,5-lactone	12.43	1915.73	217	PubChem: 7027
17	Glucose	12.55	1933.89	319	C00031
18	Glucuronate	12.82	1974.36	333	C00191

19	Glutamic acid	10.35	1628.20	246	C00302
20	Glutamine	11.52	1784.13	156	C00064
21	Glutaric acid(or anhydride)	8.50	1407.04	147	C00489
22	Glyceric acid	7.87	1339.24	147	C00258
23	Glycine	7.64	1315.40	174	C00037
24	Indole-3-acetic acid	12.51	1927.58	130	PubChem: 802
25	Inositol	13.82	2132.75	147	C00137
26	Isocitric acid + citric acid	11.90	1838.50	273	C00158+ C00311
27	Isoleucine	7.50	1300.55	158	C00407
28	Lactic acid	5.00	1063.48	117	C00186
29	Leucine	7.28	1278.59	158	C00123
30	Lyxose*	10.78	1684.91	217	C00476
31	Malic acid	9.28	1496.11	147	C00149
32	Mannitol	12.78	1968.68	147	C00392
33	Mannose*	12.46	1920.65	319	C00159
34	N-Acetyl galactosamine	13.77	2124.35	319	PubChem: 129680793
35	n-Butylamine	5.54	1112.00	174	C18706
36	n-Propylamine	4.59	1027.03	174	PubChem: 7852
37	Oxalate	5.78	1134.63	147	C00209
38	Paenoflorin	20.95	3520.64	361	C23180576
39	Phenylalanine	10.44	1640.92	218	C00079
40	Phosphate	7.30	1280.32	299	C00009
41	Phthalic acid	10.90	1699.78	147	C01606
42	Plamitic acid(16:0)	13.29	2047.66	132	PubChem: 37767
43	Proline	7.54	1304.29	142	C00148
44	Putrescine	11.32	1756.92	174	C00134
45	Quinic acid	12.26	1890.73	345	C00296
46	Quinolinic acid	11.24	1746.45	147	C03722

47	Rhamnose	11.23	1744.40	117	C01684
48	Serine	8.15	1369.03	204	C00065
49	Shikimic acid	11.77	1819.76	204	C00493
50	Sorbose	12.37	1907.03	217	C00764
51	Succinic acid(or anhydride)	7.64	1314.96	147	C00042
52	Sucrose	16.94	2706.04	361	C00089
53	Threitol	9.43	1514.89	217	C16884
54	Threonine	7.50	1300.02	117	C00188
55	Trehalose	17.47	2816.67	361	C01083
56	Unknown_15	4.92	1056.54	174	
57	Unknown_158 Amine like	8.80	1441.79	174	
58	Unknown_183 Amine like	9.35	1505.11	174	
59	Unknown_186 Amine like	9.47	1519.68	174	
60	Unknown_343	12.36	1905.65	147	
61	Unknown_347	12.37	1906.28	231	
62	Unknown_371	12.43	1915.36	307	
63	Unknown_373	12.43	1915.61	103	
64	Unknown_422	12.56	1934.77	89	
65	Unknown_425	12.56	1935.27	217	
66	Urea	6.88	1238.28	147	C00086
67	Valine	6.72	1222.78	144	C00183
68	Xylitol	11.15	1734.04	217	C00379
69	Xylonic acid	11.58	1792.90	292	C05411
70	Xylose	10.73	1678.44	103	C00181

Table S8. Solid color representative values of off-tree ripening condition and postharvest treatment. CIELAB was used to calculate the color representative values during mangosteen ripening condition. Stage 0 was used as a reference sample. dL indicates the different of lightness between the samples and reference that were measured. da and db values are chromaticity diagram that describes red-green color for da values and yellow-blue color for db values different between the samples and reference. dLab value is the total color of difference value between samples and reference.

Treatment name	day of observation	Average value						
		L*	a*	b*	dL*	da*	db*	dE*ab
"random on-tree" ripening condition	stage 1	59.36	6.41	29.59	2.21	2.94	-1.33	11.25
	stage 2	45.53	20.43	17.61	-11.63	16.96	-13.31	25.10
	stage 3	39.65	24.36	14.10	-17.50	20.89	-16.82	33.08
	stage 4	30.14	11.09	4.89	-27.01	7.62	-26.03	39.33
	stage 5	25.41	8.31	2.68	-31.74	4.84	-28.24	42.91
	stage 6	24.86	2.58	0.45	-32.29	-0.88	-30.47	44.45
Methyl jasmonate	2	27.65	14.25	5.08	-29.50	10.78	-25.84	40.86
	10	24.19	2.61	0.66	-32.96	-0.86	-30.25	44.77
KMnO4	2	27.45	14.40	5.57	-29.70	10.94	-25.35	40.81
	10	26.23	2.43	1.35	-30.92	-1.04	-29.57	42.91
Negative control	2	28.60	14.90	5.98	-28.55	11.43	-24.94	39.70
	10	24.76	2.50	1.01	-32.40	-0.97	-29.91	44.13
Combination LT and control	1	37.26	25.78	14.05	-19.89	22.31	-16.87	34.88
	3	33.38	15.80	10.04	-23.77	12.33	-20.88	34.78
	4	34.39	22.40	12.11	-22.76	18.94	-18.81	35.34
Room temperature	0	48.30	17.99	21.32	-8.85	14.52	-9.60	20.36
	1	33.98	22.49	11.33	-23.18	19.03	-19.59	36.22
	2	29.06	15.41	6.99	-28.09	11.94	-23.93	38.99
	3	26.88	11.41	4.13	-30.27	7.95	-26.79	41.50

	4	27.35	8.04	3.10	-29.80	4.57	-27.81	41.13
	5	25.04	5.66	2.41	-32.11	2.19	-28.51	43.06
	6	25.23	4.08	1.87	-31.93	0.62	-29.05	43.27
	7	24.85	3.70	1.04	-32.31	0.23	-29.88	44.04
	8	24.91	3.51	1.26	-32.24	0.05	-29.66	43.82
	9	26.42	3.69	1.90	-30.74	0.23	-29.02	42.35
	10	25.15	2.59	0.92	-32.00	-0.87	-30.00	43.89
Salicylic acid	2	24.74	3.84	1.64	-32.41	0.38	-29.28	43.86
	10	26.64	4.27	3.19	-30.52	0.80	-27.73	41.37
Low temperature	1	51.70	16.03	24.31	-5.45	12.56	-6.61	16.22
	3	48.94	19.08	22.09	-8.21	15.62	-8.83	20.76
	5	43.53	25.02	20.00	-13.62	21.55	-10.92	28.11
	7	46.27	19.96	25.45	-10.88	16.49	-5.47	23.53
	9	41.50	26.03	19.90	-15.65	22.56	-11.02	30.10
	10	45.65	19.64	24.81	-11.50	16.17	-6.11	23.32

Table S9. A list of tentatively identified metabolites GC-MS analysis in mangosteen between two ripening conditions. All metabolites are detected in both ripening conditions after alignment process and tentatively identified using our laboratory in-house library.

No	Metabolite name	
	Peel part	Flesh part
1	2-Aminoethanol	2-Aminobutyric acid
2	2-Hydroxybutyrate	2-Aminoethanol
3	2-Hydroxypyridine	4-Aminobutyric acid
4	3-Amino isobutyric acid	5-Oxoproline
5	4-Aminobutyric acid	Alanine
6	5-Oxoproline	Arabionose
7	Alanine	Arabitol
8	Arabionose	Aspartic acid
9	Ascorbic acid	b-Alanine
10	Aspartic acid	Citric acid
11	Epicatechin	Fructose
12	Ethylmalonate	Fucose
13	Fructose	Galactitol
14	Fucose	Galactose
15	Galactose	Galacturonic acid
16	Galacturonic acid	Glucarate
17	Gentiobiose	Glucono-1,5-lactone
18	Glucarate	Glucose
19	Glucono-1,5-lactone	Glucuronate
20	Glucose	Glutamic acid
21	Glucuronate	Glutamine
22	Glutamic acid	Glyceric acid
23	Glutaric acid(or anhydride)	Glycerol
24	Glyceric acid	Glycine
25	Glycerol	Hydroxyproline
26	Glycine	Isoleucine
27	Inositol	Leucine

28	Isobutylamine	Lysine
29	Isocitric acid+Citric acid	Lyxose
30	Isoleucine	Maleic acid
31	Lactic acid	Malic acid
32	Lyxose	Mannitol
33	Maleic acid	Mannose
34	Malic acid	N-Acetyl galactosamine
35	Maltose	Paeoniflorin
36	Mannitol	Phenylalanine
37	Mannose	Phosphate
38	Meso erythritol	Phthalic acid
39	N-Acetyl galactosamine	Plamitic acid
40	N-Acetyl leucine	Proline
41	n-Butylamine	Psicose
42	N-Carbamoyl aspartate	Quinic acid
43	n-Propylamine	Quinolinic acid
44	Oxalacetic acid+Pyruvate	Rhamnose
45	Oxalate	Ribose
46	Phosphate	Serine
47	Phthalic acid	Shikimic acid
48	Plamitic acid(16:0)	Sucrose
49	Psicose	Threitol
50	Pyridoxal	Threonic acid
51	Quinic acid	Tyrosine
52	Quinolinic acid	Urea
53	Rhamnose	Valine
54	Ribose	Xylitol
55	Saccharic acid	Xylonic acid
56	Sarcosine	Xylose
57	Serine	
58	Shikimic acid	
59	Sorbose	
60	Stearic acid(17:0)	
61	Succinic acid(or anhydride)	

62	Sucrose
63	Threitol
64	threo-3-Hydroxy aspartic acid
65	Tyrosine
66	Urea
67	Valine
68	Xylitol
69	Xylonic acid
70	Xylose
71	Xylulose+Ribulose

Table S10. A list of tentatively identified metabolites GC-MS analysis in mangosteen peel part during temperature treatment. All metabolites are found in both ripening condition after the alignment process and tentatively identified using our laboratory in-house library. The metabolites were marked with * are tentatively identified using both NIST library and our laboratory in-house library.

No	Peel Part				
	Metabolites name	Retention time (min)	Retention index	QuantMS	Metabolite ID
1	n-Propylamine	4.59	1027.82	174	PubChem:7852
2	2-Aminoethanol	7.25	1275.73	174	C00189
3	2-Hydroxybutyrate	5.78	1134.99	131	C05984
4	2-Hydroxypyridine	4.70	1038.22	152	C02502
5	4-Aminobutyric acid	9.60	1536.59	174	C00334
6	5-Oxoproline	9.56	1531.81	156	PubChem:7405
7	Alanine	5.47	1107.14	116	C00041
8	Arabionose	10.78	1685.79	103	C00216
9	Arabitol	11.24	1747.06	217	C01904
10	Ascorbic acid	12.82	1975.39	332	C00072
11	Aspartic acid	9.55	1530.18	232	C00049
12	Cinnamyl alcohol	8.67	1428.17	117	C02394
13	Epicatechin	17.82	2893.73	368	C09727(8)
14	Ethylmalonate	7.31	1282.41	147	PubChem:11756
15	Fructose	12.42	1915.38	103	C00085
16	Fucose	11.40	1769.03	117	C01018
17	Galactose	12.50	1927.74	319	C00124
18	Galacturonic acid	13.00	2002.20	333	C00333
19	Glucarate	12.88	1985.10	169	C00818
20	Glucono-1,5-lactone	12.42	1915.51	217	PubChem:7027
21	Glucose*	12.54	1933.91	319	C00031
22	Glucuronate	12.82	1974.89	333	C00191
23	Glutamic acid	10.34	1628.69	246	C00302

24	Glutamine	11.51	1784.29	156	C00064
25	Glutaric acid (or anhydride)	8.50	1407.86	147	C00489
26	Glycerol	7.31	1282.33	205	C00116
27	Glycine	7.64	1316.26	174	C00037
28	Homocysteine	10.73	1679.43	234	C00155
29	Inositol	13.82	2133.17	217	C00137
30	Isobutylamine	5.40	1100.38	174	C78819
31	Isocitric acid +Citric acid	11.90	1839.09	273	C00158+C00311
32	Isoleucine	7.50	1301.23	158	C00407
33	Lactic acid	4.99	1064.17	147	C00186
34	Leucine	7.28	1279.11	158	C00123
35	Maleic acid	7.50	1301.32	147	C01384
36	Malic acid	9.28	1496.91	147	C00149
37	Malonic acid	6.55	1207.16	147	C00383
38	Mannose	12.46	1920.93	319	C00159
39	Meso erythritol	9.50	1524.48	217	C00503
40	Oxalacetic acid +Pyruvate	4.92	1057.26	174	C00022+C00036
41	Oxalate	5.65	1123.56	147	C00209
42	Oxamic acid	6.99	1249.90	147	C01444
43	Paeonol	10.40	1635.71	223	C10712
44	Phosphate	7.30	1281.01	299	C00009
45	Phthalic acid	10.90	1700.27	147	C01606
46	Plamitic acid(16:0)	13.29	2048.01	117	PubChem:37767
47	Proline	7.54	1305.23	142	C00148
48	Quinic acid	12.26	1891.37	345	C00296
49	Quinolinic acid	11.24	1746.95	147	C03722
50	Rhamnose	11.22	1745.13	117	C01684
51	Serine	8.15	1369.98	204	C00065
52	Shikimic acid	11.77	1820.50	204	C00493
53	Sorbose	12.36	1905.55	103	C00764
54	Stearic acid(17:0)	14.48	2245.23	117	PubChem:5281

55	Succinic acid(or anhydride)	7.64	1315.46	147	C00042
56	Sucrose	16.89	2696.25	361	C00089
57	Threitol	9.43	1515.53	217	C16884
58	Threonic acid	9.93	1576.88	147	C01620
59	Tyramine	12.59	1940.34	174	C00483
60	Tyrosine	12.66	1951.06	218	C00082
61	Unknown_158 Amine like	8.80	1442.47	174	
62	Unknown_166	9.04	1469.45	174	
63	Unknown_177	9.35	1505.96	174	
64	Unknown_184 Amine like	9.47	1520.31	174	
65	Unknown_77	6.30	1183.56	147	
66	Urea	6.87	1238.51	147	C00086
67	Valine	6.71	1223.09	144	C00183
68	Xylitol	11.15	1734.65	217	C00379
69	Xylonic acid	11.58	1793.40	292	C05411
70	Xylose*	10.73	1679.21	103	C00181
71	Xylulose+Ribulose	10.90	1700.73	103	C00310 + C00309

Table S11. A list of tentatively identified metabolites GC-MS analysis in mangosteen peel part during temperature treatment. All metabolites are found in both ripening condition after alignment process and tentatively identified using our laboratory in-house library. The metabolites were marked with * are tentatively identified using both NIST library and our laboratory in-house library.

No	Flesh Part				
	Metabolites name	Retention time (min)	Retention index	QuantMS	Metabolite ID
1	2-Aminoethanol	7.35	1276.28	174	C00189
2	2-Hydroxybutyrate	5.75	1124.08	131	C05984
3	2-Hydroxypyridine	4.79	1039.45	152	C02502
4	3-Amino isobutyric acid	9.15	1470.84	174	C144901
5	4-Aminobutyric acid	9.75	1536.78	174	C00334
6	Alanine	5.57	1372.38	116	C00041
7	Arabionose	10.89	1686.06	217	C00216
8	Arabitol	11.34	1746.76	217	C01904
9	Aspartic acid	9.66	1531.71	232	C00049
10	b-Alanine	8.85	1437.41	248	C00099
11	Ethylmalonate	7.41	1282.61	147	PubChem:11756
12	Fructose	12.54	1915.62	103	C00085
13	Galactose	12.62	1927.88	205	C00124
14	Galacturonic acid	12.98	1982.68	333	C00333
15	Glucarate	13.00	1985.81	217	C00818
16	Glucono-1,5-lactone	12.60	1924.75	217	PubChem:7027
17	Glucose*	12.79	1934.26	147	C00031
18	Glucuronate	12.93	1975.30	333	C00191
19	Glutamic acid	10.46	1630.26	246	C00302
20	Glycine	7.75	1316.83	174	C00037
21	Hydroxyproline	9.69	1535.26	230	C51354
22	Isocitric acid+Citric	12.02	1840.40	273	C00158+

	acid				C00311
23	Isoleucine	6.36	1180.63	86	C00407
24	Lactic acid*	5.08	1064.83	147	C00186
25	Leucine	6.13	1159.19	86	C00123
26	Malic acid	9.38	1497.89	147	C00149
27	Mannose*	12.71	1920.50	319	C00159
28	N-Acetyl galactosamine	13.89	2124.96	319	PubChem: 129680793
29	N-Acetyl leucine	8.91	1444.08	86	C02710
30	n-Butylamine	5.62	1112.41	174	C18706
31	n-Propylamine	4.67	1028.23	174	PubChem:7852
32	Oxamic acid	7.09	1250.94	147	C01444
33	Phosphate	7.41	1282.28	299	C00009
34	Plamitic acid	13.40	2047.64	117	PubChem:37767
35	Proline	7.65	1306.98	142	C00148
36	Pyroglutamic acid	9.69	1534.65	156	C01879
37	Quinic acid	12.37	1891.86	345	C00296
38	Rhamnose	11.33	1745.40	117	C01684
39	Serine	7.22	1263.52	116	C00065
40	Stearic acid	14.61	2245.41	117	PubChem:5281
41	Succinic acid	7.74	1316.74	147	C00042
42	Sucrose	17.08	2707.69	361	C00089
43	Tyramine	12.70	1940.27	174	C00483
44	Tyrosine	12.82	1958.91	218	C00082
45	Unknown_10 Amine like	5.01	1058.74	174	
46	Unknown_100	8.91	1443.50	100	
47	Unknown_103 Amine like	8.91	1443.98	174	
48	Unknown_111	9.15	1470.93	86	
49	Unknown_112	9.15	1471.03	154	
50	Unknown_22	5.74	1123.78	133	
51	Unknown_23	5.74	1123.86	86	
52	Unknown_24	5.74	1123.93	146	

53	Unknown_361	13.40	2047.12	145	
54	Unknown_365	13.40	2047.77	129	
55	Unknown_37	5.99	1146.52	100	
56	Unknown_405	14.60	2245.12	145	
57	Unknown_407	14.61	2245.55	341	
58	Unknown_52	6.73	1215.81	110	
59	Unknown_8	5.01	1058.52	130	
60	Unknown_92	8.45	1392.17	99	
61	Unknown_95	8.60	1407.98	174	
62	Urea	7.00	1241.97	147	C00086
63	Valine	6.82	1223.96	144	C00183
64	Xylonic acid	11.68	1793.13	292	C05411
65	Xylose	10.84	1679.83	103	C00181

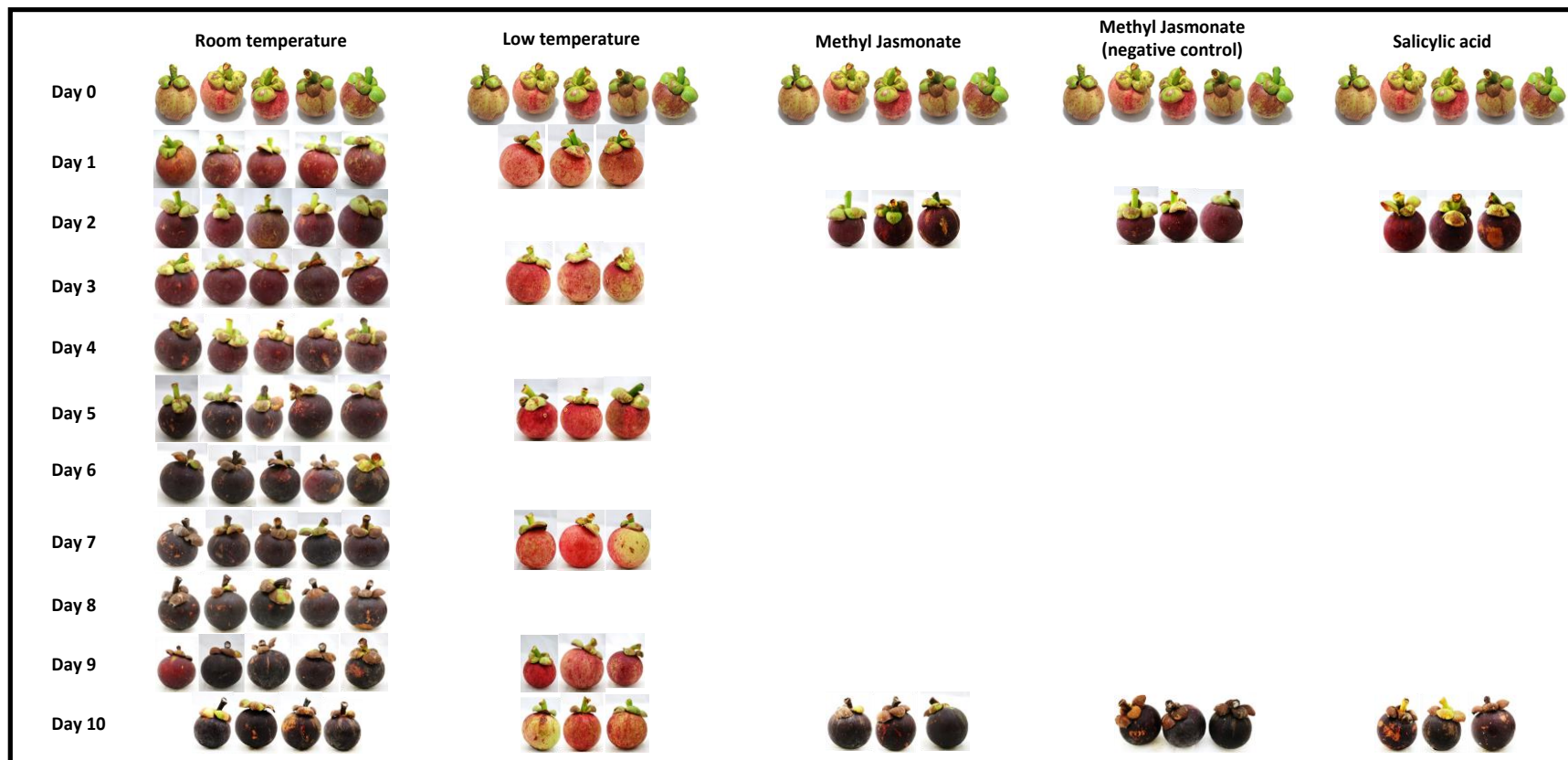


Figure S1. A photograph of all treated mangosteen using postharvest treatment

List of publications

Conferences

- 1). Anjaritha Aulia Rizky Parijadi, Sobir Ridwani, Fenny Martha Dwivany, Sastia Prama Putri, Eiichiro Fukusaki. Metabolomics-based approach for the study of *Garcinia mangostana* (mangosteen) ripening stages (poster). The 2017 Annual Conference of Society of Biotechnology Japan. September 2017. Tokyo, Japan.
- 2). Anjaritha Aulia Rizky Parijadi, Sobir Ridwani, Fenny Martha Dwivany, Sastia Prama Putri, Eiichiro Fukusaki. Metabolomics-based approach for the study of *Garcinia mangostana* (mangosteen) ripening stages (poster). The 2017 Annual Metabolomics symposium. November 2017. Osaka, Japan.
- 3). Anjaritha Aulia Rizky Parijadi, Sobir Ridwani, Fenny Martha Dwivany, Sastia Prama Putri, Eiichiro Fukusaki. Metabolomics-based approach for the study of *Garcinia mangostana* (mangosteen) ripening stages (poster). 2018 International Conference of Metabolomics Society. June 2018. Seattle, USA.
- 4). Anjaritha Aulia Rizky Parijadi, Fenny Martha Dwivany, Sastia Prama Putri, Eiichiro Fukusaki. Metabolic Profiling of Cavendish banana (*Musa acuminata* cv.AAA) to understand its color changes (oral). The 2018 Annual Conference of Society of Biotechnology Japan. September 2018. Osaka, Japan.

- 5). Anjaritha Aulia Rizky Parijadi, Sastia Prama Putri, Fenny Martha Dwivany, Eiichiro Fukusaki. Metabolome study of temperature effect in banana ripening (poster). The 2018 Annual Metabolomics symposium. October 2018. Tsuruoka, Japan.
- 6). Anjaritha Aulia Rizky Parijadi, Sobir Ridwani, Fenny Martha Dwivany, Sastia Prama Putri, Eiichiro Fukusaki. Evaluation of different postharvest treatment in mangosteen (*Garcinia mangostana*) using metabolomics approach (oral). The 2019 Annual Conference of Japan Society of Bioscience, Biotechnology and Agrochemistry. March 2019. Tokyo, Japan.
- 7). Anjaritha Aulia Rizky Parijadi, Sobir Ridwani, Fenny Martha Dwivany, Sastia Prama Putri, Eiichiro Fukusaki. An evaluation of different ripening condition and different postharvest treatment in mangosteen (*Garcinia mangostana*) using metabolomics approach (poster). The 2019 International Conference of Metabolomics Society. June 2019. The Hague, Netherland.

Review paper

- 1). Anjaritha Aulia Rizky Parijadi, Sastia Prama Putri. Aplikasi pendekatan metabolomik untuk Ilmu Tanaman. Bunga rampai ForMind 2017 – membangun Indonesia dengan ilmu pengetahuan dan keberagaman. IPB Press. Indonesia. 2017

Original papers

- 1). Anjaritha Aulia Rizky Parijadi, Sastia Prama Putri, Sobir Ridwani, Fenny Martha Dwivany, Eiichiro Fukusaki. "Metabolic profiling of *Garcinia mangostana* (mangosteen) based on ripening stages," *J Biosci Bioeng.* 2018 Feb;125(2):238-244. doi: 10.1016/j.jbiosc.2017.08.013. Epub 2017 Sep 29.
- 2). Anjaritha Aulia Rizky Parijadi, Sobir Ridwani, Fenny Martha Dwivany, Sastia Prama Putri, Eiichiro Fukusaki. "A metabolomics-based approach for the evaluation of off-tree ripening conditions and different postharvest treatments in mangosteen (*Garcinia mangostana*)," *Metabolomics.* 2019. 15: 73-89. <https://doi.org/10.1007/s11306-019-1526-1>. Epub 2019 May 03..

Acknowledgments

First of all, praises and thanks to Allah, the Almighty, for His showers of blessings and guidance throughout my life, including a chance for me to complete the study and research successfully

I sincerely thank my very kind supervisor Prof. Eiichiro Fukusaki, for his valuable and constructive suggestions during the planning and development of this research work. His kind assistances have taught me the real meaning of hard work, leadership, patience and being independent. I also would like to express my sincere gratitude to my thesis co-supervisor Prof. Toshiya Muranaka and Prof. Kazuhito Fujiyama for their insightful comments and advises to improve my doctoral thesis. I also would like to give special appreciation to Prof. Sobir and Dr. Fenny Martha Dwivany for their patient guidance, enthusiastic encouragement and useful critiques and suggestions during samples collections. Many thanks to Assoc. Prof. Suichi Shimma for their valuable comments and constructive recommendations. Assistant Professor Sastia Prama Putri for discussion, comment, and valuable guidance throughout my study.

Deepest appreciation also sent to our collaborator, Center of Tropical Horticultural studies (CENTROHS, Bogor) member during sample collection and day-to-day support and conversation and Bandung Institute of Technology (ITB) for supporting the mangosteen extraction preparation especially for Dr. Rizkita, Mr Awang, Mr. Baesuni, Mrs. Pipit, Mrs. Ike (for the administration thingy). At last, to Japan ministry of education, culture, sports, science & technology (MEXT) for financial support.

I wish to thank all Fukusaki Laboratory members who barely come and go for my five years study in Japan, for their help and warmth friendship even with the language barrier for your support not only in my research but also in my life here.

Lastly, I dedicated my thesis to my beloved family, Parijadi's Family, especially for my mother, father, and sister. Thank you for your biggest support and for everything your everlasting love means everything to me. For Mr.A, Thank you for patiently hear my story and support me in the finish line.

*So, verily, every hardship there is ease
Verily, every difficulty, there is a relief
[Quran 94:5-6]*